Journal of Visualized Experiments

Neutron Crystallography Data Collection and Processing for Modelling Hydrogen Atoms in Protein Structures

--Manuscript Draft--

Article Type:	Invited Methods Collection - JoVE Produced Video
Manuscript Number:	JoVE61903R1
Full Title:	Neutron Crystallography Data Collection and Processing for Modelling Hydrogen Atoms in Protein Structures
Corresponding Author:	Flora Meilleur North Carolina State University Raleigh, North Carolina UNITED STATES
Corresponding Author's Institution:	North Carolina State University
Corresponding Author E-Mail:	meilleurf@ornl.gov
Order of Authors:	Gabriela Schröder
	Flora Meilleur
Additional Information:	
Question	**Response**
Please indicate whether this article will be Standard Access or Open Access.	Open Access (US$4,200)
Please indicate the **city, state/province, and country** where this article will be **filmed**. Please do not use abbreviations.	Oak Ridge, TN, USA
Please confirm that you have read and agree to the terms and conditions of the author license agreement that applies below:	I agree to the Author License Agreement
Please specify the section of the submitted manuscript.	Biochemistry
Please provide any comments to the journal here.	Please note the new title.

Manuscript

Click here to access/download;Manuscript;61903_R1.docx

TITLE:

Neutron Crystallography Data Collection and Processing for Modelling Hydrogen Atoms in Protein Structures

AUTHORS AND AFFILIATIONS:

Gabriela C. Schröder[1,2], Flora Meilleur[1,2]

[1]Department of Molecular and Structural Biochemistry, North Carolina State University, Raleigh, NC, USA
[2]Neutron Scattering Division, Oak Ridge National Laboratory, Oak Ridge, TN, USA

Corresponding Author:
Flora Meilleur, fmeille@ncsu.edu

Email Addresses of Co-authors:
Gabriela C. Schröder, gcschrod@ncsu.edu

KEYWORDS:
Neutron protein crystallography, neutrons, proteins, hydrogen atoms, protonation, enzymes, metalloproteins, structural biology, polysaccharide monooxygenases, reaction mechanism, X-ray crystallography.

SUMMARY:

Neutron protein crystallography is a structural technique that permits the localization of hydrogen atoms, thereby providing important mechanistic details of protein function. We present here the workflow for mounting a protein crystal, neutron diffraction data collection, structure refinement and analysis of the neutron scattering length density maps.

ABSTRACT:

Neutron crystallography is a structural technique that allows determination of hydrogen atom positions within biological macromolecules, yielding mechanistically important information about protonation and hydration states while not inducing radiation damage. X-ray diffraction, in contrast, provides only limited information on the position of light atoms and X-ray beams rapidly induces radiation damage of redox cofactors and metal centers. Presented here is the workflow employed for the IMAGINE and MaNDi beamlines at Oak Ridge National Laboratory to obtain a neutron diffraction structure once a protein crystal of suitable size (> 0.1 mm^3) has been obtained. We demonstrate mounting of hydrogenated crystals in quartz capillaries for neutron diffraction data collection. Also presented is the vapor exchange process of the mounted crystals with D_2O-containing buffer to ensure replacement of hydrogen atoms at exchangeable sites with deuterium. The incorporation of deuterium reduces the background arising from the incoherent scattering of hydrogen atoms and prevents density cancellation caused by their negative coherent scattering length. Sample alignment and room temperature data collection strategies are illustrated using quasi-Laue data collection at IMAGINE at the High Flux Isotope Reactor (HFIR). Furthermore, crystal mounting and rapid freezing in liquid nitrogen for cryo-data

collection to trap labile reaction intermediates is demonstrated at the MaNDi time-of-flight instrument at the Spallation Neutron Source. Finally, preparation of the model coordinate and diffraction data files and visualization of the neutron scattering length density (SLD) maps will be addressed. Structure refinement against neutron data-only or against joint X-ray/neutron data to obtain an all-atom structure of the protein of interest will finally be discussed. The process of determining a neutron structure will be demonstrated using crystals of the lytic polysaccharide monooxygenase *Neurospora crassa* LPMO9D, a copper-containing metalloprotein involved in the degradation of recalcitrant polysaccharides *via* oxidative cleavage of the glycosidic bond.

INTRODUCTION:

Neutron macromolecular crystallography is a technique that provides a unique window into the structure and underlying chemistry of proteins. Conceptually similar to X-ray diffraction, neutron diffraction provides atomistic details of macromolecular structure, however, the interaction of neutrons with nuclei enables localization of light atoms, often difficult to detect with X-ray diffraction[1]. During X-ray diffraction, X-rays scatter from the electron cloud, making light atoms such as hydrogen (H) poorly visible in electron density maps that do not have near sub-Ångström resolution[2]. In contrast, the scattering intensity of neutrons depends on complex interactions with the nucleus, with isotopes of the same element displaying different scattering lengths. Therefore, light atoms and their isotopes, such as hydrogen (^{1}H) and deuterium (^{2}H or D), have comparable visibility to the backbone carbon, nitrogen and oxygen atoms in neutron scattering length density (SLD) maps. Furthermore, since the magnitude of neutron scattering is independent of the number of electrons, scattering from light elements is not obscured by heavy elements when they are in close vicinity to each other, as is observed in X-ray scattering. The enhanced visibility of H and its isotope D when employing neutron diffraction provides valuable information about the protonation state of catalytically important residues, cofactors and ligands and aids the orientation of water molecules, revealing important information about catalytic mechanisms and protein chemistry[3]. Neutron diffraction also offers the advantage of being a non-destructive technique, particularly suited to biological samples sensitive to ionization such as proteins with metal centers or photosensitive redox cofactors[2]. The primary focus of this article is to provide an overview of the workflow to obtain a high-quality neutron protein diffraction structure, we refer the interested reader to Podjarny et al.[4], Blakeley[5], Blakeley et al.[6] and O'Dell et al.[3] for an excellent overview of neutron protein diffraction and Ashkar et al.[7] for further applications of neutron scattering.

Neutrons are primarily generated during nuclear reactions employing either of two processes: nuclear fission at reactor sources or spallation at accelerator-based sources[8]. Reactor sources provide a continuous neutron beam by employing nuclear fission of the ^{235}U isotope while spallation neutron sources produce a pulsed neutron beam by bombarding a target, for example a liquid metal such as mercury, with protons[9]. Oak Ridge National Laboratory (ORNL) in Oak Ridge, Tennessee, hosts both a steady-state neutron source at the High Flux Isotope Reactor (HFIR) and a 60 Hz pulsed sourced at the Spallation Neutron Source (SNS). The IMAGINE beamline, located at the HFIR, is a neutron diffractometer optimized for biological macromolecules (**Supplementary Figure 1**)[10]. IMAGINE employs a neutron image plate detector to measure quasi-Laue data using a narrow bandpass in the range of 2.8 – 4.5 Å from single crystals with unit cell edges <150 Å. The Macromolecular Neutron Diffractometer (MaNDi), located at the SNS, is a time-of-flight (TOF) Laue neutron diffractometer equipped with a spherical detector array frame (DAF) (**Supplementary Figure 2**)[11]. MaNDi measures data from single crystals with unit cell edges in the range of 10 – 300 Å by employing a tunable 2 Å-wavelength bandwidth between 2.0 – 6.0 Å[12].

The process of generating neutrons is highly energy intensive, resulting in relatively weak neutron beam fluxes when contrasted to X-ray beam fluxes at synchrotron sources[13]. To ensure sufficient signal-to-noise ratios during data collection, it is necessary to grow crystals of suitable size and quality[14]. Typically, crystals with volumes > 0.1 mm^3 are needed to collect data with adequate statistics[15]. In addition to lower fluxes, inherent properties of the interaction between neutrons and the sample nuclei must be taken into consideration[16]. The scattering length of neutrons differs for isotopes of the same element, a property which can be advantageously exploited in small angle neutron scattering (SANS) to mask or highlight regions of a sample – a process known as contrast matching[17]. In diffraction experiments, the negative coherent neutron scattering length of H (-3.741 fm for ^{1}H) can lead to cancellation of neutron scattering density map features since the coherent neutron scattering lengths of other biologically relevant atoms, including carbon (6.6511 fm for ^{12}C), nitrogen (9.37 fm for ^{14}N), oxygen (5.803 fm for ^{16}O), phosphorus (5.13 fm for ^{31}P) and sulfur (2.804 fm for ^{32}S), are positive (**Table 1**)[12,14]. Furthermore, the large incoherent scattering length of H (25.274 fm), increases the background, hampering the quality of the dataset and compromising data resolution[7]. To circumvent these limitations introduced by H it is necessary, for neutron diffraction, to exchange H for its isotope deuterium, ^{2}H(D), which has a positive coherent neutron scattering length (6.671 fm) and significantly lower incoherent scattering length (4.04 fm)[19]. This can be achieved by perdeuteration, a process in which the protein is expressed by organisms grown in fully deuterated media ensuring complete incorporation of D at H sites[20]. It is also possible to partially deuterate protein by replacing H with D solely at the exchangeable sites (titratable groups) while the non-exchangeable carbon-bound sites remain hydrogenated[21]. This can be achieved by growth of hydrogenated protein crystals in deuterated mother liquor[22]. Most commonly however, H/D exchange of hydrogenated proteins is performed by vapor exchange following growth of suitably large crystals in H_2O-based buffer[23]. In such cases, crystals are mounted in a quartz capillary and vapor-equilibrated with deuterated mother liquor.

The limited neutron fluxes at neutron sources result in longer data collection times, ranging from days to several weeks[24]. At ORNL, both IMAGINE and MaNDi employ a narrow wavelength bandpass in the 2–6 Å range to optimize data collection[25]. Data can be collected at room temperature, or at cryo-temperature that can potentially improve data quality and opens up the possibility for freeze-trapping catalytic intermediates. Following neutron diffraction data collection, an X-ray dataset is typically collected on the same crystal at the same temperature or on a crystal grown under identical conditions[26]. Data collection at the same temperature allows structure refinement to be performed against both X-ray and neutron data, preventing any potential temperature-induced artefacts such as changes in the visibility and position of waters or the occupancies of residue alternate conformations.[27] Joint X-ray neutron data refinement increases the data-to-parameter ratio and provides the advantage of allowing the protein backbone coordinates to be refined against the X-ray data, while the neutron diffraction data is used to refine the position of the H/D atoms[28]. This is particularly useful using partially deuterated samples, and density cancellation due to H atoms at non-exchangeable sites on the protein is present. Although the number of X-ray structures far exceeds the number of neutron structures deposited in the Protein Data Bank (PDB), software packages initially designed for the refinement of X-ray data have been expanded to encompass neutron data as well[3,29,30]. Following data collection, models can be refined using refinement packages such as *phenix.refine*, CNSsolve (nCNS) or SHELXL[28, 31–33]. During the refinement process, neutron scattering density maps can be visualized for manual fitting using COOT[34]. Following structure solution, the coordinate and density files of neutron and/or X-ray data can be submitted to the PDB, who will validate and deposit the model, making it available for public acess[18,29,30].

Structural analysis of proteins is a multifaceted approach in which numerous techniques are used to probe their function and mechanism[35]. Neutron protein crystallography provides valuable chemical insights to expand on and complement findings from additional studies such as X-ray, NMR or micro crystal electron diffraction (microED)[36]. Neutron protein diffraction is uniquely positioned to provide insights into enzymatic mechanisms, since H atoms are central to their chemistry. The absence of radiation damage induced by neutrons make them a probe exceptionally suited to the study of metalloproteins[37]. We present here a representative example of the process of neutron protein diffraction from sample preparation to data collection, refinement and analysis (**Figure 1**). Crystals of sufficient size for neutron diffraction experiments have been grown of the metalloprotein *Neurospora crassa* LPMO9D (*Nc*LPMO9D). *Nc*LPMO9D is a copper-containing metalloprotein involved in the degradation of recalcitrant cellulose by oxygen atom insertion at the glycosidic bond[38,39]. The *Nc*LPMO9D active site contains a mononuclear copper center within a characteristic “histidine-brace” composed of the N-terminal histidine and a second conserved histidine (**Supplementary Figure 3**)[40]. The N-terminal of fungal LPMOs is methylated but the post-transitional modification does not occur during recombinant expression in yeast. In the *Nc*LPMO9D resting state, the copper center is present in a Cu^{2+} oxidation state and is activated by single electron reduction to Cu^{1+}, allowing molecular oxygen to bind and be activated by rapidly being reduced to a superoxide species[41,42]. The overall *Nc*LPMO9D reaction requires further addition of one electron and two protons to form the hydroxylated polysaccharide product[43]. The identity of the activated oxygen species responsible for hydrogen atom abstraction (HAA) from the polysaccharide substrate has not been identified and intensive structural and computational studies are currently ongoing[44,45]. Given the redox chemistry at the *Nc*LPMO9D active site, mitigation of radiation damage is particularly pertinent. We illustrate here room temperature and cryo-temperature data collection on *Nc*LPMO9D to determine its structure in the resting state and its activated reduced form, respectively[46]. Emphasis will be given to protein crystal mounting, beamline instrument setup for data collection, the preparation of the data and coordinate files and the refinement steps necessary to model an all-atom neutron structure.

PROTOCOL:

1. Crystal size evaluation

1.1. Measure the size of the crystals using a microscope equipped with normal and polarized light. Select crystals with a minimum volume of ~0.1 mm^3.

1.2. Label wells with sufficiently large crystals and note the crystallization conditions used to generate these crystals.

2. Preparation of deuterated crystallization buffer

2.1. Dissolve crystallization buffer components in D_2O to generate deuterated crystallization buffer.

2.2. Adjust pH of the buffer by calculating the pD of the solution using the following equation:

$$pD = pH_{meas} + 0.4 \tag{1}$$

where pH_{meas} is the pH measured with a standard glass electrode. The original pH of the *Nc*LPMO9D crystallization buffer was 6.0, therefore we will use a pH_{meas} of 5.6 for the deuterated crystallization buffer at pD 6.0.

2.3. Immerse the pH meter electrode in D_2O for ten minutes prior to use (**Supplementary Figure 5**).

2.4. Adjust the pH_{meas} to 5.6 by use of the base NaOD or the acid DCl.

3. Crystal harvesting

3.1. Place siliconized 22 mm round glass slides next to the crystallization tray from which crystals will be harvested. Use a clean glass slide per crystal (**Figure 2A**).

3.2. Open the sealed sandwich box containing the protein crystals in the 9-well large volume siliconized glass plate.

3.3. Remove 10-20 µL from the crystallization reservoir solution with a micropipette and place the solution on the glass slide (**Figure 2B**).

3.4. Harvest the crystal using a microloop of appropriate size and place the crystal in the reservoir solution drop on the glass slide to remove debris that are often harvested along with the crystal (**Figure 2C** and **Figure 2D**).

NOTE: It will be necessary to work quickly since the small-volume droplets may evaporate. Exposed crystals are also at risk of drying out when exposed to the atmosphere. It may be necessary to add some reservoir solution to the protein drop to prevent crystals from drying out in small crystallization drop volumes.

4. Crystal mounting

NOTE: Capillary mounting protocols vary with experimentalist preferences. To prevent damage to crystals, capillaries that need to be shortened should be scored with a cutting stone or sandpaper to ensure a smooth break.

4.1. Fill one end of a 2 mm diameter 50 mm length quartz capillary with reservoir buffer by capillary action or by directly pipetting ~10 μL of reservoir buffer into the capillary (**Figure 3A**).

NOTE: Users are encouraged to make use of quartz capillary tubes because in, addition to its mechanical strength, it is essential to limit neutron beam absorption and lower background contributions from the capillary. Glass capillaries introduce high background and absorb neutrons, compromising data quality.

4.2. Gently place the crystal in the reservoir buffer in the quartz capillary using the mounting loop (**Figure 3B** and **Figure 3C**).

4.3. Tap the tube to move the reservoir buffer and the therein suspended crystal down the capillary (**Figure 3D**).

4.4. Place the crystal no closer than 13.5 mm and no further 27.5 mm from one end of the capillary; this will be the mounting end (**Supplementary Figure 6**).

4.5. Aspirate the buffer solution around the crystal using a long thin pipette tip, leaving the slightly crystal wet. Do not touch the crystal (**Supplementary Figure 7A**).

4.6. Dry the capillary walls with a thin paper wick (**Supplementary Figure 7B**).

4.7. Pipette 20-50 μL of deuterated buffer solution into the end of the capillary opposite the mounting end (**Figure 4A**).

4.8. Melt beeswax with a heat "wand" and gently insert the capillary in this melted beeswax. Repeat until an airtight seal forms (**Figure 4B** and **Figure 4C**).

4.9. Pipette a very small amount of deuterated buffer, approximately 5 μL in the mounting end of the capillary to act as a "heat sink" for the hot beeswax. Dip this end in melted beeswax to generate an airtight seal as described previously to form a capillary sealed on both ends (**Figure 4D**).

4.10. Inspect the mounted crystal using a microscope after mounting to ensure airtightness (**Figure 4E**).

4.11. Carefully secure the mounted crystals with Kim wipes in a container such as a 15-ml Falcon tube or Petri Dish and store horizontally at the temperature at which the crystals were grown (**Figure 4F**).

5. Vapor exchange

5.1. Replace the deuterated buffer with fresh buffer two days after crystal mounting.

5.2. Melt the wax seal furthest from the crystal with a heating loop, and use a pipette and paper wicks to remove the buffer.

5.3. Refill the capillary with 20-50 μL of deuterated buffer solution and seal with a wax seal.

5.4. Repeat the deuterated buffer replacement twice more at four day intervals to ensure that deuterated buffer vapor exchange is complete and allow vapor exchange for at least two weeks.

6. Neutron protein diffraction

NOTE: Readers interested in the IMAGINE beam line specifics are encouraged to consult Meilleur et al. 2013, Meilleur et al. 2018[10, 47].

6.1. Room temperature data collection at the IMAGINE beamline at HFIR

6.1.1. Sample mounting

6.1.1.1. Secure the capillary-mounted quartz capillary on the goniometer with putty.

6.1.1.2. Mount the goniometer on the sample stick and center the crystal in the beam using the off-line alignment station.

6.1.1.3. Secure the sample stick on the instrument sample stage (**Figure 1B**).

6.1.1.4. Ensure that the experimental hutch is vacated and open the beamline shutter for neutron data collection.

6.1.2. **Data collection**

6.1.2.1. Open the data acquisition program on the beamline control computer and click on the **Setup** tab to set up the data collection strategy. Under **Experiment Parameters** type the sample name next to **Sample Name** and input the proposal number next to **Proposal**. Under **Image Naming** select **Folder template** and set the destination for the acquired data to be saved and select Image Prefix and type relevant frame name (**Supplementary Figure 8**).

NOTE: Data collection at both IMAGINE and MaNDi will be performed in quasi-Laue mode, using methodology and software developed for Laue diffraction data collection as developed by

Helliwell et al.[48] and Nieh et al.[49].

6.1.2.2. Open the Optics GUI and click on **2.78** for λ_{min} and **4.78** for λ_{max} to set the quasi-Laue range for data collection (**Supplementary Figure 9**).

6.1.2.3. Toggle to the **Collect** tab and under **Next Scan Parameters** insert the exposure time in seconds under **Exposure**, the number of frames under **N Frames** and the angles for data collection under **Δφ/Frame**. Name the frame to be collected under **Image Prefix** and initiate the data collection by clicking the **Start Scan** button (**Supplementary Figure 10**).

6.1.2.4. The diffracted neutrons will be detected by the Image Plate Detector. At the end of each exposure, the image plate will be read and the pattern displayed on the data acquisition GUI (**Supplementary Figure 11**).

6.1.2.5. Index, integrate, wavelength normalize, and scale frames using Lauegen, Lscale[50] and Scala by the responsible beamline scientist, who will provide the user with the merged reflection file following data collection (**Supplementary Figure 12**).

6.1.2.6. Collect a corresponding X-ray dataset on the same crystal at the same temperature following neutron diffraction data collection (**Supplementary Figure 13**).

NOTE: A crystal grown from the same drop or under the same crystallization conditions can also be used for collecting X-ray diffraction data for joint neutron/X-ray refinement.

6.2. Cryo data collection at the MaNDi beamline at the SNS

NOTE: Readers interested in the beam line specifics are encouraged to consult Coates et al. (2015), Meilleur et al. 2018[10, 11].

6.2.1. Sample mounting

6.2.1.1. Prepare the deuterated ascorbate soaking solution for the reduction of the crystals and the deuterated cryoprotectant. Place 20 μL drops of each of these solutions into sitting drop wells in a crystallization plate.

NOTE: The cryoprotectant solution is usually the cryoprotectant that has proven effective for cryo-temperature X-ray diffraction data collection prepared in D_2O. This cryoprotectant can be further optimized (e.g. concentration) for neutron data collection if necessary.

6.2.1.2. Select loops for sample mounting and attach them to a cryo crystal mount following the MaNDi guidelines (**Supplementary Figure 14**).

6.2.1.3. Fill a foam cryo-Dewar with liquid nitrogen. Place a metal cryo-protection sleeve within the liquid nitrogen to cool (**Supplementary Figure 15A**).

6.2.1.4. Remove the wax plugs from both ends of the capillary and tap the capillary to move the buffer plug so that the mounted crystal is immersed in buffer. Wash the crystal out into the 20 µL reservoir solution drop in the sitting drop well (**Supplementary Figure 15B** and **Supplementary Figure 15C**).

NOTE: This step is not required if H/D exchange was performed by equilibration of the crystallization drops against deuterated buffer or by direct soaking of the crystal in deuterated buffer.

6.2.1.5. Immerse the crystal in the ascorbate soaking solution for two hours. Mount the crystal in a microloop attached to a cryo crystal mount. Immerse the mounted crystal in the cryoprotectant for 10 seconds and plunge the crystal and cryo mount into the liquid nitrogen to freeze (**Supplementary Figure 15D**).

6.2.1.6. Once the crystal is frozen, use pre-cooled cryo pin tong and mount the crystal on the MaNDi sample stage fitted with a cryo-stream. Gently open the cryo pin tong and ensure that the crystal remains in the cryo-stream.

6.2.2. Data collection

6.2.2.1. Open the data collection software in which the experiment information will have auto-populated.

6.2.2.2. Click on the center of the crystal to center it with the computer-controlled goniometer (**Supplementary Figure 16**).

6.2.2.3. Under **Table**, set up the data collection strategy by inputting the angles for data collection under “phi” as well as the total neutron beam exposure per frame under “Value” (**Figure 21**).

6.2.2.4. Click on **Submit** to start data collection.

6.2.2.5. As data collects, diffracted neutron will be visible (**Supplementary Figure 17**). Diffraction spots will become clearer as the exposure time increases, improving the signal-to-noise ratio (**Figure 5**).

6.2.2.6. Index, integrate, wavelength normalize, and scale frames using Mantid and Lauenorm by the responsible beamline scientist, who will provide the user with the merged intensity file following data collection[51].

7. Structure refinement

7.1. Joint X-ray and neutron data refinement

7.1.1. Structure preparation

7.1.1.1. Refine the X-ray data to obtain a protein structure using the *phenix.refine* software package and Coot for manual building to obtain a completed structure.

7.1.1.2. Open CCP4 and select the **Convert to/modify/extend MTZ** program to match the R-free data flags of the neutron data to those of the X-ray data. Select to import the reflection file in **MTZ** format. Under **In** upload the obtained neutron MTZ file and upload the X-ray mtz file under **Import FreeR MTZ** (**Supplementary Figure 18**). Give a name for the new MTZ file under **Out** and click **Run**.

7.1.1.3. Open the Phenix software package and click on **ReadySet** under Refinement Tools. Next to **PDB file** upload the PDB coordinate file refined against the X-ray data. Select to **Add hydrogens to model if absent** and select **H/D at exchangeable sites, H elsewhere** from the drop-down menu. Select **Add deuteriums to solvent molecules** and leave the remaining options on their default values (**Supplementary Figure 19A**).

NOTE: If a perdeuterated protein is used, select the option **Add hydrogens to model if absent** and select **H/D at exchangeable sites, D elsewhere**.

7.1.2. **Structure refinement**

7.1.2.1. Open the *phenix.refine* program under the **Refinement** tab to set up the refinement using both X-ray and neutron data. In the **Configure** tab in **Input files** input the PDB file from the X-ray structure which has been processed with ReadySet and the necessary CIF restrains file for any relevant ligands. Upload the MTZ file from the neutron data with the Rfree flags assigned using CCP4 and assign this as “Neutron data” and “Neutron R-free” under the “Data type” heading. Upload the MTZ file from the X-ray data and assign this as “X-ray data” and “X-ray R-free” under the “Data type” heading. The “Space group” and “Data labels” will auto-populate once the data has been uploaded (**Supplementary Figure 19B**).

NOTE: When performing the refinement, and inputting the crystal information, use the unit cell determined from the X-ray data.

7.1.2.2. Under the **Configure** tab in the **Refinement settings** keep the standard refinement strategy. Increase the number of cycles to five (**Supplementary Figure 20**)

7.1.2.3. Select **All parameters**, click on **Advanced** and select **Hydrogens…**. Change the **Hydrogen refinement model** to **individual** and turn off the **Force riding adp** (**Supplementary Figure 20**).

7.1.2.4. Select **All parameters** and open the **Search parameters** option. Search for the word **nuclear** and select to **Use the nuclear distances for X-H/D** (**Supplementary Figure 20**).

7.1.2.5. Select **Run** to initiate the refinement.

7.1.3. **Model building**

7.1.3.1. Following the refinement in Phenix, click on **Open in Coot** in the **Results** tab to visualize the X-ray electron density and neutron SLD maps. Click on the **Display Manager** tab and under **Maps** click on **Delete Map** next to the **_neutron** maps to remove the neutron maps (**Supplementary Figure 21**). Click on **File > Open MTZ, mmCIF fcf or phs…**. Select the current refinement files and open the .mtz file. For both the **Amplitudes** and **Phases** option select the **$2F_OF_C$WT_no_fill_neutron** data from the dropdown menu. Repeat this and open the F_OF_CWT_neutron data. Open **Display Manager** and toggle to **Scroll** for both the neutron and X-ray $2F_OF_C$WT maps then scroll to decrease the rmsd of the $2F_OF_C$WT maps to 1.00 (**Supplementary Figure 21**). Toggle to **Scroll** for both the neutron and X-ray F_OF_CWT maps and scroll to decrease the rmsd of the F_OF_CWT maps to 3.00.

7.1.3.2. Perform visual inspection of the residues to determine whether the model fits the data. Determine the correct orientation and H/D occupancy of all exchangeable sites by analyzing difference density map peaks. This includes the hydroxyl groups of Serines, Threonines and Tyrosines; the nitrogen of Histidine, Glutamine, Asparagine and Lysine; the sulfhydryl of Cysteine; the carboxyl groups of Aspartate and Glutamate; backbone amide groups; ligands; cofactors and any potential functionalized residues.

7.1.3.3. Reorient water molecules according to neutron density and hydrogen bond interactions by rotating them using the **Rotate Translate Zone/Chain/Molecule** feature (**Supplementary Figure 22A** and **Supplementary Figure 22B**). Adjust positions of protein residue H/D exchangeable sites using the **Edit Chi Angles** tool and the **Rotate Translate Zone/Chain/Molecule** feature (**Supplementary Figure 22C** and **Supplementary Figure 22D**).

7.2. **Structure refinement – neutron data-only refinement**

7.2.1. **Structure preparation**

7.2.1.1. Open Phenix and select "**Molecular Replacement**" and select "**Phaser-MR (full featured)**" to phase the density file of scaled intensities provided by the instrument scientist by molecular replacement to generate a starting coordinate file in pdb format. Input the starting pdb structure in the "**Input and general options** tab and complete the **Ensembles**, **ASU contents** and **Search Procedure** options.

7.2.1.2. Open **Model tools** and select **PDB Tools**. Insert the pdb file as the **Input file**. Navigate to the **Options** tab and under **Remove atom selection** select the names of the solvent, ligands, cofactors and metals. This removes all water molecules, cofactors, ligands and metal ions to generate a minimal model. Additionally, select to Remove alternate conformers from the model (**Supplementary Figure 23**).

7.2.1.3. Select **Refinement** in Phenix and open **ReadySet**. Input the edited pdb coordinate file next to **PDB file**. Select to **Add hydrogens to model if absent** and select **H/D at exchangeable sites, H elsewhere** from the drop-down menu of **Neutron refinement options** (**Supplementary Figure 23**).

7.2.2. **Structure refinement**

7.2.2.1. Open the *phenix.refine* program under the **Refinement** tab in Phenix. In the **Configure** tab input the PDB file which has been processed with ReadySet under the **input files** box . In the **Input files** box upload the MTZ file from the neutron data and assign this as X-ray data and X-ray R-free under the **Data type** column even though it is neutron data. The refinement configuration set up in the next step will be used to treat the reflection files as neutron data. The Space group and Data labels will auto-populate once the data has been uploaded (**Supplementary Figure 24A**).

7.2.2.2. Under the **Configure** tab in the **Refinement settings** keep the standard refinement strategy. Increase the number of cycles to five. Under **Other options** select **neutron** from the **Scattering table** dropdown menu. Deselect the option to **Update waters** (**Supplementary Figure 24B**).

7.2.2.3. Select **Allparameters>Advanced>Hydrogens**. In the new window select **Individual** from the **Hydrogen refinement model** dropdown menu and turn off the **Force riding adp** (**Supplementary Figure 20**).

7.2.2.4. Select **All parameters > Search parameters**… option. Search for the word **nuclear** and select to **Use the nuclear distances for X-H/D** (**Supplementary Figure 20**).

7.2.2.5. Select to **Run** to initiate the refinement.

NOTE: Following the initial refinement, it will be necessary to visually inspect the neutron SLD maps and perform manual model building in Coot. It may be necessary to insert ligands/cofactors present in the model. Subsequent refinements will require the necessary CIF restraints file for any relevant ligands and these should be uploaded in the **Configure** tab of *phenix.refine.*

7.2.3. **Model building**

7.2.3.1. Following the refinement in Phenix, click on **Open in Coot** in the **Results** tab to visualize the neutron SLD maps and structure. Click on the **Display Manager** tab and under **Maps** click on **Delete Map** to delete both the $2F_OF_CWT$ and F_OF_CWT maps (**Supplementary Figure 25**). Click on **File > Open MTZ, mmCIF fcf or phs…**. Select the current refinement folder and select the .mtz file. For both the **Amplitudes** and **Phases** option select the **$2F_OF_C$WT_no_fill** data from the dropdown menu. Repeat by clicking on **File > Open MTZ, mmCIF fcf or phs…** and select the **F_OF_CWT** data from the dropdown menu for both the **Amplitudes** and **Phases** option. Open **Display Manager** and toggle to **Scroll** for the $2F_OF_C$WT_no_fill map then scroll to decrease the rmsd of the 2F_OF_CWT_no_fill data to 1.00 (**Supplementary Figure 25**). Toggle to **Scroll** for the F_OF_CWT map and scroll to decrease the rmsd of the F_OF_CWT data to 3.00.

7.2.3.2. Perform visual inspection of the protein structure to determine whether the model fits the neutron SLD map.

7.2.3.3. As described in **7.1.3.2**, determine the correct orientation and H/D occupancy of residues and groups with H/D exchangeable sites. Adjust residue positions using the **Rotate Translate** tool and **Edit Chi Angles** (**Figure 6**). If necessary, **Real Space Refine Zone** can be used. Fix D atoms that explode from the residue manually by using the text editor to insert the correct atom coordinates

NOTE: **Real Space Refine Zone** is not optimized for neutron SLD maps in Coot and may result in irregular bond lengths for atoms bound to D, termed exploding residues (**Supplementary Figure 26**). It is preferable to manually edit the necessary atomic coordinates and avoid use of **Real Space Refine Zone**.

7.2.3.4. Insert and reorient water molecules according to neutron density. To add waters in Coot select the **Place atom at pointer** icon and select to insert a water molecule (**Supplementary Figure 27A**). Coot will insert an O atom at this position by default.

7.2.3.5. To add D atoms to the O atoms of waters inserted in Coot use Phenix. Open the **Refinement** menu and click on **ReadySet**. Next to **Neutron Refinement Options** select only the option to **Add deuteriums to solvent molecules**. Deselect **Add hydrogens to model if absent** (**Supplementary Figure 27B** and **Supplementary Figure 27C**).

NOTE: Model building using neutron-only data differs from model building of a joint X-ray/neutron structure because there is no X-ray data to contribute to the refinement of the coordinates of the backbone and heavier atoms. In a joint refinement, the electron density map is initially used to determine the protein backbone and sidechain coordinates. This model is subsequently used in a joint X-ray/neutron data refinement in which the orientation and occupancy of H/D atoms is derived from the neutron SLD map. In a neutron-only refinement, the entire structure is derived from analysis of the neutron SLD maps, requiring building of the backbone, side-chains and ligands in addition to the H/D atoms. The data-to-parameter ratio is low in refinements against neutron data lone and caution should be taken not too overfit the data.

REPRESENTATIVE RESULTS:

Neutron diffraction data on crystals of a lytic polysaccharide monooxygenase from *Neurospora crassa* (*Nc*LPMO9D) were collected on IMAGINE at the HFIR at room temperature and at MaNDi at the SNS under cryo-conditions following the protocol described above. Crystals of the hydrogenated protein grown in H_2O-based buffer measuring ~1000 μm by ~900 μm with an approximate volume of 0.1 mm^3 were used (illustrative example of large crystals are shown in **Supplementary Figure 4** and figures thereafter). Crystals were mounted in quartz capillaries and vapor exchange with the D_2O-based buffer was performed for three weeks prior to data collection (**Figure 4**).

Room temperature data collection was performed on the IMAGINE beamline (**Figure 1**). A four-hour white beam test lead to high resolution diffraction suggesting that the crystal was of suitable size and quality for a full dataset to be collected. In addition to providing preliminary information on the diffraction quality of the crystal, the broad bandpass exposure can be used to index the diffraction pattern and determine the crystal orientation matrix. Given the P_{21} space group of the crystal, a data collection strategy of 18 frames with a collection time of 20 hours per frame was implemented. As with X-ray diffraction data collection, higher symmetry space groups require fewer frames (i.e. less angular coverage) to collect a complete dataset. The data were collected in quasi-Laue mode using a wavelength range of 2.8 – 4.0 Å. Following data collection, the data were indexed, integrated scaled and merged to give a neutron SLD file in MTZ format at a resolution of 2.14 Å. Data were evaluated to be of sufficient quality following similar guidelines for X-ray data analysis, although a completeness of 80 % and a $CC_{1/2}$ of at least 0.3 were considered acceptable since neutron protein diffraction is a flux-limited technique.

Following room-temperature neutron diffraction data collection, the same crystal was used to collect a room temperature X-ray diffraction dataset at 1.90 Å resolution (**Figure 17**). The X-ray data were used to determine the positions of the “heavier” atoms including C,N,O and S. The structure refined against the X-ray data alone was then used as the starting model to perform a joint refinement against the X-ray and neutron data. Phenix ReadySet was used to add H atoms at non-exchangeable sites, H and D atoms at exchangeable sites and D atoms to water molecules of the starting X-ray model. Following this model preparation, iterative refinements were performed against both datasets (**Figure 24**). Interactive model building was performed in Coot by visually inspecting the density maps to orientate side-chains and water molecules accordingly. The neutron data were primarily used to determine protonation states and water molecule orientations. Comparison of the electron density map of residues such as serine and tryptophan and the corresponding neutron SLD map illustrate the information that can be gained on protonation states at H/D exchangeable sites from neutron protein diffraction (**Figure 7**). A map overlay of electron and neutron SLD maps for water molecules also indicate that while hydrogen bond interactions can be inferred from X-ray data, neutrons provide clear information regarding the position of these hydrogen bonds (**Figure 8**). Neutron SLD F_O-F_C omit maps were generated to determine protonation states and H/D orientation of side-chains. Illustrated are the neutron SLD maps obtained for tyrosine and threonine residues, in which the neutron F_o-F_C maps clearly indicate positive peaks signifying the presence of H/D (**Figure 9**). The collected neutron diffraction data also provided valuable information about multiple protonation states, such as the $-ND_3^+$ group of Lys (**Figure 10**). Refinement statistics (R_{work} and R_{free}) were closely monitored during model optimization to prevent over-fitting. Final statistics gave an X-ray R_{work} of 12.77 % and an R_{free} of 18.21%, and a neutron R_{work} of 14.48% and an R_{free} of 21.41% with 389 water molecules present (**Supplementary Figure 28**).

Cryo-temperature data were collected on *Nc*LPMO9D following an ascorbate soak to reduce the copper active site from Cu^{II} to Cu^{I} on the MaNDi beamline (**Figure 2** and **Figure 19**) [45]. Data were collected using TOF Laue mode following a neutron diffraction test using a 4 hour exposure to verify the quality of diffraction. Given the space group of the crystal, a data collection strategy of 18 frames with a collection dose of 80 Coulombs per frame was devised. The data were collected in TOF-Laue mode at a wavelength range of 2.15 – 4.3 Å. Following data collection, the data were indexed, integrated, scaled and merged to give a neutron SLD file in MTZ format at a resolution of 2.40 Å[51, 52].

Following data collection, the 2.40 Å cryo-temperature *Nc*LPMO9D neutron diffraction dataset was used for neutron-only data refinement. The neutron data were phased by molecular replacement using PDB 5TKH as the starting model. Phenix ReadySet was used to add H atoms at non-exchangeable sites and H/D atoms with partial occupancies at exchangeable sites. Water molecules were removed from the starting model with PDB Tools (**Supplementary Figure 23**). Model preparation was followed by refinement with *phenix.refine* using the neutron scattering table (**Supplementary Figure 24**). Interactive model building was performed in Coot, with water molecules being added using the positive peaks of F_O-F_c maps and positioned according to potential hydrogen bond interactions (**Figure 11A** and **Figure 11B**). When analyzing neutron SLD maps, water molecules are clearly visible if they are highly ordered, however their density may be spherical or ellipsoidal if they are not well-ordered (**Figure 11C-E**). Neutron SLD maps were used to provide valuable information on the orientation of residues such as asparagine, in which differentiating between the carbonyl and amino groups can be challenging when using X-ray diffraction data alone (**Figure 12A** and **Figure 12B**). Peaks in F_O-F_C neutron SLD omit maps were also very informative in determining the protonation states of His residues at the N_δ- or N_ε-position (**Figure 12C** and **Figure 12D**). The protonation state of residues with multiple H/D exchangeable sites can also be determined using neutron SLD maps. This was clearly illustrated with an F_O-F_C neutron SLD omit map of Arginine, which is known to have a positive charge (**Figure 12E** and **Figure 12F**). As previously, over-fitting was prevented by monitoring R_{work} and R_{free}. Final statistics gave an R_{work} of 22.58% and an R_{free} of 30.84% with 414 water molecules present (**Supplementary Figure 29**). Given that neutron protein diffraction is a flux limited technique in which the negative scattering length and large incoherent scattering factor of H must be taken in to account, it can be expected that a neutron data-only refinement would have poorer statistics than a joint X-ray/neutron-data refinement with fewer visible water molecules (**Supplementary Figure 28** and **Supplementary Figure 29**).

When analyzing neutron SLD maps, it will become apparent that density cancellation due to the negative neutron scattering length of H will be present in hydrogenated proteins that were subjected to vapor exchange with D_2O-containing crystallization buffer. Due to this reason, neutron SLD maps in which non-exchangeable H atoms are attached to carbon appear incomplete when compared to their electron density map counterpart (**Figure 13A**). The effect of cancellation is often more apparent at poorer resolutions, making it imperative to obtain protein crystals of a high quality. It is therefore preferable to perform a joint refinement of a sample with both X-ray and neutron data in which the X-ray data can be used to determine the position of the protein backbone (**Figure 13B**). Furthermore, sulfur atoms in Cys and Met may be poorly visible, requiring X-ray data for exact atom placement (**Figure 13C** and **Figure 13D**). Metal with weak neutron scattering lengths may also be challenging to model in neutron SLD maps, as is apparent in our LPMO9D maps. Collection of an X-ray dataset on the same crystal is therefore useful, since it permits metal atom positioning using electron density maps (**Figure 13E** and **Figure 13F**).

FIGURE AND TABLE LEGENDS:

Figure 1: Flow chart of neutron protein crystallography workflow. Protein Production: In order to obtain a neutron structure, protein is first expressed. Bacterial expression in H_2O- or D_2O-based media is typically used to produce a high yield of hydrogenated or perdeuterated recombinant protein, respectively. The protein is purified in H_2O-based buffer and then crystallized in either H_2O- or D_2O-based crystallization buffer to grow crystals to a minimum size of 0.1 mm^3. **Sample Preparation:** Prior to neutron diffraction data collection, H_2O-grown crystals undergo H/D exchange to exchange the protein titratable H atoms with D. H/D exchange can be done by direct soaking of the crystals in deuterated crystallization buffer, equilibration of the crystallization drop with a D_2O-based reservoir, or by mounting the crystals in quartz capillaries for vapor exchange with deuterated crystallization buffer. **Neutron Data Collection:** Following H/D exchange, potential crystals are screened to determine the diffraction quality. Crystals with a minimum resolution of 2.5 Å are considered suitable for a full dataset to be collected. Crystals are mounted in quartz capillaries for data collection at room temperature or flash frozen in a cryo-loop for data collection at cryogenic temperature. An X-ray dataset is collected on the same (or an identical) crystal at the same temperature. **Model Building:** Refinement is performed using *phenix.refine* against both neutron and X-ray data or against the neutron data only. Manual model building of the protein structure is performed in Coot using the neutron SLD maps. **Complete Structure:** Following completion of the protein structure, the coordinate model is validated and deposited in the Protein Data Bank.

Figure 2: Harvesting protein crystals. (**A**) Crystals are handled under a microscope. (**B**) The sealed sandwich box containing the siliconized glass plate is opened. Reservoir buffer is pipetted onto siliconized glass slides. (**C**) A crystal is harvested with a microloop. (**D**) The crystal is placed in drop of mother liquor to wash off any debris that are often harvested along with the crystal.

Figure 3: Transfer of crystal to quartz capillary. (**A**) The end of a quartz capillary is filled with reservoir buffer. (**B**) The crystal is transferred into the quartz capillary and (**C)** immersed in reservoir buffer. (**D**) The crystal is carried down capillary using reservoir buffer.

Figure 4: Sealing of the quartz capillary. (**A**) Deuterated buffer is added at the end of the capillary to form a “plug”. (**B**) Wax is melted with a “wand”. (**C**) The capillary is placed in the melted wax to seal. (**D**) Wax plugs are formed on both ends to seal the capillary. (**E**) The crystal after mounting. (**F**) The sealed capillary is placed in a Petri dish and held in place with putty.

Figure 5: Increased signal-to-noise of the neutron diffraction pattern. As data collection proceeds, diffracted spots become more intense. (NOTE: the live diffraction images presented here are for illustration and were taken from different crystals.)

Figure 6: Interactive model building using neutron data in Coot. (**A**) A positive F_O-F_C neutron SLD

density peak (green) indicating serine must be reoriented by editing chi angles. The $2F_O-F_C$ neutron SLD map is displayed in purple and $2F_O-F_C$ electron density map is displayed in blue. (**B**) Correctly positioned serine. (**C**) Positive and negative F_O-F_C neutron SLD density peaks (green and red, respectively) indicating that tryptophan must be rotated/translated to match difference density peak. (**D**) Correctly oriented tryptophan.

Figure 7: Additional information from neutron SLD maps. (**A**) $2F_O-F_C$ electron density map (blue) displays the positions of the “heavier” atoms in Serine. (**B**) $2F_O-F_C$ neutron SLD map (purple) clearly displays the position of the “lighter” D atom in Serine. (**C**) $2F_O-F_C$ electron density map (blue) displays the positions of the “heavier” atoms in Tryptophan. (**D**) $2F_O-F_C$ neutron SLD map (purple) clearly displays the position of the “lighter” D atom in Tryptophan.

Figure 8: Water molecule positioning. (**A**) The spherical shape of an $2F_O-F_C$ electron density map (blue) feature for water. (**B**) The $2F_O-F_C$ neutron SLD map (purple) provides information about the water orientation and hydrogen bond interaction. (**C**) Map overlay of electron and neutron SLD maps of water. The $2F_O-F_C$ neutron SLD map is displayed in purple and $2F_O-F_C$ electron density map is displayed in blue.

Figure 9: Neutron SLD F_O-F_C omit maps. (**A**)**:** The F_O-F_C neutron SLD map (green) provides clear information on the H/D orientation of Tyrosine residues. The $2F_O-F_C$ neutron SLD map is displayed in purple and $2F_O-F_C$ electron density map is displayed in blue. (**B**) Tyrosine residue with correct H/D orientation. (**C**) F_O-F_C neutron SLD map (green) provides clear information on the H/D orientation of Threonine residues. (**D**) Threonine residue with correct H/D orientation

Figure 10: Multiple protonation states displayed with neutron SLD maps. (**A**) The $2F_O-F_C$ electron density map (blue) only provides the position of the N atom of Lysine ε-ammonium group**.** (**B-E**) The F_O-F_C neutron SLD omit map (green) clearly demonstrates the positively charged $-NH_3$ group. The $2F_O-F_C$ neutron SLD map is displayed in purple and $2F_O-F_C$ electron density map is displayed in blue. (**F**) Overlay of electron density and neutron SLD maps.

Figure 11: Appearance of water molecules in neutron SLD maps. (**A**) Water molecules are positioned according to F_O-F_C neutron SLD maps (green) and potential hydrogen bonds. The $2F_O-F_C$ neutron SLD map is displayed in purple. (**B**) Correctly positioned water molecule. (**C-E**) The various shapes of neutron SLD maps for water molecules depending on B-factors and hydrogen bond interactions.

Figure 12: Information about amino acid orientation and protonation provided by neutron SLD maps. (**A**) The neutron SLD F_O-F_C map peaks (green) indicate incorrect orientation of an Asparagine residue. The $2F_O-F_C$ neutron SLD map is displayed in purple and $2F_O-F_C$ electron density map is displayed in blue. (**B**) $2F_O-F_C$ neutron SLD map (purple) of the correct Asparagine orientation. (**C**) The neutron SLD F_O-F_C map peak (green) indicates single protonation of the Histidine at N_ε. (**D**) $2F_O-F_C$ neutron SLD map (purple) of Histidine N_ε-protonation. (**E**) Neutron SLD F_O-F_C omit map peaks (green) confirm the positive charge of Arginine. (**F**) $2F_O-F_C$ neutron SLD map (purple) of positively charged Arginine.

Figure 13: Discontinuous neutron SLD maps. (**A**) $2F_O$-F_C neutron SLD map (purple) of a hydrogenated, vapor H/D exchanged protein. Glutamic acid displays neutron SLD map cancellation due to the negative scattering length of non-exchangeable H atoms. (**B**) An overlayed $2F_O$-F_C electron density map (blue) clearly displays the density of the Glutamic Acid. (**C**) Sulfur atom in Methionine is poorly visible in $2F_O$-F_C neutron SLD maps (purple). (**D**) An overlayed electron density map clearly displays the density of the Methionine. (**E**) Metal atoms, here Copper, are poorly visible in neutron $2F_O$-F_C SLD maps (purple). (**F**) An overlayed $2F_O$-F_C electron density map (blue) clearly displays the density of the coordinated Copper atom.

Table 1: Neutron scattering lengths and incoherent scattering values. Adapted from Sears, 1992[16].

Supplementary Figure 1: The IMAGINE Instrument at the High Flux Isotope Reactor. (**A**) The IMAGINE instrument in the cold neutron guide hall. (**B**) Sample in mounted in a quartz capillary attached with putty to the goniometer. The sample and detector table closes to position the crystal and the cylindrical image plate in the neutron beam. Modified with permission of the International Union of Crystallography[53]. Images provided with permission of Genevieve Martin, Oak Ridge National Laboratory.

Supplementary Figure 2: The MaNDi Instrument at the Spallation Neutron Source. (**A**) The MaNDi Anger camera detector array. Reproduced with permission the International Union of Crystallography[11]. (**B**) MaNDi moveable sample stage. (**C**) Sample mounted in quartz capillary mounted on the goniometer at MaNDi for room temperature data collection. Images provided with permission of Genevieve Martin, Oak Ridge National Laboratory.

Supplementary Figure 3: Structure of the lytic polysaccharide monooxygenase *Nc*LPMO9D. The *Nc*LPMO9D copper-active site is located on a flat polysaccharide binding surface. The copper is coordinated by two histidine residues in a classical “histidine brace” as well as an axial tyrosine residue.

Supplementary Figure 4: Crystal with sufficient volume in sitting drop crystallization tray. (**A**) Large crystals are grown in sitting drops set up in 9-well siliconized glass plates. (**B** and **C**) Crystals are measured to identify those with volume > 0.1 mm^3.

Supplementary Figure 5: pH meter set up for deuterated buffer readings. The pH electrode is soaked in D_2O prior to use. NaOD and DCl are used to adjust the pH of deuterated buffers.

Supplementary Figure 6: MaNDi sample mounting guidelines. Maximum dimensions of the quartz capillary and sample position for room temperature data collection.
Reproduced from: https://neutrons.ornl.gov/mandi/sample-environment

Supplementary Figure 7: Removal of excess buffer. (**A**) Excess buffer is aspirated from the quartz capillary with microcapillary tips. (**B**) The remaining buffer is removed with a thin paper wick to completely dry the capillary.

Supplementary Figure 8: The data acquisition GUI. Input window of the "Experiment Parameters" for data collection.

Supplementary Figure 9: The Optic GUI. Selection of the quasi-Laue range for data collection and monitoring of the neutron count rate.

Supplementary Figure 10: Data collection in data acquisition GUI. The exposure time, number of frames and angles for data collection are specified in the "Collect" tab. Data collection is then initiated using "Start Scan".

Supplementary Figure 11: Diffracted neutrons detected and displayed. At the end of the exposure time**,** the neutron sensitive image plate detector is read out and the diffraction pattern is displayed in the data acquisition GUI.

Supplementary Figure 12: Data processing following neutron diffraction. Frames are indexed, integrated, wavelength normalized and scaled using Lauegen, Lscale and Scala to generate a merged reflection file following data collection.

Supplementary Figure 13: X-ray data collection. Home source X-ray generator set up with quartz capillary mounted crystal for room temperature data collection.

Supplementary Figure 14: Mounting guidelines for MaNDi cryo-data collection. Dimensions of CrystalCaps and pin height for cryo-data collection at MaNDi.
Reproduced from: https://neutrons.ornl.gov/mandi/sample-environment

Supplementary Figure 15: Flash freezing for cryo neutron diffraction data collection. (**A**) Setup for crystal soaking, harvesting with a microloop and freezing in liquid nitrogen using a cryo compatible container foam Dewar. The mounted crystal is transferred directly onto the beamline cryo goniometer using precooled cryo pin tongs**.** (**B**) The wax seal is melted for crystal removal. (**C**) The crystal is flushed to end of quartz capillary for harvesting. (**D**) The crystal is sequentially soaked in ascorbate soak buffer and then cryoprotectant followed by flash freezing in liquid nitrogen.

Supplementary Figure 16: Sample alignment interface. Crystal alignment in the neutron beam, represented by the blue cross, is done by point and click centering.

Supplementary Figure 17: The CSS GUI for data collection. The data collection strategy, including exposure doses and angles, are uploaded in the CSS GUI. As data collection proceeds the diffracted neutrons detected on the real-time detector will be displayed in the upper panel.

Supplementary Figure 18: Matching R-free flags. The R-free flags of the neutron data are matched with the R-free flags of X-ray data collected on the same or an identical crystal for joint refinement.

Supplementary Figure 19: Structure preparation and refinement. A) The Phenix ReadySet tool is used to add dual H/D occupancy at exchangeable sites. **B**) Both the neutron data and X-ray data are used for a joint refinement, while the initial input model was refined against the X-ray dataset collected on the same crystal or an identical crystal.

Supplementary Figure 20: Configuration of refinement settings. The refinement model as well as the nuclear distances are configured for joint X-ray/neutron data refinement.

Supplementary Figure 21: Data selection for Coot model building. The phenix mtz file output containing X-ray and unfilled neutron data is opened in Coot to generate electron and neutron SLD maps for interactive model building.

Supplementary Figure 22: Interactive model building in Coot during a joint refinement. (**A**) A positive and negative F_O-F_C neutron SLD density peak (green and red, respectively) indicating that the water must be reoriented by rotation/translation. The $2F_O$-F_C neutron SLD map is displayed in purple and $2F_O$-F_C electron density map is displayed in blue. (**B**) Correctly positioned water. (**C**) A positive F_O-F_C neutron SLD map peak (green) indicate that threonine must be rotated to match difference density peak by editing chi angles. (**D**) Correctly oriented threonine.

Supplementary Figure 23: Structure preparation for neutron-only data refinement. The starting coordinate file is prepared for refinement by water atom removal in PDBTools and by addition of dual H/D occupancy at exchangeable sites.

Supplementary Figure 24: Neutron data-only refinement. (**A**) Neutron data is uploaded as well as the prepared starting model. (**B**) The settings for neutron data refinement use the neutron scattering table**.**

Supplementary Figure 25: Data selection for Coot model building. The unfilled neutron data are opened in Coot for interactive model building.

Supplementary Figure 26: Real space refinement in Coot for deuterated residues. (**A**) Positive and negative F_O-F_C neutron SLD density peaks (green and red, respectively) indicating that an arginine residue must be moved to fit the F_O-F_C density peak. The $2F_O$-F_C neutron SLD map is displayed in purple and $2F_O$-F_C electron density map is displayed in blue. (**B**) Utilizing Real Space Refine results in “exploding” D atoms due to missing Coot geometry restraints libraries. (**C**) The D atoms do not move with the rest of the residue atoms. (**D**) The D atom positions can be manually fixed using a text editor.

Supplementary Figure 27: Addition of water molecules. (**A**) Water molecules can be manually added to the positive F_O-F_C neutron SLD map density peaks (green). The inserted water molecules will initially be represented by an O atom in Coot. (**B**) Phenix ReadySet is used to add D atoms to the O atoms for water molecules. (**C**) The deuterated water molecule is successfully added.

Supplementary Figure 28: Refinement statistics. Final data refinement statistics following joint X-ray/neutron refinement.

Supplementary Figure 29: Refinement statistics. Final data refinement statistics following neutron data-only refinement.

DISCUSSION:

Neutron protein crystallography is a highly sensitive technique to probe protonation states and water molecule orientation in proteins. This information sheds light on protein catalytic mechanisms since changes in protonation and hydrogen bonding interactions are often central to enzyme chemistry[10]. Neutron protein crystallography, albeit an informative technique, has a number of factors that should be taken into consideration before planning to conduct a neutron diffraction experiment, namely:

1. The requirement for large protein crystals for data collection.
2. The scattering properties of hydrogen and other elements, such as metal ions.
3. Limitations in the structure refinement and model building software when working with deuterated samples.

Neutron protein crystallography is a flux limited technique. In contrast to X-ray diffraction datasets, neutron diffraction data statistics possess a lower completeness, redundancy and signal-to-noise ratios due to the inherent limitations (flux limited, quasi-Laue, longer wavelengths) of the technique. Data collection of a single frame is typically 12 – 18 hours. Success of an experiment is highly dependent on sample size and quality with crystals of 0.1 mm^3 often being the minimum requirement[3]. Neutron diffraction requires production of large amounts of protein to set up crystallization drops ranging from 10 to 800 μL. The minimum volume for growing sufficiently large crystals can be estimated using a Volume Calculator given the crystal and sample parameters (https://neutrons.ornl.gov/imagine). Growth of large crystals has most prevalently been accomplished by vapor diffusion[3]. Hanging drop crystallization permits growth of crystals in large drops ranging from 10-25 μL, while larger drops ranging up to ~ 50 μL can be set up using commercially available sitting drop equipment[14, 54]. Siliconized nine-well glass plates can be used to set up very large drops, with volume up to 800 μL. These glass plates are placed in “sandwich boxes” commercially available from Hampton Research. Further crystallization techniques include batch crystallization, in which the limit of the drop size is dictated by the vessel. Batch crystallization experiment set up can range from microliters to milliliters[55]. Crystallization can also be performed using the dialysis technique in which the protein is equilibrated with the precipitant *via* a dialysis membrane or by counter-diffusion along a precipitant concentration gradient or through a porous plug such as agarose[56, 57]. Seeding offers another alternative to obtain crystals of the desired volume. Micro- and macroseeding have been successfully employed for large crystal growth, including large crystal of *Nc*LPMO9D[45]. Some knowledge of the protein phase diagram, including the influence of temperature on solubility, aid in large crystal growth.

When planning a neutron diffraction experiment, optimization of the protein preparation to maximize signal-to-noise ratio during diffraction data collection is essential[7]. To circumvent density cancellation and high incoherent scattering caused by H atoms, neutron SLD maps can be improved by exchanging H atoms for its isotope D, which possesses a positive coherent scattering length and low incoherent scattering length. To accomplish this vapor exchange of the hydrogenated protein crystal against deuterated crystallization buffer is performed. This ensures H/D exchange of solvent molecules and the labile, titratable H atoms[23]. Vapor exchange is performed by mounting the hydrogenated crystal mounted in a quartz capillary with deuterated crystallization buffer “plugs” and it represents an effective, gentle technique that is most often applied[14, 23, 35]. The exchange can take several weeks and preferably requires the deuterated buffer to be frequently changed to ensure maximum H/D exchange. H/D exchange can also be performed by directly soaking the crystal in deuterated buffer. To avoid placing the crystal under stress due to D_2O exposure, the soaking process should be performed gradually by incrementally increasing the D_2O:H_2O ratio[58]. In addition to this, crystallization of hydrogenated protein can also be performed in deuterated buffer for H/D at labile H sites [22, 59]. It should be noted, however, that D_2O-based buffer has an effect on protein solubility requiring further adjustment of the known H_2O-based conditions[3,59]. D_2O-based buffers have also been observed to lead to smaller crystals in some cases[59]. Full exchange of titratable and carbon-bound H atoms to D can be achieved by expressing proteins in deuterated media to generate a perdeuterated sample[20]. The resulting neutron SLD maps of the perdeuterated sample will be significantly improved, no longer displaying the density cancellation of the hydrogenated sample counterpart. This is beneficial when characterizing H/D bound at non-exchangeable sites in a protein or cofactor. However, expression of perdeuterated protein is both high in cost and low in yield[60]. The Oak Ridge National Laboratory (ORNL) Center for Structural Molecular Biology (CSMB) offers a deuteration facility for users seeking to generate a perdeuterated sample (https://www.ornl.gov/facility/csmb). Perdeuterated expression is typically performed in a bioreactor on the 1 L scale yielding ~50 mg of purified protein[61].

Following the collection of neutron diffraction data, refinement and interactive model building is performed. Refinement can be run using multiple software suites including *phenix.refine,* nCNS or SHELXL[28,31–33]. The Phenix suite is the most commonly utilized software for refinement of neutron diffraction data in conjunction with Coot which is used to manually build the model from the neutron SLD maps[34]. Although both Phenix and Coot allow for the processing of neutron diffraction data, they may lack certain features necessary to process the idiosyncrasies associated with neutron data and deuterated samples. For example, Coot does not contain geometry optimization for deuterated residues, which can lead to complications during model building since the “Real Space Refine” feature results in “exploding” residues (**Supplementary Figure 26**)[62]. This can be resolved by generating restraint files for all the deuterated residues. However, this is an intensive process and such libraries are not currently publicly available. When performing refinements in Phenix, exchangeable H/D sites will initially be set to 0.50 occupancy for H and D. As refinements are performed, the occupancy of H and D will be refined according to the neutron SLD maps. During interactive model building, difference density F_o-F_c maps are very informative in assessing H/D occupancies. Maps can be used to determine which sites possess high D occupancy, which is particularly informative at the active site where protonation states are catalytically relevant[63]. Ambiguous situations do arise, however, when the H:D occupancy is close to 0.70:0.30 which results in complete signal cancellation in neutron SLD maps[64]. It should also be taken into account that neutron diffraction data usually has a completeness of ~80%, which is lower than the routinely observed ≥ 98% for X-ray diffraction data. When refining neutron diffraction data in Phenix, the missing observed amplitudes (F_o) are therefore calculated from the model to complete the reflection list, thus introducing model bias. To account for this potential bias "no_fill" maps should be examined during interactive model building as opposed to "fill" maps.

Users can choose to perform a joint X-ray/neutron data refinement of their structure, or a neutron-data only refinement. Visualizing neutron SLD maps, particularly at lower resolution, may initially be disconcerting especially for a hydrogenated protein in which H is still present at non-exchangeable sites despite H/D vapor exchange. This results in neutron density map cancellations, giving the impression of discontinuous maps[65,66]. Collecting a corresponding X-ray dataset advantageously complements these cancellations in a joint refinement (**Figure 13A** and **Figure 13B**). A joint-refinement strategy typically involves refining the protein backbone coordinates against the X-ray data, while the neutron diffraction data is used to refine the position and occupancy of the H/D atoms at exchangeable sites[28]. Since introduction of joint H/D occupancy at exchangeable sites increases the number of parameters being refined, a joint refinement with X-ray data also increases the data-to-parameter ratio. A joint refinement requires a corresponding X-ray dataset to be collected at the same temperature on the same crystal or a crystal grown under the same conditions. For neutron diffraction data collected at room temperature (300K), the corresponding X-ray dataset should be collected at room temperature using a low-dose data collection strategy to limit radiation damage. Perdeuterated samples, in contrast, provide improved and continuous neutron SLD maps since they do not possess the same magnitude of H/D signal cancellation. However, the neutron scattering length of certain elements including metals and sulfur make them poorly visible in neutron SLD maps, even if the protein has been perdeuterated (**Figure 13C-F**)[18]. If a metal needs to be characterized, it is best to utilize X-ray diffraction in a joint refinement or apply spectroscopic techniques to complement diffraction experiments. Neutron-only data refinements are often performed when the neutron dataset has high resolution or if a perdeuterated protein was used. In addition, neutron-only data refinement is particularly useful if a protein highly sensitive to radiation damage is being studied, since an X-ray derived structure may possess radiation-induced artefacts. If a neutron-data-only refinement is to be performed, it must be ascertained whether the corresponding neutron dataset has sufficient completeness and resolution.

ORNL offers two facilities for collection of neutron diffraction data: the IMAGINE beamline at the HFIR as well as the MaNDi beamline at the SNS[36, 67]. While both instruments provide effective means for collecting a neutron diffraction dataset employing similar principles, each instrument has unique specifications that should be taken into account when applying for beam time. IMAGINE collects quasi-Laue data and is optimized for room temperature data collection on crystals with unit cells up to ~100 Å. MaNDi can be used for the collection of room temperature and cryo-temperature data employing TOF-Laue collection on crystals with unit cells up to ~ 300 Å. Prior to collecting a complete dataset, a test is performed on the crystal to evaluate the quality of the obtained diffraction pattern in which the crystal is exposed to the neutron beam for a single frame. If the crystal is of sufficient quality, a full neutron diffraction dataset will be collected, indexed, integrated, scaled and merged in a process analogous to X-ray data processing. IMAGINE makes use of Lauegen and Lscale and MaNDi utilizes the Mantid package and employs three-dimensional profile fitting[48,50,51,68–70]. Scientists who become users at either of these facilities will be provided with a dataset in MTZ or HKL format for further analysis.

Neutron protein diffraction is a non-destructive, highly sensitive technique for probing the protonation state and hydrogen bond interactions of biological macromolecules. It is particularly useful for photo-sensitive proteins and metalloproteins. Several considerations regarding the technique as well as the processing of the data must be taken into consideration before conducting an experiment, however the outcome yields results which may give valuable insight into the catalytic mechanism of the protein of interest. Neutron protein crystallography complements computational, structural, biochemical and spectroscopic studies, making it a valuable tool in the biologist's toolbox of techniques used to characterize biological macromolecules.

ACKNOWLEDGEMENTS:

Protein expression, purification and crystallization experiments were conducted at the Center for Structural Molecular Biology (CSMB), a U.S. Department of Energy Biological and Environmental Research User Facility at Oak Ridge National Laboratory. Neutron diffraction data was collected at BL-11B MaNDi at the Spallation Neutron Source (SNS) at ORNL which is sponsored by the Scientific User Facilities Division, Office of Basic Energy Sciences, U.S. Department of Energy. The authors thank Brendan Sullivan for assistance with data reduction. X-ray diffraction data was collected at the Molecular Education, Technology, and Research Innovation Center (METRIC) facilities at North Carolina State University, which is supported by the State of North Carolina. GCS acknowledges support in part from the National Research Foundation (NRF), South Africa and the Graduate Opportunities (GO!) program at ORNL. FM acknowledges support from USDA NIFA Hatch 211001.

DISCLOSURES:

The authors have nothing to disclose.

REFERENCES:

1. Neumann, P., Tittmann, K. Marvels of enzyme catalysis at true atomic resolution: distortions, bond elongations, hidden flips, protonation states and atom identities. *Current Opinion in Structural Biology*. **29**, 122–133 (2014).
2. Pynn, R. Neutron Scattering—A Non-destructive Microscope for Seeing Inside Matter. *Neutron Applications in Earth, Energy and Environmental Sciences*. 15–36 (2009).
3. O'Dell, W.B., Bodenheimer, A.M., Meilleur, F. Neutron protein crystallography: A complementary tool for locating hydrogens in proteins. *Archives of Biochemistry and Biophysics*. **602**, 48–60 (2016).
4. Niimura, N., Podjarny, A. *Neutron Protein Crystallography: Hydrogen, Protons, and Hydration in Bio-macromolecules*. Oxford University Press. Oxford, UK. (2011).
5. Blakeley, M.P.P. Neutron macromolecular crystallography. *Crystallography Reviews*. **15**

(3), 157–218 (2009).

6. Blakeley, M.P., Cianci, M., Helliwell, J.R., Rizkallah, P.J. Synchrotron and neutron techniques in biological crystallography. *Chemical Society Reviews*. **33** (8), 548–557 (2004).
7. Ashkar, R. et al. *Neutron scattering in the biological sciences: progress and prospects*. *Acta Crystallographica Section D: Structural Biology*. **74** (12) (2018).
8. Teixeira, S.C.M. et al. New sources and instrumentation for neutrons in biology. *Chemical Physics*. **345** (2–3), 133–151 (2008).
9. Furrer, A., Mesot, J., Strässle, T. *Neutron Scattering in Condensed Matter Physics*. World Scientific Publishing Company. Singapore (2009).
10. Meilleur, F., Coates, L., Cuneo, M.J., Kovalevsky, A., Myles, D.A.A. The neutron macromolecular crystallography instruments at Oak Ridge national laboratory: Advances, challenges, and opportunities. *Crystals*. **8** (10), 1–10 (2018).
11. Coates, L. et al. The Macromolecular Neutron Diffractometer MaNDi at the Spallation Neutron Source. *Journal of Applied Crystallography*. **48**, 1302–1306 (2015).
12. Coates, L., Stoica, A.D., Hoffmann, C., Richards, J., Cooper, R. The macromolecular neutron diffractometer (MaNDi) at the Spallation Neutron Source, Oak Ridge: enhanced optics design, high-resolution neutron detectors and simulated diffraction. *Journal of Applied Crystallography*. **43** (3), 570–577 (2010).
13. Koetzle, T.F., Piccoli, P.M.B., Schultz, A.J. Single-crystal neutron diffraction studies of hydrogen-bonded systems: Two recent examples from IPNS. *Nuclear Instruments and Methods in Physics Research, Section A: Accelerators, Spectrometers, Detectors and Associated Equipment*. **600** (1), 260–262 (2009).
14. Ng, J.D. et al. Large-volume protein crystal growth for neutron macromolecular crystallography. *Acta Crystallographica Section F:Structural Biology Communications*. **71**, 358–370 (2015).
15. Blakeley, M.P., Langan, P., Niimura, N., Podjarny, A. Neutron crystallography: opportunities, challenges, and limitations. *Current Opinion in Structural Biology*. **18** (5), 593–600 (2008).
16. Sears, V.F. Neutron scattering lengths and cross sections. *Neutron News*. **3** (3), 26–37 (1992).
17. Weik, M., Patzelt, H., Zaccai, G., Oesterhelt, D. Localization of glycolipids in membranes by in vivo labeling and neutron diffraction. *Molecular Cell*. **1** (3), 411–419 (1998).
18. Helliwell, J.R. *Fundamentals of neutron crystallography in structural biology*. *Methods in Enzymology*. **634** Elsevier Inc. (2020).
19. Niimura, N., Bau, R. Neutron protein crystallography: Beyond the folding structure of biological macromolecules. *Acta Crystallographica Section A: Foundations of Crystallography*. **64** (1), 12–22 (2008).
20. Hazemann, I. et al. High-resolution neutron protein crystallography with radically small crystal volumes: Application of perdeuteration to human aldose reductase. *Acta Crystallographica Section D: Biological Crystallography*. **61** (10), 1413–1417 (2005).
21. Niimura, N., Chatake, T., Ostermann, A., Kurihara, K., Tanaka, I. High resolution neutron protein crystallography. Hydrogen and hydration in proteins. *Zeitschrift für Kristallographie - Crystalline Materials*. **218** (2) (2003).
22. Meilleur, F., Contzen, J., Myles, D.A.A., Jung, C. Structural stability and dynamics of

hydrogenated and perdeuterated cytochrome P450cam (CYP101). *Biochemistry*. **43** (27), 8744–8753 (2004).

23. Bennett, B.C., Gardberg, A.S., Blair, M.D., Dealwis, C.G. On the determinants of amide backbone exchange in proteins: A neutron crystallographic comparative study. *Acta Crystallographica Section D: Biological Crystallography*. **64** (7), 764–783 (2008).
24. Meilleur, F., Kovalevsky, A., Myles, D.A.A. *IMAGINE: The neutron protein crystallography beamline at the high flux isotope reactor*. *Methods in Enzymology*. **634**, Elsevier Inc. (2020).
25. Wang, X.P. et al. A suite-level review of the neutron single-crystal diffraction instruments at Oak Ridge National Laboratory. *Review of Scientific Instruments*. **89** (9), 092802 (2018).
26. Wlodawer, A., Hendrickson, W.A. A procedure for joint refinement of macromolecular structures with X-ray and neutron diffraction data from single crystals. *Acta Crystallographica Section A*. **38** (2), 239–247 (1982).
27. Halle, B. Biomolecular cryocrystallography: Structural changes during flash-cooling. *Proceedings of the National Academy of Sciences of the United States of America*. **101** (14), 4793–4798 (2004).
28. Adams, P.D., Mustyakimov, M., Afonine, P. V., Langan, P. Generalized X-ray and neutron crystallographic analysis: More accurate and complete structures for biological macromolecules. *Acta Crystallographica Section D: Biological Crystallography*. **65** (6), 567–573 (2009).
29. Berman, H.M. et al. The Protein Data Bank. *Acta Crystallographica Section D Biological Crystallography*. **58** (6), 899–907 (2002).
30. Liebschner, D., Afonine, P. V., Moriarty, N.W., Langan, P., Adams, P.D. Evaluation of models determined by neutron diffraction and proposed improvements to their validation and deposition. *Acta Crystallographica Section D: Structural Biology*. **74**, 800–813 (2018).
31. Afonine, P. V., Mustyakimov, M., Grosse-Kunstleve, R.W., Moriarty, N.W., Langan, P., Adams, P.D. Joint X-ray and neutron refinement with phenix.refine. *Acta Crystallographica Section D: Biological Crystallography*. **66** (11), 1153–1163 (2010).
32. Brünger, A.T. et al. Crystallography & NMR system: A new software suite for macromolecular structure determination. *Acta Crystallographica Section D: Biological Crystallography*. **54** (5), 905–921 (1998).
33. Gruene, T., Hahn, H.W., Luebben, A. V., Meilleur, F., Sheldrick, G.M. Refinement of macromolecular structures against neutron data with SHELXL2013. *Journal of Applied Crystallography*. **47** (1), 462–466 (2014).
34. Emsley, P., Lohkamp, B., Scott, W.G., Cowtan, K. Features and development of Coot. *Acta Crystallographica Section D Biological Crystallography*. **66** (4), 486–501 (2010).
35. Lakey, J.H. Neutrons for biologists: A beginner's guide, or why you should consider using neutrons. *Journal of the Royal Society Interface*. **6** (SUPPL. 5) (2009).
36. Schröder, G.C., O'Dell, W.B., Myles, D.A.A., Kovalevsky, A., Meilleur, F. IMAGINE: Neutrons reveal enzyme chemistry. *Acta Crystallographica Section D: Structural Biology*. **74**, 778–786 (2018).
37. Halsted, T.P. et al. Catalytically important damage-free structures of a copper nitrite reductase obtained by femtosecond X-ray laser and room-temperature neutron crystallography. *IUCrJ*. **6**, 761–772 (2019).
38. Meier, K.K. et al. Oxygen Activation by Cu LPMOs in Recalcitrant Carbohydrate

Polysaccharide Conversion to Monomer Sugars. *Chemical Reviews*. **118** (5), 2593–2635 (2018).

39. Beeson, W.T., Vu, V. V., Span, E.A., Phillips, C.M., Marletta, M.A. Cellulose Degradation by Polysaccharide Monooxygenases. *Annual Review of Biochemistry*. **84** (1), 923–946 (2015).
40. Walton, P.H., Davies, G.J. On the catalytic mechanisms of lytic polysaccharide monooxygenases. *Current Opinion in Chemical Biology*. **31**, 195–207 (2016).
41. Bertini, L. et al. Catalytic Mechanism of Fungal Lytic Polysaccharide Monooxygenases Investigated by First-Principles Calculations. *Inorganic Chemistry*. **57** (1), 86–97 (2018).
42. Hedegård, E.D., Ryde, U. Molecular mechanism of lytic polysaccharide monooxygenases. *Chemical Science*. **9** (15), 3866–3880 (2018).
43. Hangasky, J.A., Detomasi, T.C., Marletta, M.A. Glycosidic Bond Hydroxylation by Polysaccharide Monooxygenases. *Trends in Chemistry*. **1** (2), 198–209 (2019).
44. Bacik, J.P. et al. Neutron and Atomic Resolution X-ray Structures of a Lytic Polysaccharide Monooxygenase Reveal Copper-Mediated Dioxygen Binding and Evidence for N-Terminal Deprotonation. *Biochemistry*. **56** (20), 2529–2532 (2017).
45. O'Dell, W.B., Agarwal, P.K., Meilleur, F. Oxygen Activation at the Active Site of a Fungal Lytic Polysaccharide Monooxygenase. *Angewandte Chemie - International Edition*. **56** (3), 767–770 (2017).
46. O'Dell, W.B., Swartz, P.D., Weiss, K.L., Meilleur, F. Crystallization of a fungal lytic polysaccharide monooxygenase expressed from glycoengineered Pichia pastoris for X-ray and neutron diffraction. *Acta Crystallographica Section:F Structural Biology Communications*. **73** (2), 70–78 (2017).
47. Meilleur, F. et al. The IMAGINE instrument: First neutron protein structure and new capabilities for neutron macromolecular crystallography. *Acta Crystallographica Section D: Biological Crystallography*. **69** (10), 2157–2160 (2013).
48. Helliwell, J.R. et al. The recording and analysis of synchrotron X-radiation Laue diffraction photographs. *Journal of Applied Crystallography*. **22** (5), 483–497 (1989).
49. Nieh, Y.P. et al. Accurate and highly complete synchrotron protein crystal Laue diffraction data using the ESRF CCD and the Daresbury Laue software. *Journal of Synchrotron Radiation*. **6** (5), 995–1006 (1999).
50. Arzt, S., Campbell, J.W., Harding, M.M., Hao, Q., Helliwell, J.R. LSCALE - The new normalization, scaling and absorption correction program in the Daresbury Laue software suite. *Journal of Applied Crystallography*. **32** (3), 554–562 (1999).
51. Sullivan, B. et al. Improving the accuracy and resolution of neutron crystallographic data by three-dimensional profile fitting of Bragg peaks in reciprocal space. *Acta Crystallographica Section D: Structural Biology*. **74** (11), 1085–1095 (2018).
52. Sullivan, B. et al. BraggNet: integrating Bragg peaks using neural networks. *Journal of Applied Crystallography*. **52** (4), 854–863 (2019).
53. Schröder, G.C., O'Dell, W.B., Myles, D.A.A., Kovalevsky, A., Meilleur, F. IMAGINE: Neutrons reveal enzyme chemistry. *Acta Crystallographica Section D: Structural Biology*. **74** (2018).
54. Blum, M.M. et al. Preliminary time-of-flight neutron diffraction study on diisopropyl fluorophosphatase (DFPase) from Loligo vulgaris. *Acta Crystallographica Section F: Structural Biology and Crystallization Communications*. **63** (1), 42–45 (2007).
55. Tomanicek, S.J. et al. Neutron and X-ray crystal structures of a perdeuterated enzyme

inhibitor complex reveal the catalytic proton network of the Toho-1 β-lactamase for the acylation reaction. *Journal of Biological Chemistry*. **288** (7), 4715–4722 (2013).

56. Metcalfe, C. et al. The tuberculosis prodrug isoniazid bound to activating peroxidases. *Journal of Biological Chemistry*. **283** (10), 6193–6200 (2008).
57. Hughes, R.C. et al. Inorganic pyrophosphatase crystals from Thermococcus thioreducens for X-ray and neutron diffraction. *Acta Crystallographica Section F: Structural Biology and Crystallization Communications*. **68** (12), 1482–1487 (2012).
58. Bennett, B.C., Meilleur, F., Myles, D.A.A., Howell, E.E., Dealwis, C.G. Preliminary neutron diffraction studies of Escherichia coli dihydrofolate reductase bound to the anticancer drug methotrexate. *Acta Crystallographica Section D: Biological Crystallography*. **61** (5), 574–579 (2005).
59. Snell, E.H. et al. Optimizing crystal volume for neutron diffraction: D-xylose isomerase. *European Biophysics Journal*. **35** (7), 621–632 (2006).
60. Golden, E., Attwood, P. V., Duff, A.P., Meilleur, F., Vrielink, A. Production and characterization of recombinant perdeuterated cholesterol oxidase. *Analytical Biochemistry*. **485**, 102–108 (2015).
61. Munshi, P. et al. Rapid visualization of hydrogen positions in protein neutron crystallographic structures. *Acta Crystallographica Section D: Biological Crystallography*. **68** (1), 35–41 (2012).
62. Logan, D.T. *Interactive model building in neutron macromolecular crystallography*. *Methods in Enzymology*. **634**. Elsevier Inc. (2020).
63. Koruza, K., Lafumat, B., Végvári, Knecht, W., Fisher, S.Z. Deuteration of human carbonic anhydrase for neutron crystallography: Cell culture media, protein thermostability, and crystallization behavior. *Archives of Biochemistry and Biophysics*. **645** (March), 26–33 (2018).
64. Fisher, S.J. et al. Perdeuteration: Improved visualization of solvent structure in neutron macromolecular crystallography. *Acta Crystallographica Section D: Biological Crystallography*. **70** (12), 3266–32722014).
65. Chen, J.C.-H., Hanson, B.L., Fisher, S.Z., Langan, P., Kovalevsky, a. Y. Direct observation of hydrogen atom dynamics and interactions by ultrahigh resolution neutron protein crystallography. *Proceedings of the National Academy of Sciences*. **109** (38), 15301–15306 (2012).
66. Cuypers, M.G. et al. Near-atomic resolution neutron crystallography on perdeuterated Pyrococcus furiosus rubredoxin: Implication of hydronium ions and protonation state equilibria in redox changes. *Angewandte Chemie - International Edition*. **52** (3), 1022–1025 (2013).
67. Coates, L., Sullivan, B. *The macromolecular neutron diffractometer at the spallation neutron source*. *Methods in Enzymology*. **634**, . Elsevier Inc. (2020).
68. Ren, Z., Kingman, N.G., Borgstahl, G.E.O., Getzoff, E.D., Moffat, K. Quantitative Analysis of Time-Resolved Laue Diffraction Patterns. *Journal of Applied Crystallography*. **29** (3), 246–260 (1996).
69. Campbell, J.W., Hao, Q., Harding, M.M., Nguti, N.D., Wilkinson, C. LAUEGEN version 6.0 and INTLDM. *Journal of Applied Crystallography*. **31** (3), 496–502 (1998).
70. Arnold, O. et al. Mantid - Data analysis and visualization package for neutron scattering

and µ SR experiments. *Nuclear Instruments and Methods in Physics Research, Section A: Accelerators, Spectrometers, Detectors and Associated Equipment*. **764**, 156–166 (2014).

Figure 1

Click here to access/download;Figure;Figure1.eps

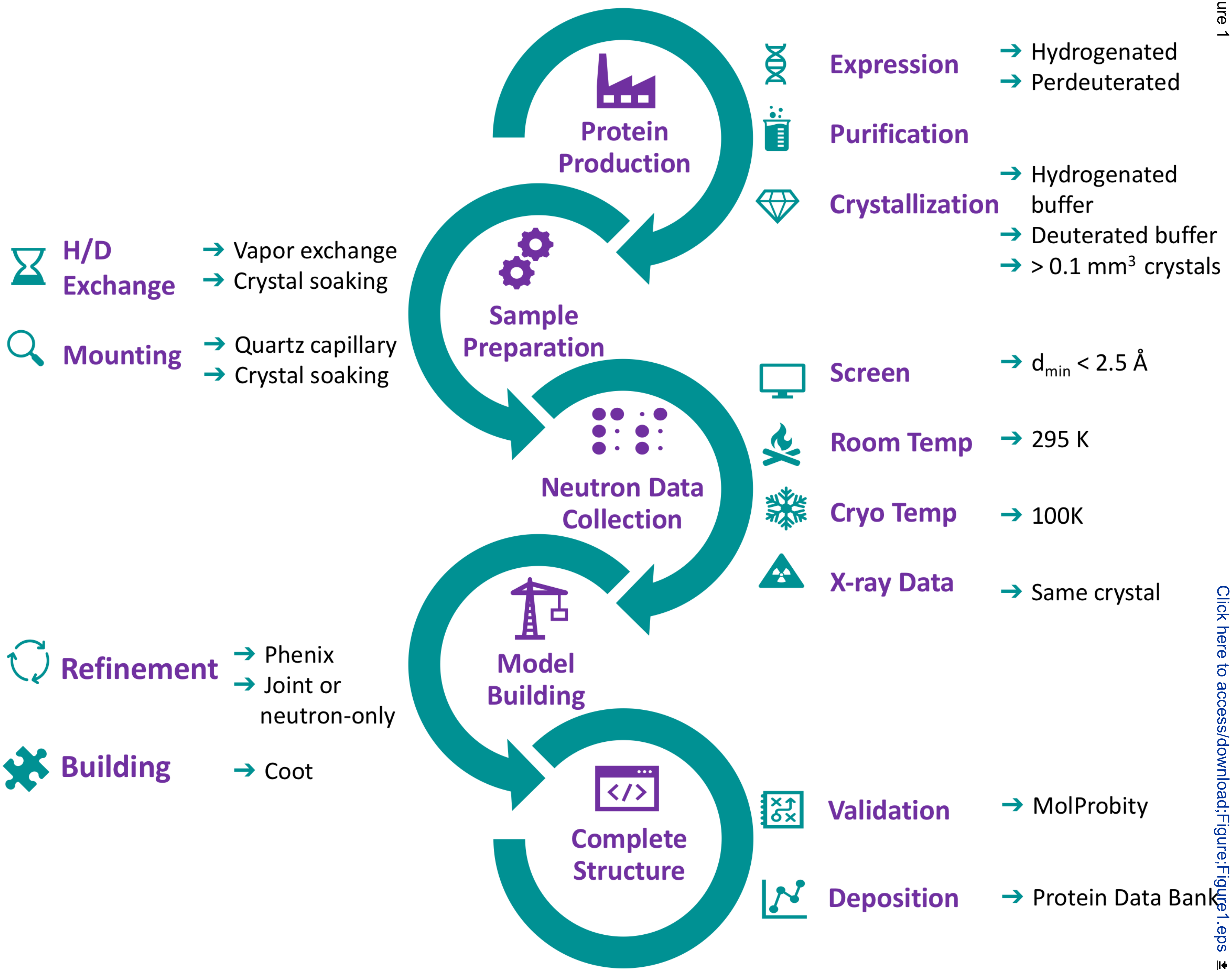
Protein Production
Sample Preparation
Neutron Data Collection
Model Building
Complete Structure
Expression → Hydrogenated → Perdeuterated
Purification
Crystallization → Hydrogenated buffer → Deuterated buffer → > 0.1 mm³ crystals
H/D Exchange → Vapor exchange → Crystal soaking
Mounting → Quartz capillary → Crystal soaking
Screen → dmin < 2.5 Å
Room Temp → 295 K
Cryo Temp → 100K
X-ray Data → Same crystal
Refinement → Phenix → Joint or neutron-only
Building → Coot
Validation → MolProbity
Deposition → Protein Data Bank

Figure 2

Click here to access/download;Figure;Figure2.eps

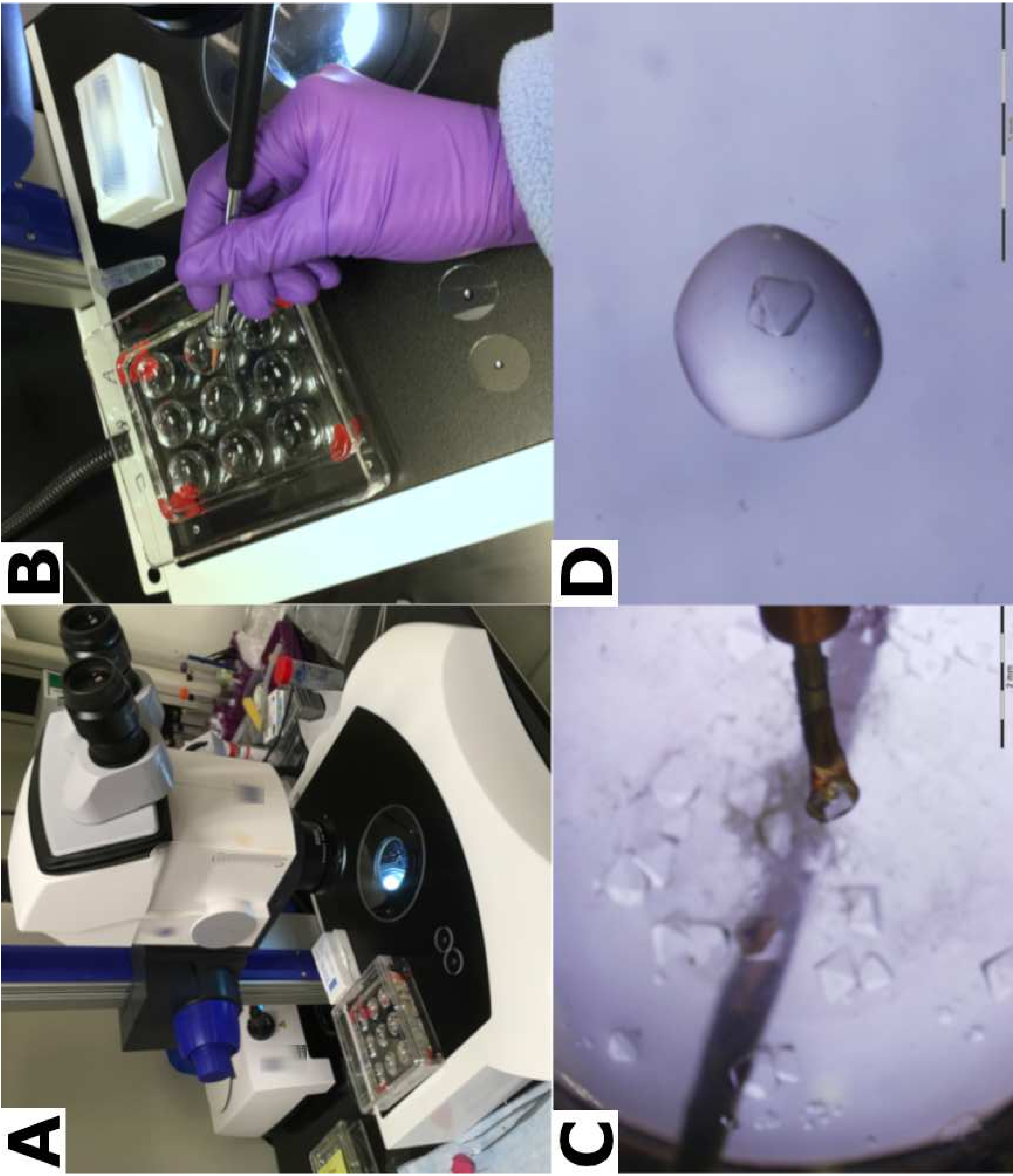

Figure 3

Click here to access/download;Figure;Figure3.eps

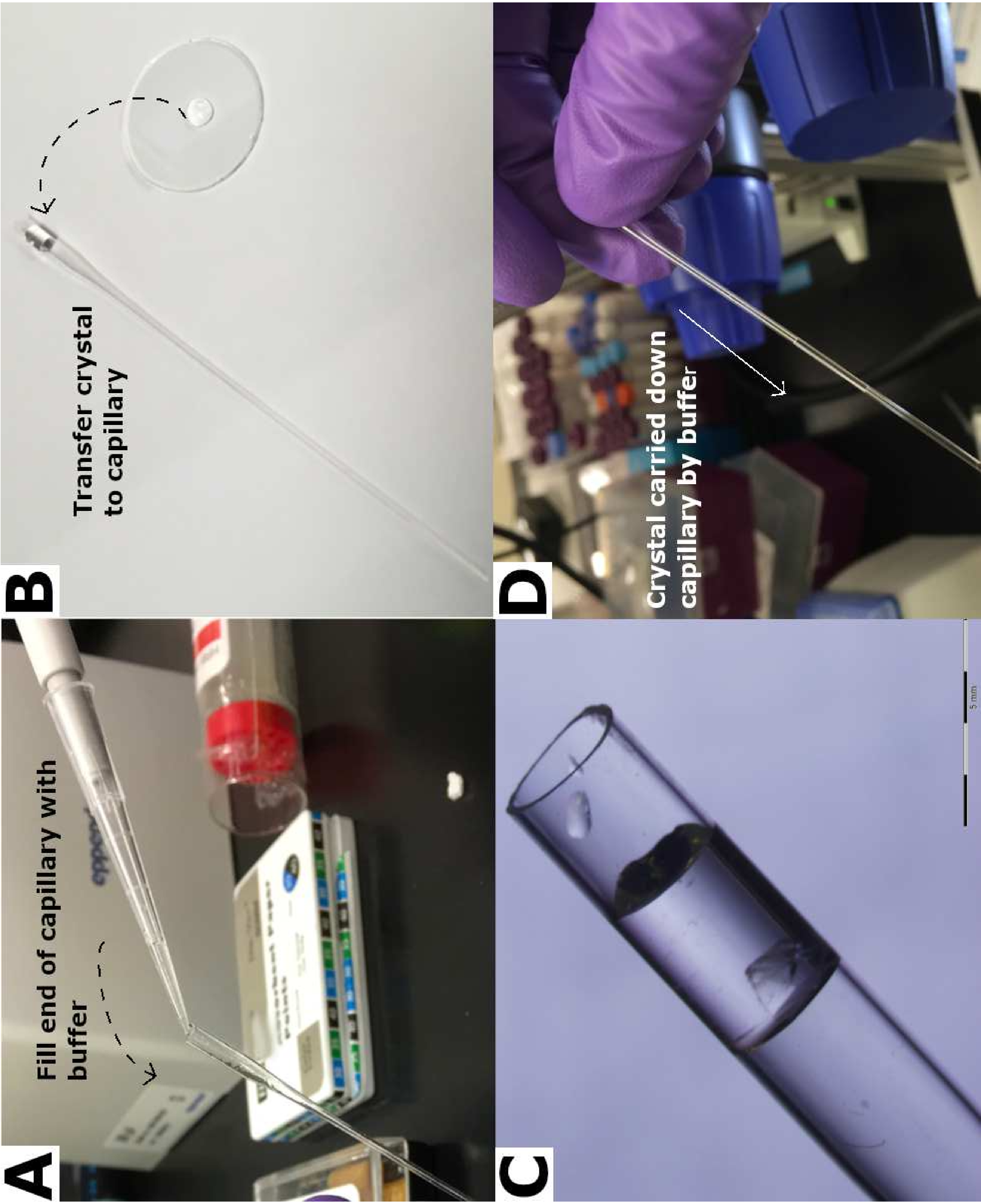
A
Fill end of capillary with buffer
B
Transfer crystal to capillary
C
5 mm
D
Crystal carried down capillary by buffer

Figure 4

Click here to access/download;Figure;Figure4.eps

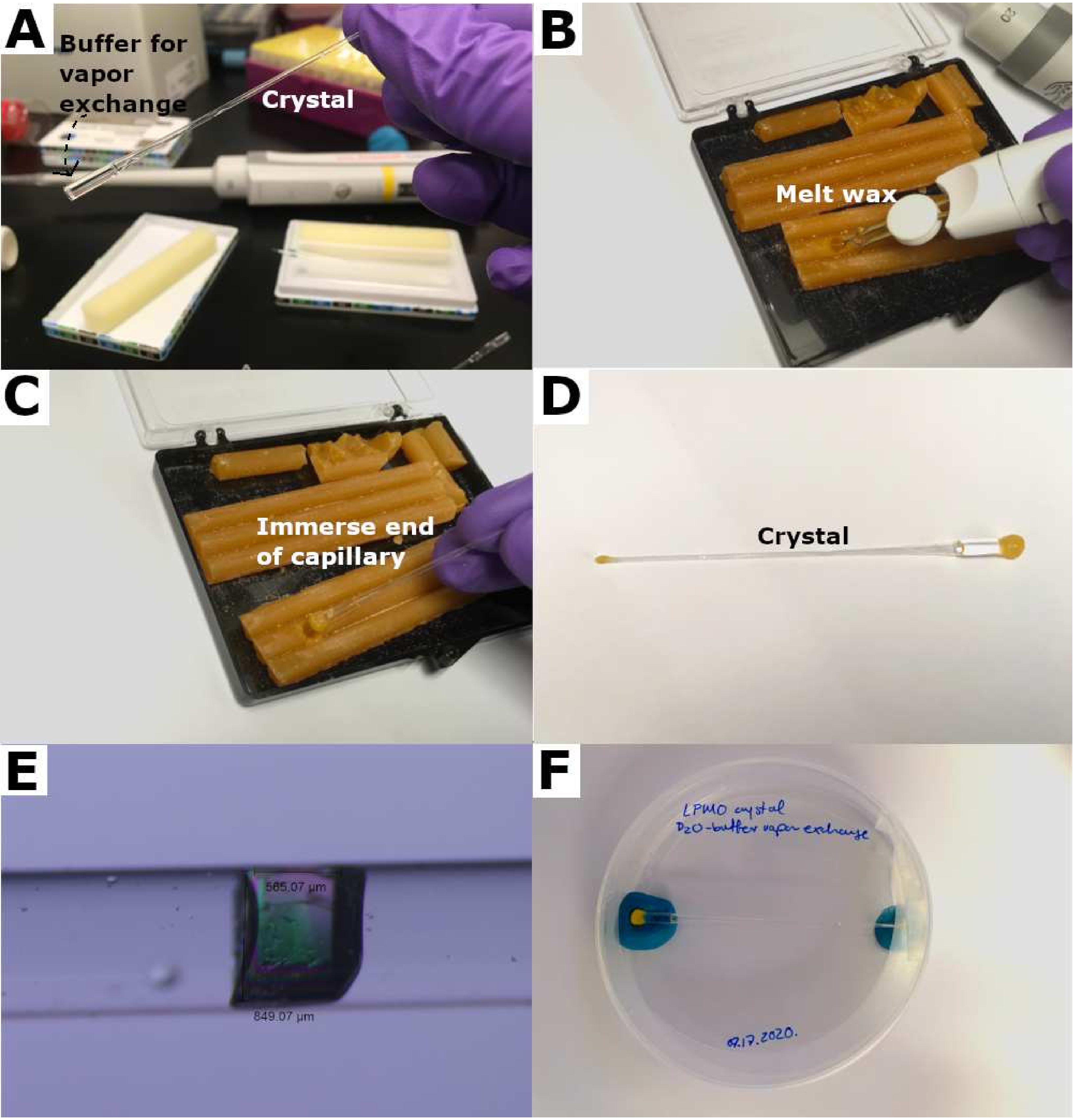
A
Buffer for vapor exchange
Crystal
B
Melt wax
C
Immerse end of capillary
D
Crystal
E
565.07 µm
849.07 µm
F
LPMO crystal
D2O-buffer vapor exchange
02.17.2020.

Figure 5

Click here to access/download;Figure;Figure5.eps

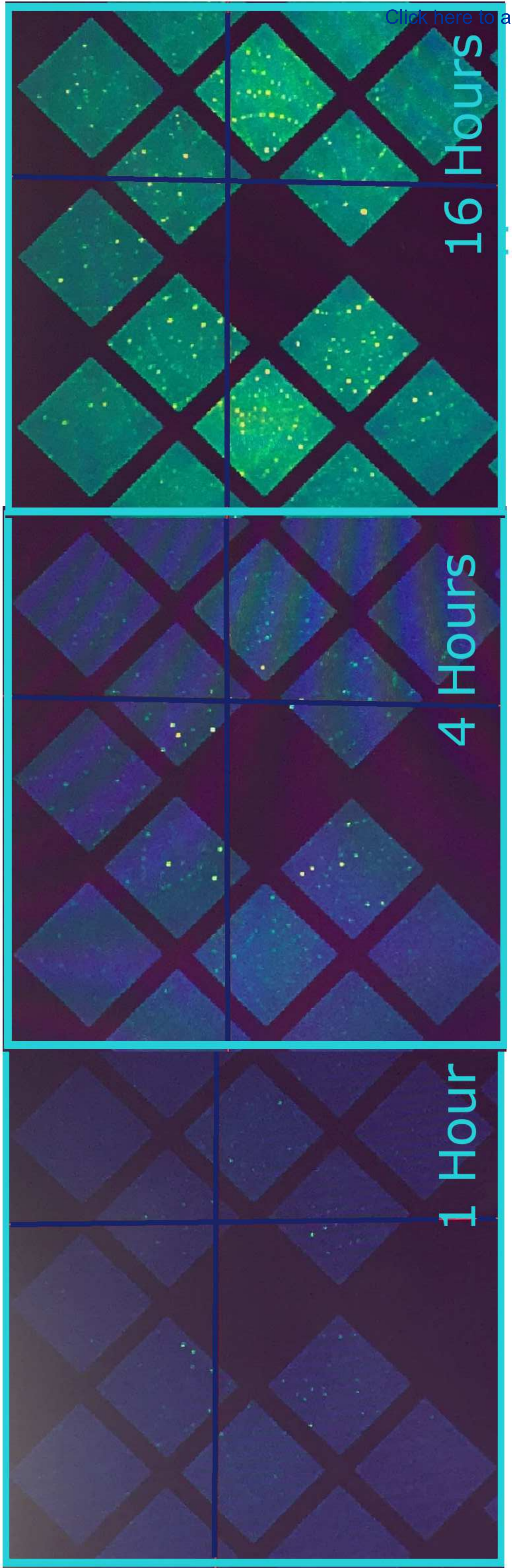
16 Hours
4 Hours
1 Hour

Click here to access/download;Figure;Figure6.eps

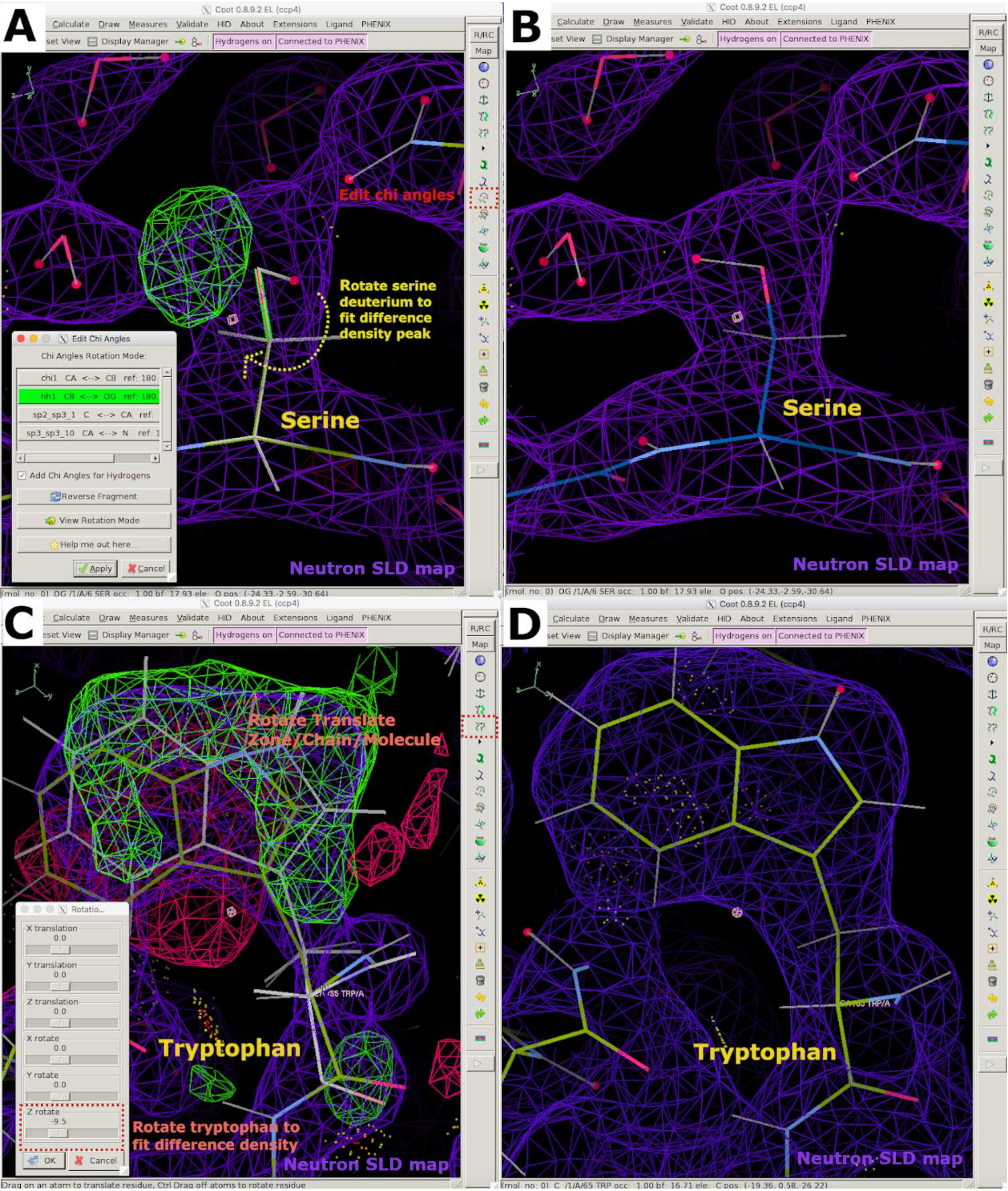
A
Coot 0.8.9.2 EL (ccp4)
Calculate Draw Measures Validate HID About Extensions Ligand PHENIX
set View Display Manager Hydrogens on Connected to PHENIX
R/RC
Map
Edit chi angles
Rotate serine deuterium to fit difference density peak
Serine
Neutron SLD map
Edit Chi Angles
Reverse Fragment
View Rotation Mode
Help me out here...
Apply
Cancel
B
Coot 0.8.9.2 EL (ccp4)
Serine
Neutron SLD map
C
Coot 0.8.9.2 EL (ccp4)
Rotate Translate Zone/Chain/Molecule
Tryptophan
Rotate tryptophan to fit difference density
Neutron SLD map
Rotatio...
OK
Cancel
/A/65 TRP/A
D
Coot 0.8.9.2 EL (ccp4)
Tryptophan
Neutron SLD map
CA/65 TRP/A

Chi Angles Rotation Mode:

chi1 CA <--> CB ref: 180
hh1 CB <--> OG ref: 180
sp2_sp3_1 C <--> CA ref:
sp3_sp3_10 CA <--> N ref: 1

☑ Add Chi Angles for Hydrogens

(mol. no: 0) OG /1/A/6 SER occ: 1.00 bf: 17.93 ele: O pos: (-24.33,-2.59,-30.64)

(mol. no: 0) OG /1/A/6 SER occ: 1.00 bf: 17.93 ele: O pos: (-24.33,-2.59,-30.64)

X translation 0.0
Y translation 0.0
Z translation 0.0
X rotate 0.0
Y rotate 0.0
Z rotate -9.5

Drag on an atom to translate residue, Ctrl Drag off atoms to rotate residue

(mol. no: 0) C /1/A/65 TRP occ: 1.00 bf: 16.71 ele: C pos: (-19.36, 0.58,-26.22)

Figure 7

Click here to access/download;Figure;Figure7.eps

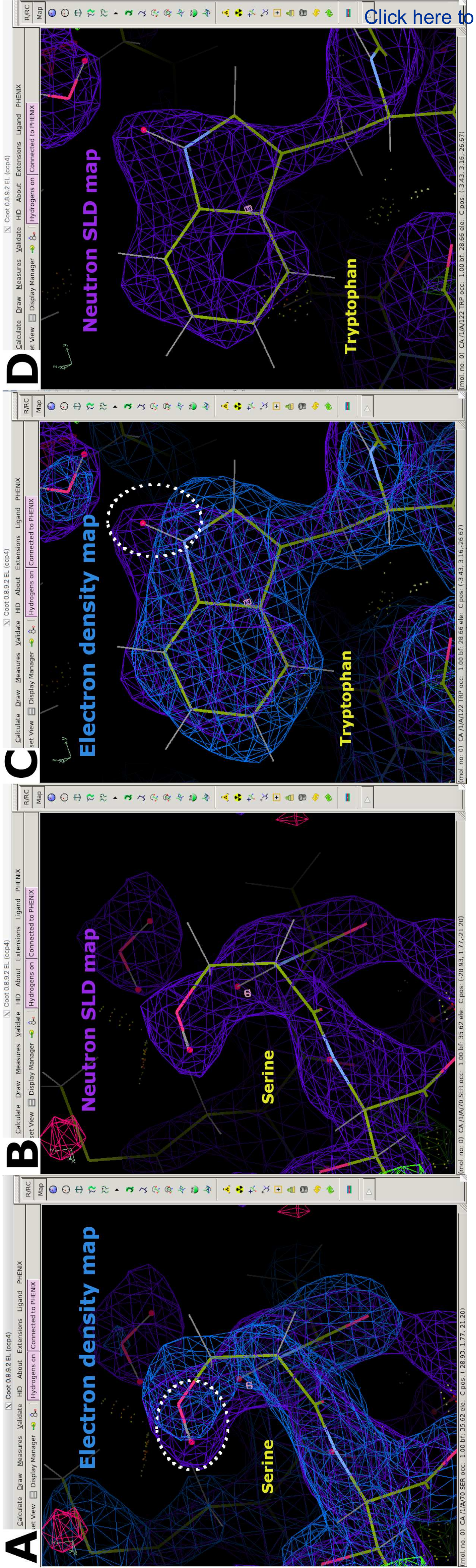
A
Electron density map
Serine
B
Neutron SLD map
Serine
C
Electron density map
Tryptophan
D
Neutron SLD map
Tryptophan
Coot 0.8.9.2 EL (ccp4)
Calculate Draw Measures Validate HID About Extensions Ligand PHENIX
Display Manager
Hydrogens on
Connected to PHENIX
R/RC
Map

(mol. no: 0) CA /1/A/70 SER occ: 1.00 bf: 35.62 ele: C pos: (-28.93, 1.77,-21.20)

(mol. no: 0) CA /1/A/122 TRP occ: 1.00 bf: 28.66 ele: C pos: (-3.43, 3.16,-26.67)

Figure 8

Click here to access/download;Figure;Figure8.eps

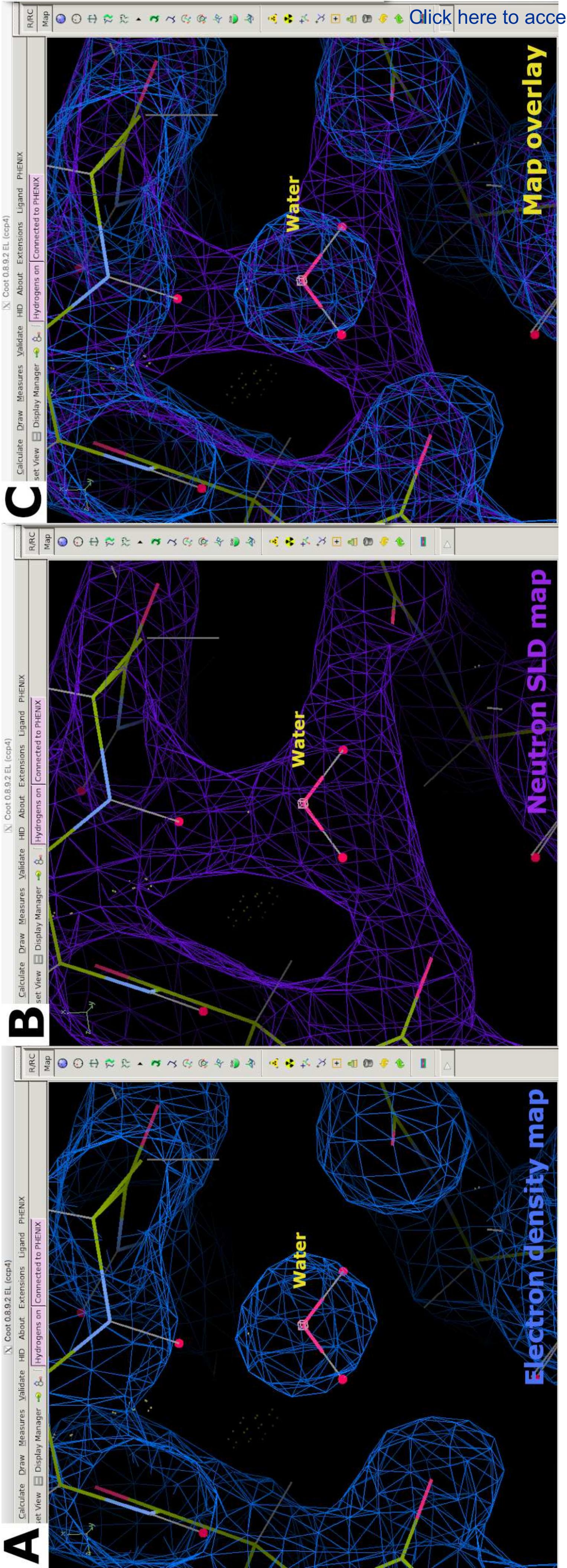
A
Electron density map
Water
B
Neutron SLD map
Water
C
Map overlay
Water
Coot 0.8.9.2 EL (ccp4)
Calculate Draw Measures Validate HID About Extensions Ligand PHENIX
set View Display Manager Hydrogens on Connected to PHENIX
R/RC
Map

Figure 9

Click here to access/download;Figure;Figure9.eps

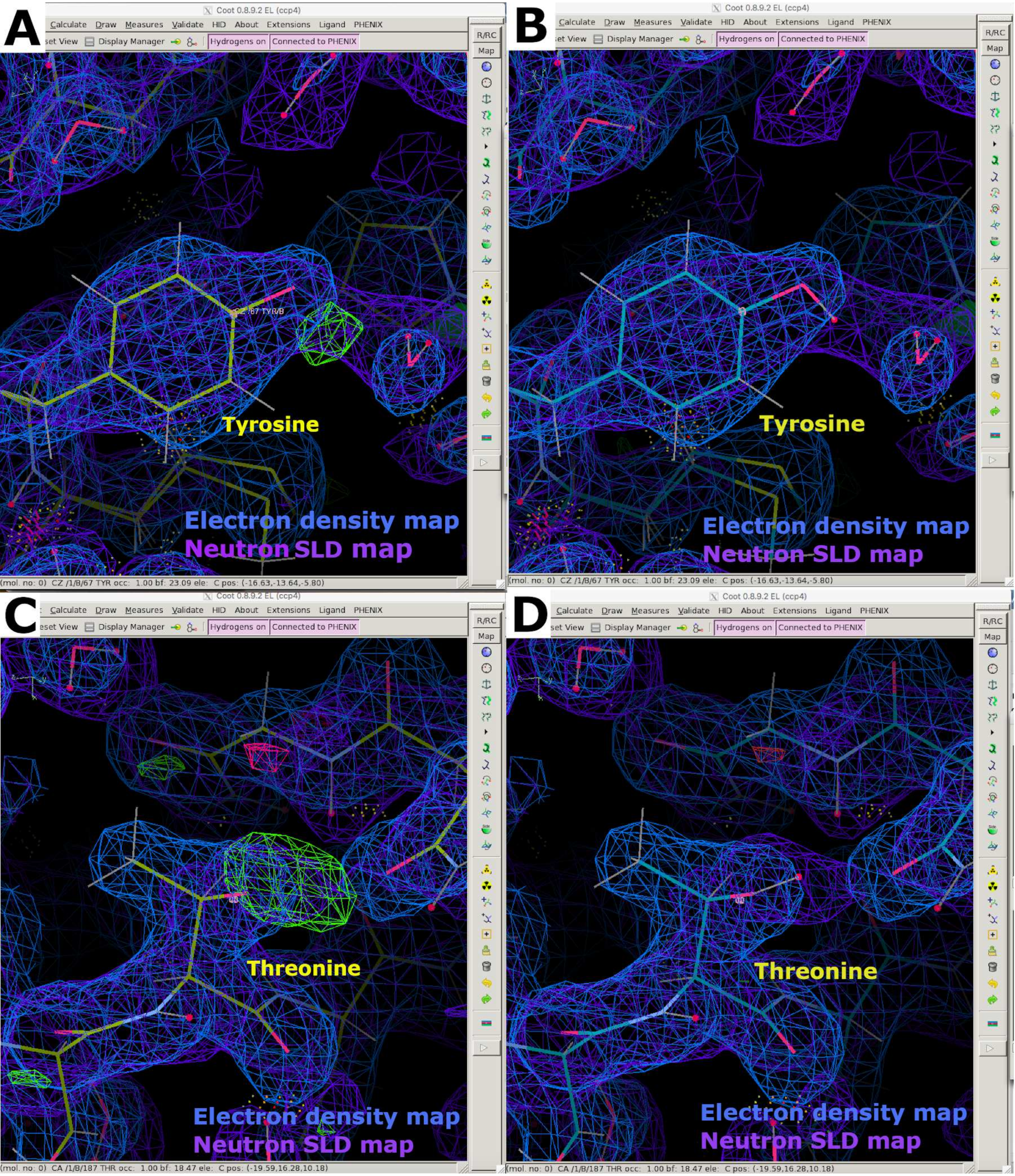
A
B
C
D
Coot 0.8.9.2 EL (ccp4)
Calculate Draw Measures Validate HID About Extensions Ligand PHENIX
set View
Display Manager
Hydrogens on
Connected to PHENIX
R/RC
Map
CZ /67 TYR/B
Tyrosine
Threonine
Electron density map
Neutron SLD map

```
(mol. no: 0)  CZ /1/B/67 TYR occ:  1.00 bf: 23.09 ele:  C pos: (-16.63,-13.64,-5.80)
```

```
(mol. no: 0)  CZ /1/B/67 TYR occ:  1.00 bf: 23.09 ele:  C pos: (-16.63,-13.64,-5.80)
```

```
(mol. no: 0)  CA /1/B/187 THR occ:  1.00 bf: 18.47 ele:  C pos: (-19.59,16.28,10.18)
```

```
(mol. no: 0)  CA /1/B/187 THR occ:  1.00 bf: 18.47 ele:  C pos: (-19.59,16.28,10.18)
```

Figure 10

Click here to access/download;Figure;Figure10.eps

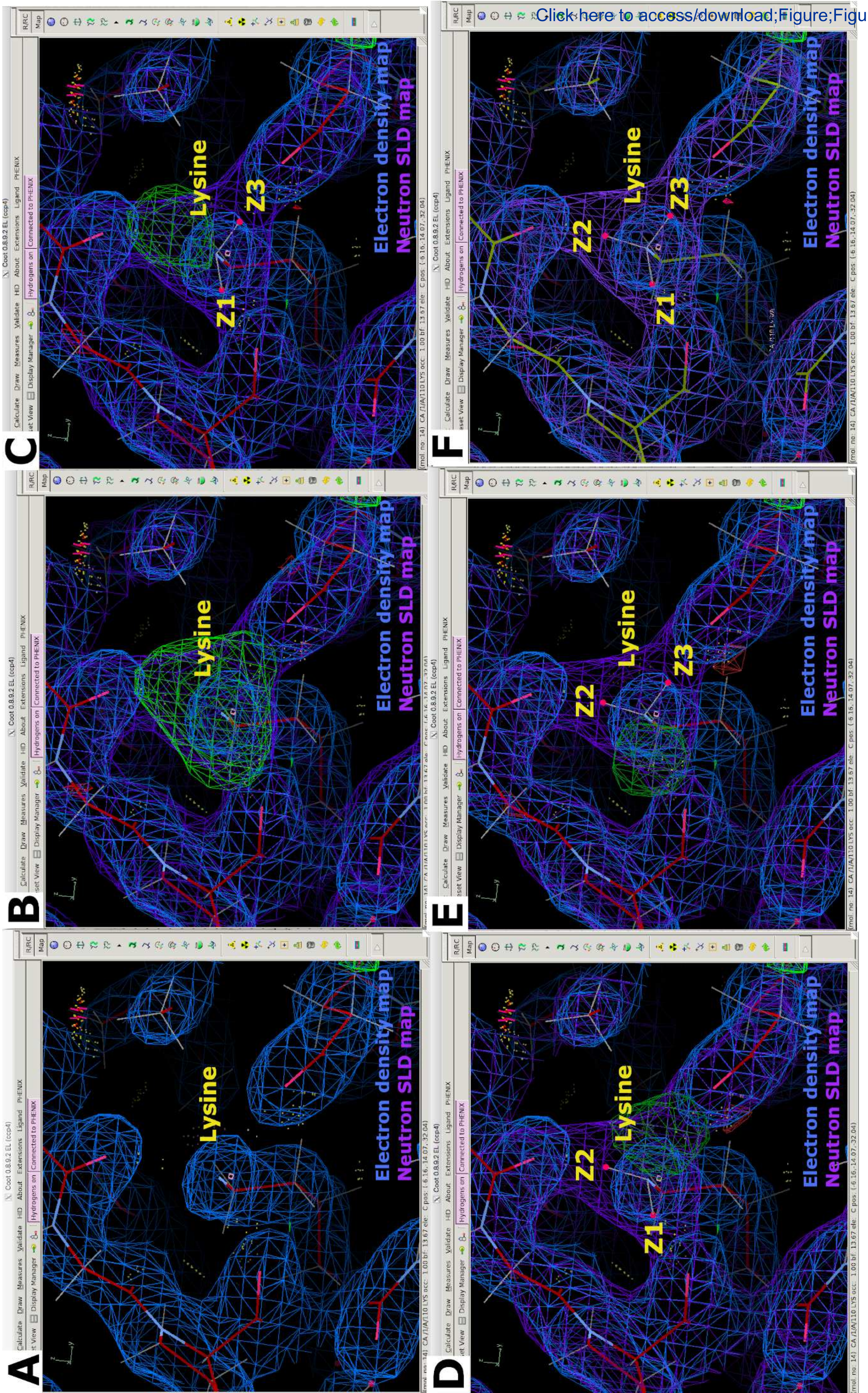
A
Lysine
Electron density map
Neutron SLD map
B
Lysine
Electron density map
Neutron SLD map
C
Z1
Z3
Lysine
Electron density map
Neutron SLD map
D
Z1
Z2
Lysine
Electron density map
Neutron SLD map
E
Z2
Z3
Lysine
Electron density map
Neutron SLD map
F
Z1
Z2
Z3
Lysine
Electron density map
Neutron SLD map
Coot 0.8.9.2 EL (ccp4)
Calculate Draw Measures Validate HID About Extensions Ligand PHENIX
Display Manager
Hydrogens on
Connected to PHENIX
R/RC
Map

Figure 11

Click here to access/download;Figure;Figure11.eps

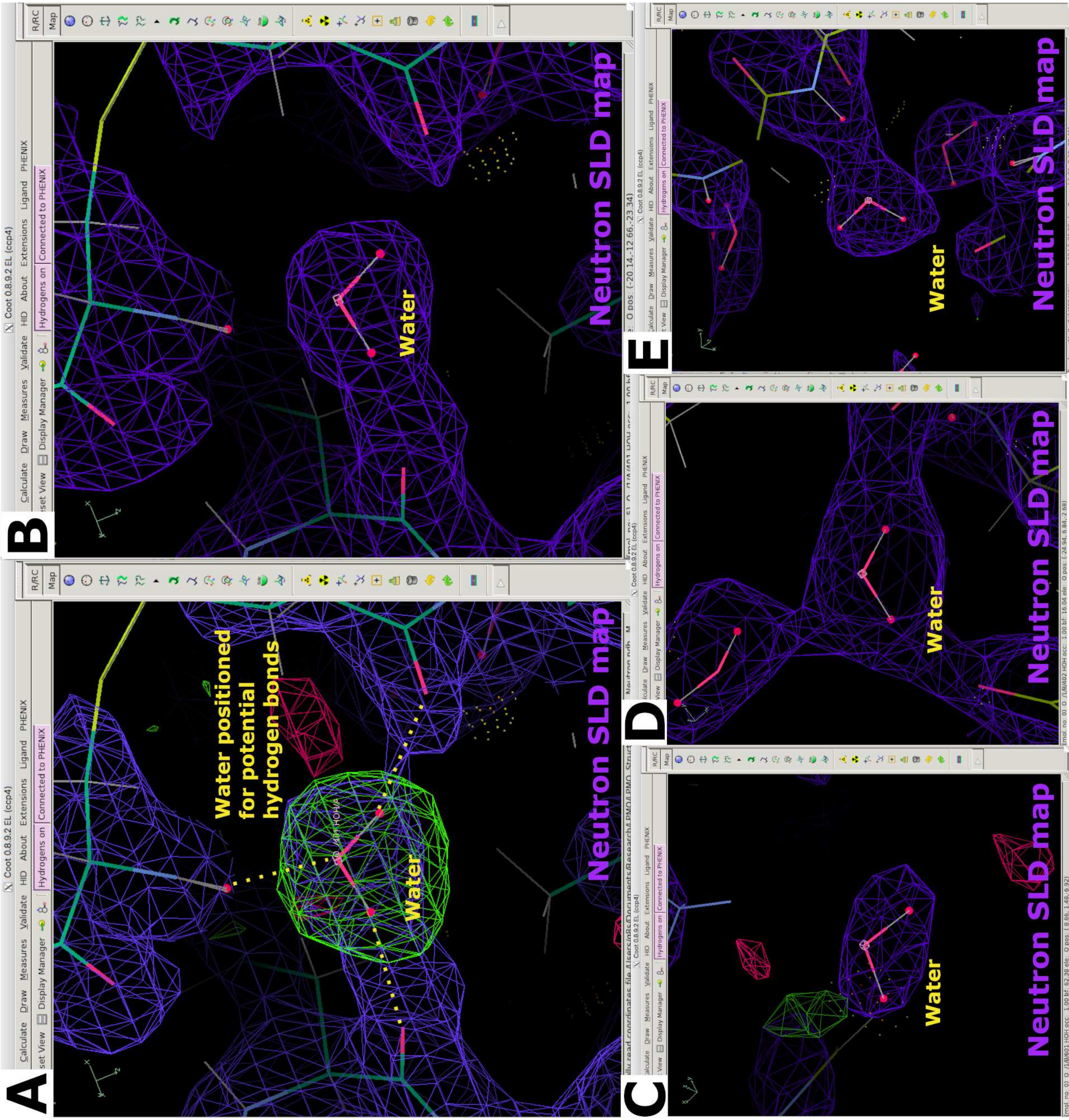
A
B
C
D
E
Water positioned for potential hydrogen bonds
Water
Neutron SLD map
Coot 0.8.9.2 EL (ccp4)
Calculate Draw Measures Validate HID About Extensions Ligand PHENIX
Display Manager
Hydrogens on
Connected to PHENIX
R/RC
Map

Figure 12

Click here to access/download;Figure;Figure12.eps

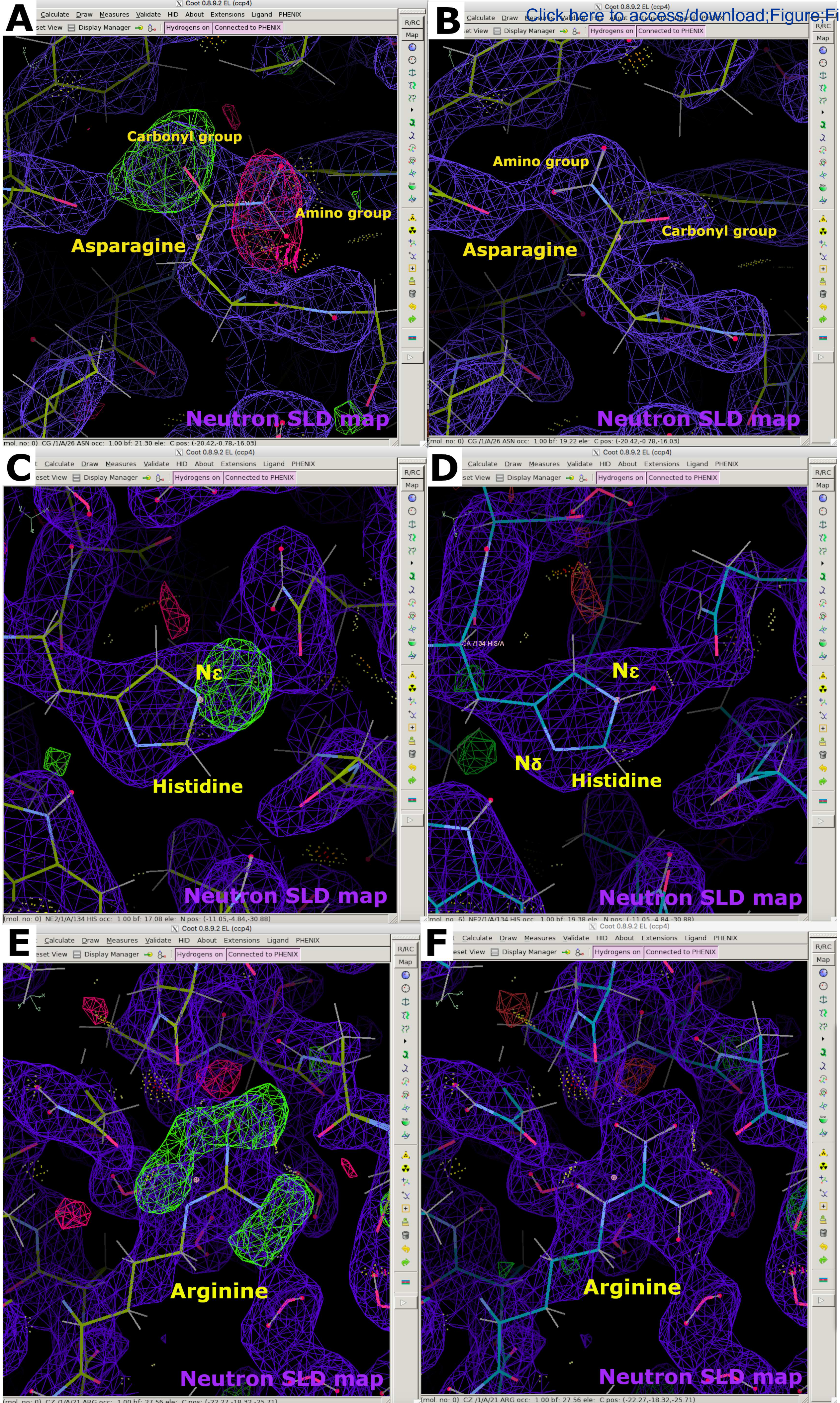
A
Carbonyl group
Amino group
Asparagine
Neutron SLD map
mol. no: 0) CG /1/A/26 ASN occ: 1.00 bf: 21.30 ele: C pos: (-20.42,-0.78,-16.03)
B
Amino group
Carbonyl group
Asparagine
Neutron SLD map
mol. no: 0) CG /1/A/26 ASN occ: 1.00 bf: 19.22 ele: C pos: (-20.42,-0.78,-16.03)
C
Nε
Histidine
Neutron SLD map
mol. no: 0) NE2/1/A/134 HIS occ: 1.00 bf: 17.08 ele: N pos: (-11.05,-4.84,-30.88)
D
CA /134 HIS/A
Nε
Nδ
Histidine
Neutron SLD map
E
Arginine
Neutron SLD map
F
Arginine
Neutron SLD map
mol. no: 0) CZ /1/A/21 ARG occ: 1.00 bf: 27.56 ele: C pos: (-22.27,-18.32,-25.71)
Coot 0.8.9.2 EL (ccp4)
Calculate Draw Measures Validate HID About Extensions Ligand PHENIX
Reset View Display Manager Hydrogens on Connected to PHENIX
R/RC
Map

Figure 13

Click here to access/download;Figure;Figure13.eps

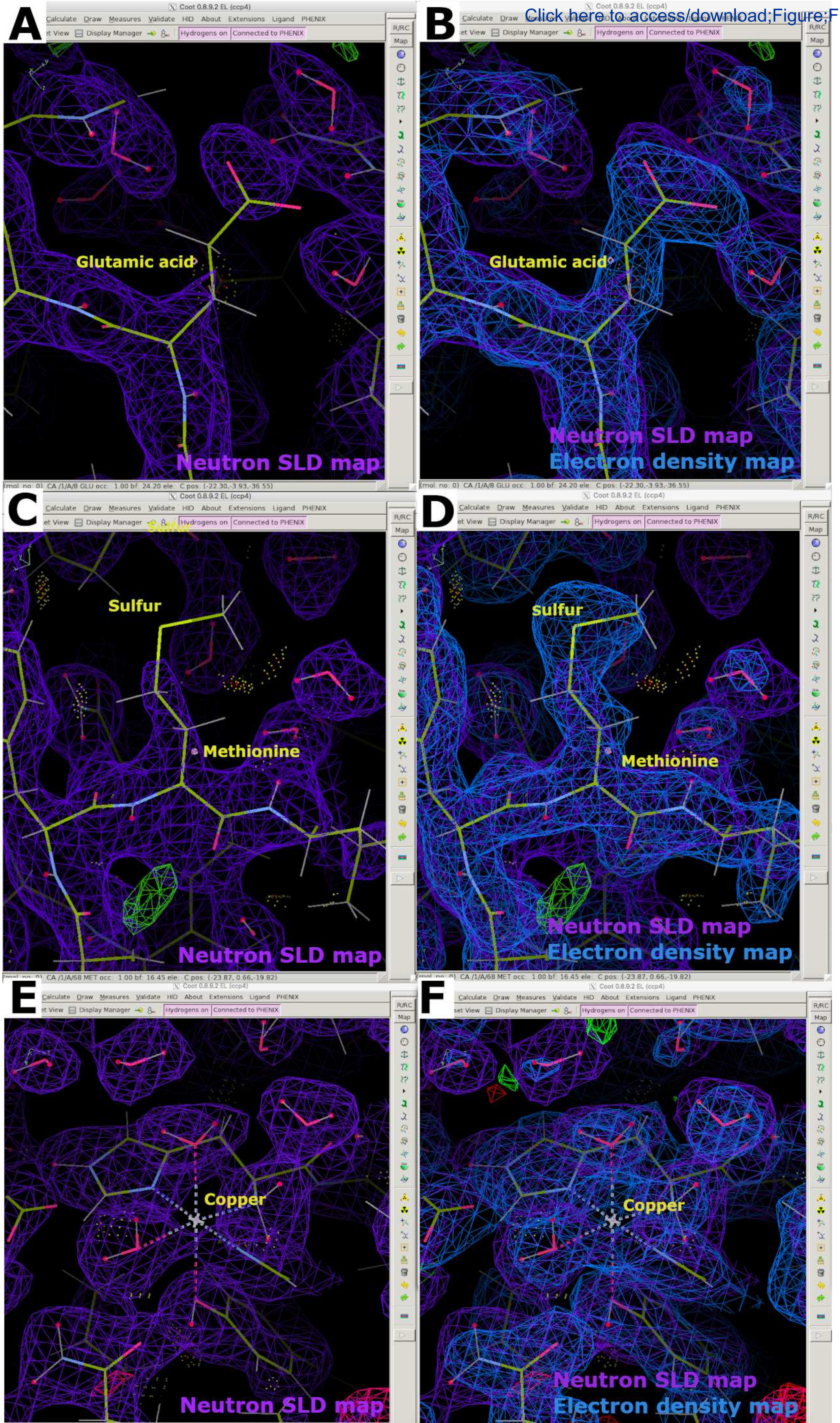
A
Coot 0.8.9.2 EL (ccp4)
Calculate Draw Measures Validate HID About Extensions Ligand PHENIX
et View Display Manager Hydrogens on Connected to PHENIX
R/RC
Map
Glutamic acid
Neutron SLD map
B
Glutamic acid
Neutron SLD map
Electron density map
C
Sulfur
Methionine
Neutron SLD map
D
Sulfur
Methionine
Neutron SLD map
Electron density map
E
Copper
Neutron SLD map
F
Copper
Neutron SLD map
Electron density map

(mol. no: 0) CA /1/A/8 GLU occ: 1.00 bf: 24.20 ele: C pos: (-22.30,-3.93,-36.55)

(mol. no: 0) CA /1/A/68 MET occ: 1.00 bf: 16.45 ele: C pos: (-23.87, 0.66,-19.82)

Click here to access/download;Table;Table 1.xlsx

Isotope	Coherent scattering length (fm)	Incoherent scattering length (fm)
1H	-3.741	25.274
2H	6.671	4.04
12C	6.6511	0
14N	9.37	2
16O	5.803	0
23Na	3.63	3.59
24Mg	5.66	0
31P	5.13	0.2
32S	2.804	0
35Cl	11.65	6.1
39K	3.74	1.4
40Ca	4.8	0
55Mn	-3.73	1.79
56Fe	9.94	0
63Cu	6.43	0.22
64Zn	5.22	0

Click here to access/download;Table of Materials;JoVE_Table_of_Materials.xlsx

Name of Material/Equipment	Company	Catalog Number	Comments/Description
Absorbent Paper Points Size #30-#40, 60 mm length	DiaDent/DiaVet	218-292	
Capillary wax	Hampton	HR4-328	
CCP4		Version 7.0.077	
Conical Centrifuge Tubes (15 mL)	Corning	CLS430790	
Conical Centrifuge Tubes (50mL)	Corning	CLS430828	
Coot		Version 0.8.9.2	
CrystalCap ALS	Hampton	HR4-779	
Curved-Tip Forceps	Mitegen	TW-CTF-1	
Deuterium chloride solution, 35 wt. % in D2O, ≥99 atom % D	Sigma-Aldrich	543047	
Deuterium oxide 99.9 atom % D	Sigma-Aldrich	151882	
Dual Thickness MicroLoops 1000 µm	Mitegen	M5-L18SP-1000	
FiveEasy pH meter F20-Std-Kit	Mettler Toledo	30266626	
Foam Dewars Standard Vessel 800 ml	Spearlab	M-FD-800	
Four Color Mounting Clay	Hampton	HR4-326	
HEPES, BioUltra, for molecular biology, ≥99.5% (T),	Sigma-Aldrich	54457	
High flux rotating anode X-ray diffractomemeter with EIGER 4M detector	Rigaku, Oxford Cryostream and Dectris	XtaLAB Synergy-R	Home source X-ray diffractometer
Magnetic Wand Straight	Mitegen	M-R-1013198	

Microloader, tip for filling Femtotips and other glass microcapillaries (for research use only), 0.5 – 20 µL, 100 mm, light gray, 192 pcs. (2 racks × 96 pcs.)	Eppendorf	930001007	
Microtubes volume 1.5 mL	Eppendorf	Z606340	
Petri Dishes with Clear Lid 100 mm diameter	Fischerbrand	FB0875713	
Phenix		Version 1.14-3260	
Pin Tong 18 mm	Mitegen	M-R-1013196	
Pipette Volume 0.1-2.5 µL	Eppendorf Research	Z683779	
Pipette Volume 100-1000 µL	Eppendorf Research	Z683825	
Pipette Volume 10-100 µL	Eppendorf Research	Z683809	
Pipette Volume 20-200 µL	Eppendorf Research	Z683817	
Poly(ethylene glycol) BioXtra, average mol wt 3,350, powder	Sigma-Aldrich	P4338	
Quartz Capillary , 1.00 mm inner diameter, 80 mm length	Hampton	HR6-146	Thin-walled capillary
Research Stereomicroscope System	Olympus	SZX16	
Reusable B3 (SSRL/SAM Style) Goniometer Bases	Mitegen	GB-B3-R	
Round - Miniature Hollow Glass Tubing (VitroTubes) Clear Fused Quartz / 1.00 mm inner diameter, 100 mm length	VitroCom	CV1012	Thick-walled capillary
Sandwich Box with cover	Hampton	HR3-132	
Siliconized 9 Well Glass Plate	Hampton	HR3-134	
Sitting Drop Crystallization Plate (24 Big Well)	Mitegen	XQ-P-24S-A	

Sodium deuteroxide solution, 40 wt. % in D2O, 99 atom % D	Sigma-Aldrich		176788
Thick Siliconized circle cover slides (22 mm x 0.96 mm)	Hampton	HR3-247	
Universal Pipet Tips, 0.1 - 10 µL	VWR	76322-528	
Universal Pipet Tips, 1 - 100 µL	VWR	76322-136	
Universal Pipet Tips, 100 - 1000 µL	VWR	76322-154	
Universal Pipet Tips, 20 - 200 µL	VWR	76322-150	
Universal Pipet Tips, 1 - 20 µL	VWR	76322-134	
Wax pen	Hampton	HR4-342	

Click here to access/download;Rebuttal Letter;Reviewer Response.docx

Reviewer #1:
Manuscript Summary:
This is an excellent and very well executed description of neutron macromolecular crystallography (nMX) procedures. It is perfect for a JoVE article and video contribution. Furthermore the authors and the ORNL neutron center facilities are amongst the very best leading exponents in the world today of these instruments, procedures and results.

Minor Concerns:
The list below is a mix of minor-major or major-minor concerns, ie not sure how to define:-

For JoVE

This is an excellent and very well executed description of neutron macromolecular crystallography (nMX) procedures. It is perfect for a JoVE article and video contribution. Furthermore the authors and the ORNL neutron center facilities are amongst the very best leading exponents in the world today of these instruments, procedures and results.

We thank the reviewer for positively appraising our manuscript.

I commend that the following are attended to:

(i) Electrons are sensitive to hydrogens, albeit not yet shown for MX. Somewhere in their manuscript a mention is needed.

We have revised the text to mention that hydrogen atoms are visible in X-ray diffraction structures if the resolution is sufficiently high:

Line 65: "During X-ray diffraction, X-rays scatter from the electron cloud, making light atoms such as hydrogen poorly visible in electron density maps that do not have near sub-Ångström resolution.[2] In contrast, the scattering intensity of neutrons depends on complex interactions with the nucleus. Light atoms and their isotopes, such as hydrogen and deuterium, therefore have comparable visibility to the backbone carbon, nitrogen and oxygen atoms in neutron scattering length density maps."

(ii)A teaching review article aimed at these topics is Blakeley et al Chem Soc Reviews 2004 33, 548-557 ie of complementarity of nMX and X-ray MX; I suggest that this article could be cited.

We have included Blakeley, M.P., Cianci, M., Helliwell, J.R., Rizkallah, P.J. Synchrotron and neutron techniques in biological crystallography. *Chemical Society Reviews*. **33** (8), 548–557, doi: 10.1039/b312779f (2004) in the manuscript line 75-78.

Line 79-83: "The primary focus of this article is to provide an overview of the workflow to obtain a high-quality neutron protein diffraction structure, we refer the interested reader to

Podjarny *et al.*[4], Blakeley[5]*,* Blakeley *et al.*[6] *and* O'Dell *et al.*[3] for an excellent overview of neutron protein diffraction and Ashkar *et al.*[7] for further applications of neutron scattering."

(iii) The deposition of nMX results at the PDB, has been strongly criticised by Afonine et al. So, some level of teaching how to guarantee that the underpinning data are FAIR (Findable, Accessible, Interoperable, and Reusable) is essential really e.g. at its most simple via the facility itself and or attached to the journal article, in case the PDB fails to archive data FAIRly. The Afonine et al article needs to be cited I think. In addition the current policy is that the raw diffraction images should be archived with a doi (IUCr). This policy article, Acta Cryst D75, 455-457, needs citing.

Although deposition of the neutron protein diffraction data and structure to the Protein Data Bank (PDB) is an important aspect and currently presents challenges that must be addressed by the community, we believe that this topic is beyond the scope of this paper.

We have cited Liebschner, D., Afonine, P. V., Moriarty, N.W., Langan, P., Adams, P.D. Evaluation of models determined by neutron diffraction and proposed improvements to their validation and deposition. *Acta Crystallographica Section D: Structural Biology*. **74**, 800–813, doi: 10.1107/S2059798318004588 (2018) which addresses issues related to neutron structure deposition and validation in line 192 and line 197.

(iv) The procedures and software on Imagine and at Mandi comes back at its base to the Daresbury Laue software development and so Helliwell et al 1989 and or Arzt et al and or Nieh et al JSR (1999). 6, 995-1006 needs to be cited.

We have included the following citations in the protocol section (line 583):

Helliwell, J.R. *et al.* The recording and analysis of synchrotron X-radiation Laue diffraction photographs. *Journal of Applied Crystallography*. **22** (5), 483–497, doi: 10.1107/s0021889889006564 (1989).
Nieh, Y.P. *et al.* Accurate and highly complete synchrotron protein crystal Laue diffraction data using the ESRF CCD and the Daresbury Laue software. *Journal of Synchrotron Radiation*. **6** (5), 995–1006, doi: 10.1107/S0909049599006342 (1999).
Arzt, S., Campbell, J.W., Harding, M.M., Hao, Q., Helliwell, J.R. LSCALE - The new normalization, scaling and absorption correction program in the Daresbury Laue software suite. *Journal of Applied Crystallography*. **32** (3), 554–562, doi: 10.1107/S0021889898015350 (1999).

(v) In papers reporting the diffraction resolutions of MX and or nMX data there are inconsistent cut offs used. Some comments on these cut offs are needed. i.e. to encourage good practice. Such as at least the need to state where the crosses 2.0 and what diffraction resolution is the CC1/2 value. Also some discussion is needed of the needed data completeness. Whilst X+n and X then n studies can surely rest on the X-ray diffraction data (very high) completeness then at least 80% neutron data completeness should be strived for. (A forward reference to line 884 can be made from here.) Furthermore if a publication ends up featuring a "never seen before" piece of protein structure the whole experiment should be repeated so as to claim "reproducibility" of that feature. Reproducibility is an issue for science as a whole and no special exemption should be claimed by crystallography.

We have expanded on the recommended guidelines for evaluating data in the text:

Line 1452 “Data were evaluated to be of sufficient quality following similar guidelines for X-ray data analysis, although a completeness of 80 % and a $CC_{1/2}$ of at least 0.3 were considered acceptable since neutron protein diffraction is a flux-limited technique.”
Line 2086: “In contrast to X-ray diffraction datasets, neutron diffraction data statistics possess a lower completeness, redundancy and signal-to-noise ratios due to inherent limitations (flux limited, quasi-Laue, longer wavelengths) of the technique.”

Discussion of the reproducibility of structural data obtained both with X-ray and neutron diffraction data is beyond the scope of this paper. It is a highly relevant concern for all structural studies, however we primarily seek to instruct the uninitiated neutron protein crystallographer on the experimental aspects of sample preparation and data collection.

(vi) At page 2 line 111 some mention of cryo-artefacts should be made whereby certain types of details are different from a room temperature structure i.e. that an investigator needs to be made aware of. Top of this list of types of artefact is that many more bound waters are observed, also that those at both RT and cryo can be in different places. Also the split occupancy residues can be different at each temperature. Halle 2004 PNAS 101 (14) 4793-4798 has summarised these cryo-artefacts well and again could be usefully cited.

Discussion of the artefacts that may be induced using cryo-conditions has been included in the text, particularly that since temperature artefacts may be introduced, it is necessary to collect X-ray and neutron datasets on the same crystal at the same temperature.

Line 168: “Data collection at the same temperature allows structure refinement to be performed against both X-ray and neutron data, preventing any potential temperature-induced artefacts such as changes in the visibility and position of waters or the occupancies of residue alternate conformations.”

We have accordingly referenced Halle, B. Biomolecular cryocrystallography: Structural changes during flash-cooling. *Proceedings of the National Academy of Sciences of the United States of America*. **101** (14), 4793–4798, doi: 10.1073/pnas.0308315101 (2004) in line 171.

(vii) At line 118 mention is made of many more X-ray structures than neutron ones in the PDB. I think this is a flawed metric. The role of neutrons is to resolve mechanistic questions unresolved by X-ray, NMR or electron methods. This role is pivotal and solves controversies in whole areas of biochemistry and or molecular biology. This sentence could be usefully rephrased. This is captured well in the text of the next paragraph although the word "complement" is a bit weak, although typical in the field.

To expand on the role of neutron protein crystallography as a valuable standalone technique, we have added the following:
Line 200-202: “Neutron protein crystallography provides valuable chemical insights to expand on and complement findings from additional studies such as X-ray, NMR or micro crystal electron diffraction (microED). Neutron protein diffraction is uniquely positioned to provide insights into enzymatic mechanisms, since hydrogen atoms are central to their chemistry.”

(viii) page 4 line 206. Quartz capillary is good for nMX since its mechanical strength is wanted. But for X-ray work quartz generates a lot of extra background in the diffraction image than a glass capillary does.

To emphasize the importance of using quartz capillaries as opposed to glass capillaries we have included the following note:

Line 312: “Note: Users are encouraged to make use of quartz capillary tubes because in, addition to its mechanical strength, it is essential to limit neutron beam absorption and lower background contributions from the capillary. Glass capillaries introduce high background and absorb neutrons, compromising data quality.”

(ix) page 6 line 271, define "sweeps".

We have rephrased this for clarity:

Line 469: “Ensure that the experimental hutch is vacated and open the beamline shutter for neutron data collection.”

(x) page 6 line 280 I learnt in a visit to Imagine at ORNL that a broad bandpass exposure can be useful to identify zones for indexing. That I think is a very neat procedure and quick as the neutron beam over its full bandpass is at a higher total flux. (A forward ref to line 512 could be made from here.)

We have included this additional information that can be gained from a broad bandpass exposure:

Line 1443: “In addition to providing preliminary information on the diffraction quality of the crystal, the broad bandpass exposure can be used to index the diffraction pattern and determine the crystal orientation matrix.”

(xi) Page 7 I think more detail on the cryo-protectant is needed here not least which compounds are preferred? In any case, since Blakeley et al 2004 PNAS, which should be cited, there have still been rather few such publications, Therefore the freezing behaviour of cryo-compounds under D2O, and their protein crystal, is a topic of biophysical chemistry research maybe worthy of more detailed basic experiments….

Preparation of a cryoprotectant suitable for cryo-data collection of protein crystals is case-dependent since crystallization conditions vary widely. We recommend that for a cryo-neutron diffraction experiment, users utilize cryoprotectants optimized when having performed X-ray diffraction.

The article to which the reviewer refers (Blakeley, M.P., Kalb, A.J., Helliwell, J.R., Myles, D.A.A. The 15-K neutron structure of saccharide-free concanavalin A. *Proceedings of the National Academy of Sciences of the United States of America*. **101** (47), 16405–16410, doi: 10.1073/pnas.0405109101 (2004)) reports neutron protein diffraction at 15K, which requires the use of a cryostat. In contrast, the cryo-data collection at MaNDi is performed at 100 K by use of a nitrogen cryo-stream which is the same sample environment used during cryo-X-ray data collection. Therefore, use of an established cryo-protectant as used for X-ray data collection is recommended for neutron cryo-data collection.

To clarify this, we have included the following:

Line 618: “Note: The cryoprotectant solution is usually the cryoprotectant that has proven effective for cryo-temperature X-ray diffraction data collection prepared in D_2O. This cryoprotectant can be further optimized (e.g. concentration) for neutron data collection if necessary.”

(xii) page 8 line 372 for fully deuterated protein the H/D option would not be chosen.

The example given here pertains to a hydrogenated protein that has undergone vapor exchange with deuterated buffer.

We have added the following note to accommodate for perdeuterated proteins:

Line 902: “Note: If a perdeuterated protein is used, select the option “Add hydrogens to model if absent” and select “H/D at exchangeable sites, D elsewhere”.

(xiii) page 9 line 418 re water molecules some mention is needed that both deuteriums are not always seen ie due to mobility, spinning, of the water along on axis. (A forward reference to line 564 could be made from here.)

The effect of water mobility (i.e. high B-factors) on the form of neutron scattering length density maps has been addressed in Line 1519: “When analyzing neutron scattering length density maps, water molecules are clearly visible if they are highly ordered, however their density may be spherical or ellipsoidal if they are not well-ordered (**Figure 11C-E**).”

(xiv) Page 10 line 447 for neutron only a specific point should be made that the wavelength used for the MR X-ray model was a particular monochromatic value and therefore, along with the absolute unit cell distances, the neutron refinement is in effect also calibrated to that specific wavelength via the X-ray structure bond lengths. The point being that Laue data, neutron or X-ray, must be tethered to a monochromatic X-ray wavelength value. Obviously where monochromatic neutron diffraction data are used then that wavelength should be used.

In a Laue experiment (X-ray or neutron), only the ratio of the unit cell parameters can be accurately determined. Therefore the refinement should be performed using the unit cell parameters determined by the accompanying monochromatic X-ray experiment.

(xv) page 11 lines 495 to 500 this statement is not applicable to the quite often used case of "X then n" MX refinement whereby all non-hydrogen atoms are fixed at the X-ray positions. Obviously this still requires the X and the n data sets to be measured from identically prepared protein crystals and at the same temperature.

We have deleted this note to not complicate the discussion with a third type of refinement that we do not otherwise present in the manuscript.

(xvi) Figure 33C, the nuclear density to guide placing deuteriums on a bound water, is there surely a better example ie one that shows a boomerang shape? (Or, add a forward reference to Figure 39.) Otherwise, excellent figures. :-)

We were not able to observe F_O-F_C neutron SLD map density peaks with the “boomerang” shape since the resolution of the presented data was not sufficiently high, yet this resolution is typical of most neutron data sets.

(xvii) Some comment needed somewhere encouraging the PDB to introduce a Validation report for neutron MX structures.

Although this is a very relevant concern for neutron data deposition, we believe that it is beyond the scope of this manuscript which seeks to visually inform potential users on sample preparation, data collection and analysis.

(xviii) Line 533:- "…indicate that while hydrogen bond interactions can be deduced from X-ray data, neutrons provide clear information regarding the position of these hydrogen bonds (Figure 35)." Deduced is a strong word, maybe 'inferred' or 'indicated' is more the actuality?

The sentence has been reformulated:

Line 1473: “A map overlay of electron and neutron scattering length density maps for water molecules also indicate that while hydrogen bond interactions can be inferred from X-ray data, neutrons provide clear information regarding the position of these hydrogen bonds (**Figure 8**).”

Reviewer #2:

Manuscript Summary:

The authors present the workflow of neutron protein crystallography. This manuscript focuses on mounting a protein crystal, neutron diffraction data collection, structure refinement, and analysis of SLD maps. The study is well conducted, and the methods used are appropriate. The data is presented clearly. This paper is very useful for researchers with little experience in neutron crystallography because the explanations in the text are very practical. This paper will be of interest to many protein crystallographers, as well as researchers in the field.

We thank the reviewer for positively appraising our manuscript.

Major Concerns:
No

Minor Concerns:

In discussion, I think the authors should give more information about the benefit of the high-resolution neutron diffraction data using H/D exchanged crystal. Thus, we can detect SLD map of hydrogen at non-exchangeable sites using high-resolution data. This is important information to evaluate the nature of the ligand and the cofactor in the protein (e.g., pKa of the group).

We agree with the reviewer that if the protein is perdeuterated (so that the non-exchangeable hydrogen atom sites are occupied by deuterium) it is possible to see the deuterium positions of these non-exchangeable atoms on neutron scattering length density maps. However these positions are not titratable (non-exchangeable) and as such do not have pKas.

To further elaborate on the value of perdeuterated structure in neutron protein diffraction we have included the following In the Discussion:

Line 2141: “This is beneficial when characterizing hydrogen/deuterium bound at non-exchangeable sites in a protein or cofactor.”

L354
I can perform neutron data refinement in "Basic" user level in Phenix. This may depend on the version of Phenix and OS. I think it would be useful if the authors gave more information about the version of the software (Phenix, CCP4, and Coot) and OS used in the study.

We have included the software used for structure refinement in the Table of Materials and have removed the requirement to use the “Advanced” level in Phenix for structure refinement.

L879
Recently, many neutron diffraction data collection are carried out at cryo-temperature. "Since neutron diffraction data is generally collected at room temperature (300K)" would be better as "When neutron diffraction data is collected at room temperature (300K) ".

We note that while reviewer 2 states that "Recently, many neutron diffraction data collection are carried out at cryo-temperature", reviewer 1 noted that "there have still been rather few such publications". Therefore we do not comment on frequency of one method over the other but rather focus on describing the steps of each method as we include both examples in our manuscript.

We have reformulated this to highlight that if X-ray data is collected at room temperature, it should be done using a low-dose data collection strategy.

Line 2263: "For neutron diffraction data collected at room temperature (300K), the corresponding X-ray dataset will should be collected at room temperature using a low-dose data collection strategy to limit radiation damage."

We have also reformulated Line 164 to read: "Data can be collected at room temperature, ~~currently the most employed method for neutron diffraction~~, or at cryo-temperature which can potentially improve data quality and opens up the possibility for freeze-trapping catalytic intermediates."

L883 (L407)
The authors should briefly describe the difference between "fill" map and "no_fill" map.

We have included a more detailed explanation of the difference between "fill and no_fill" maps and their role in model bias.

Line 2244: "It should also be taken into account that neutron diffraction data usually has a completeness of ~80%, which is lower than the routinely observed ≥ 98% for X-ray diffraction data. When refining neutron diffraction data in Phenix, the missing observed amplitudes (F_o) are therefore calculated from the model to complete the reflection list, thus introducing model bias. To account for this potential bias "no_fill" maps should be examined during interactive model building as opposed to "fill" maps. "

Reviewer #3:

This manuscript walks the reader through what is a rather intensive diffraction technique (macromolecular neutron crystallography) that remains difficult, despite 20 years of new beamlines, and over a decade of streamlining the data collection and structure refinement process. The two instruments at Oak Ridge are the only suitable beamlines for large unit cell crystals available in the US at present, and the manuscript presents a fair amount of detail into the data collection specifics at MaNDi and IMAGINE. Overall, this should be published, with some revisions that address the issues outlined below.

Pg. 1, lines 57-58: It is worth mentioning that it is difficult to see hydrogen atoms even in the highest resolution X-ray structures, especially the mobile and mechanistically important ones. One of the strengths of neutron diffraction is visualizing hydrogen atom positions, at moderate resolutions.

To further highlight the strengths of neutron protein crystallography, we have included the following:

Line 62: "Conceptually similar to X-ray diffraction, neutron diffraction provides atomistic details of macromolecular structure, however, the interaction of neutrons with nuclei enables localization of light atoms, often difficult to detect with X-ray diffraction[1]. During X-ray diffraction, X-ray photons scatter from the electron cloud, making light atoms such as hydrogen poorly visible in electron density maps that do not have near sub-Ångström resolution.[2] In contrast, the scattering intensity of neutrons depends on complex interactions with the nucleus. Therefore, light atoms and their isotopes, such as hydrogen and deuterium, have comparable visibility to the backbone carbon, nitrogen and oxygen atoms in neutron scattering length density maps."

Pg. 2, lines 89-95: The hydrogen isotopes need to be consistently labeled, maybe it is best to use 1H and 2H with D in parentheses. The NIST scattering lengths should be included in the text, with + and - for emphasis. Table 1 could include some of the more commonly metal ions in biological systems (Zn, Ca, Fe, etc.).

We have included designation of hydrogen (^{1}H) and deuterium ($^{2}H(D)$) in the introduction. The values of the scattering lengths has been included for the elements discussed in paragraph 3. Furthermore, Table 1 has been modified to include more elements commonly found in biological systems.

It should also be mentioned in the text that the neutron coherent scattering lengths of C, N, O are similar to D atoms, and that unlike X-rays, the scattering across the periodic table is not related to the number of electrons. This obscures electron density of light elements in the vicinity of heavy elements such as those in metal clusters, whereas with neutrons this is not an issue- it should be mentioned as yet another advantage of using neutrons to study metalloproteins, in addition to the lack of radiation damage of these rather sensitive assemblies.

We have elaborated on the differences between X-ray and neutron scattering:

Line 65: “During X-ray diffraction, X-ray photons scatter from the electron cloud, making light atoms such as hydrogen poorly visible in electron density maps that do not have near sub-Ångström resolution[2]. In contrast, the scattering intensity of neutrons depends on complex interactions with the nucleus, with isotopes of the same element displaying different scattering lengths. Therefore, light atoms and their isotopes, such as hydrogen (^{1}H) and deuterium (^{2}H or D), have comparable visibility to the backbone carbon, nitrogen and oxygen atoms in neutron scattering length density maps. Furthermore, since the magnitude of neutron scattering is independent of number of electrons, scattering from light elements is not obscured by heavy elements when they are in close vicinity to each other, as is observed in X-ray scattering.”

Pg. 2, line 115, similarly Pg. 11, lines 495-500: "neutron diffraction data provides information solely on the position of the hydrogen / deuterium atoms". This is not true. Each reflection is composed of scattering contributions from each atom in the unit cell and vice versa.

In the cases discussed in the text in those instances, the intention was not to suggest that the data obtained from neutron diffraction only provides signal from H and D. The intent was to emphasize that during a joint refinement, during which both X-ray and neutron data are used, the neutron scattering length density maps are used to determine the position of the H/D atoms while the X-ray density maps are used for the backbone and C,N,O and S coordinates.

This has been rephrased for clarity:

Line 170: “Joint X-ray neutron data refinement increases the data-to-parameter ratio and provides the advantage of allowing the protein backbone coordinates to be refined against the X-ray data, while the neutron diffraction data is used to refine the position of the hydrogen/deuterium atoms[28].”

Line 1375: “ **NOTE:** Model building using neutron-only data differs from model building of a joint X-ray/neutron structure because there is no X-ray data to contribute to the refinement of the coordinates of the backbone and “heavier” atoms. In a joint refinement, the electron density map is initially used to determine the protein backbone and sidechain coordinates. This model is subsequently used in a joint X-ray/neutron data refinement in which the orientation and occupancy of H/D atoms is derived from the neutron SLD map. In a neutron-only refinement, the entire structure is derived from analysis of the neutron SLD maps, requiring building of the backbone, side-chains and ligands in addition to the H/D atoms. The data-to-parameter ratio is low in refinements against neutron data lone and caution should be taken not too overfit the data.”

Pg. 4, sections 3 and 4: A couple of technical suggestions, one is to invert the cover slide with the mother liquor facing down to slow the evaporation. The capillary should be cut smooth at the ends to avoid damaging the crystal(s), which tend to be pretty fragile at the size they grow to. Sandpaper is a good way to score the capillary to get a smooth break.

There are many techniques that can be applied during crystal mounting, and we are presenting only one of the possibilities. We do however not think that it is technically feasible to invert the cover slide during crystal harvesting.

Line 305: “**NOTE**: Capillary mounting protocols vary with experimentalist preferences. To prevent damage to crystals, capillaries that need to be shortened should be scored with a cutting stone or sandpaper to ensure a smooth break.”

Pg. 5, section 4.10: maybe not reference the specific crystal (NcLPMO9), as this should be more of a general flowchart for neutron diffraction-ready crystal preparation.

We have removed *Nc*LPMO9D to keep the protocol more general.

Pg. 5, section 5.2: "furthest the crystal", should be "furthest from the crystal".

This has been corrected.

Pg. 5, section 5.4: "twice more with four days intervals", should be "twice more at four day intervals".

This has been corrected.

Pg. 10, section 7.2.3.3: Real space refine in Coot is really not advisable against the nuclear density maps, best not to use this option at all. With very few exceptions, the nuclear density maps just are not resolved enough to do this. Also this option is to be avoided when placing the D2O molecules. In practice the water orientation is guided more by hydrogen bonding geometry than by the maps. Figure 32 shows the real space refine option applied to the electron density maps- the manuscript should at least make this clear that it's a more suitable option for the electron density maps and will likely fail for the nuclear density maps.

The authors agree with the reviewer, “Real Space Refine Zone” is not recommended for neutron SLD maps in Coot. However, since this protocol is aimed at X-ray crystallographers interested in neutron protein crystallography, we considered it informative to highlight the shortcomings of “Real Space Refine Zone” and how to fix the “exploding” atoms that result since it is routine to use “Real Space Refine Zone” when performing interactive model building for X-ray structures.

To highlight the pitfalls of “Real Space Refine Zone”, we have included the following:

Line 1378: “Note: “Real Space Refine Zone” is not optimized for neutron SLD maps in Coot and may result in irregular bond lengths for atoms bound to deuterium, termed “exploding residues” (Supplementary **Figure 26**). It is preferable to manually edit the necessary atomic coordinates and avoid use of “Real Space Refine Zone”.”

Pg. 11, line 513: Which space group is it? Figure 24 shows P21- maybe it should be stated in the manuscript that fewer frames are required for higher symmetry space groups.

We have included the *N*cLPMO9D space group and clarified that higher symmetry is beneficial because fewer frames have to be collected.

Line 1479: “Given the $P2_1$ space group of the crystal, a data collection strategy of 18 frames with a collection time of 20 hours per frame was implemented. As with X-ray diffraction data collection, higher symmetry space groups require fewer frames (i.e. less angular coverage) to collect a complete dataset.”

Pg. 14, line 652: misspelling.

This has been corrected.

Pg. 18, lines 845-869: The choice of vapor exchange of labile hydrogen atoms needs a clearer explanation, vs. completely unexchanged, vs. perdeuterated crystals. Perdeuteration of crystals seems to have mixed results in terms of crystal size, diffraction quality, and also yield of protein, c.f. perdeuterated rubredoxin (Munshi / Meilleur Acta cryst D 2012), perdeuterated beta-lactamase (ref. 47), haloalkane dehydrogenase (Liu / Viola Acta cryst D 2007), perdeuterated DFPase (Blum / Chen 2010), and others.

It should be added that the most straightforward, cost-effective, and practical option is vapor exchange, that will replace a certain percentage of hydrogen atoms in proteins and solvent and will decrease the background from the incoherent scattering of 1H atoms, and also yield some basic information about the dynamics of the protein by the exchange of backbone amide protons (Kossiakoff Nature 1982, Bennett / Dealwis PNAS 2006, Blum / Chen PNAS 2009, and others).

Easiest thing is to move the perdeuteration discussion to the end of the paragraph, and start with the description of soaking in deuterated buffer / deuteration via vapor exchange in capillary. Personally, the reviewer would attempt perdeuteration as a last resort, for many of the reasons the authors mention in the paragraph.

This has been addressed by rephrasing paragraph 2 of the discussion as suggested by the reviewer to first describe H/D vapor exchange of a hydrogenated protein crystal and then mention the additional alternatives such as perdeuteration.

Pg. 19-20, lines 871-894: The structure refinement protocols are rather confusingly laid out. The authors discuss the use of joint X-ray and neutron refinement, and also neutron-only refinement, but do not say why it is done this way. At some point it would be good to explain the need for joint X-ray / neutron refinement vs. neutron refinement on its own. Introducing the data-to-parameters ratio is a good idea here- that the addition of H / D atoms and relative H / D occupancies increases the number of parameters being refined and can de-stabilize refinement. Having X-ray data, generally containing many more observations, higher resolution, higher completeness, can alleviate this issue to a certain extent.

The authors have included both joint X-ray/neutron and neutron-only refinement to provide readers with instructive examples of both. The joint technique was discussed first because, as the reviewer mentions, it has the advantage of higher completeness and resolution, and provides the backbone upon which a neutron data-derived structural information can be built.

In paragraph 4, we have elaborated on the advantages that a joint refinement offers i.e. using the X-ray data to determine the backbone coordinates since neutron SLD maps are often incomplete due to H atom negative scattering lengths and the improvement of the data-to-parameter ratio. We also discuss that if the neutron data is of sufficient resolution or a perdeuterated sample was used, neutron-only refinement is recommended. In addition, neutron-only data refinement is particularly useful if a protein highly sensitive to radiation damage is being studied, since an X-ray derived structure may possess radiation-induced artefacts.

Pg. 20, line 888: High-resolution neutron structures (Chen et al., PNAS, 2012; Cuypers, et al., Angew. Chemie, 2013) should be referenced. The cancellation effects noted in nuclear density maps are less obvious at these resolutions, but this is of course rarely seen in the majority of macromolecular neutron structures which are at moderate resolutions.

We have referenced the recommended articles.

Pg. 20, 896-925: This section could use some discussion about occupancy refinement of exchangeable H / D sites in Phenix, which atoms should be refined, which ones should be set to full D occupancy, etc. This is important for active site residues where protonation states are most relevant.

We have included a discussion about occupancy refinement in paragraph 3 of the discussion since this paragraph addresses refinement procedures, programs and model bias in maps.

Line 2187: "When performing refinements in Phenix, exchangeable H/D sites will initially be set to 0.50 occupancy for H and D. As refinements are performed, the occupancy of H and D will be refined according to the neutron SLD maps. During interactive model building, difference density F_o-F_c maps are very informative in assessing H/D occupancies. Maps can be used to determine which sites possess high D occupancy, which is particularly informative at the active site where protonation states are catalytically relevant[62]. Ambiguous situations do arise, however, when the H:D occupancy is close to 0.70:0.30 which results in signal cancellation in neutron SLD maps[63].”

Supplementary Figure 1

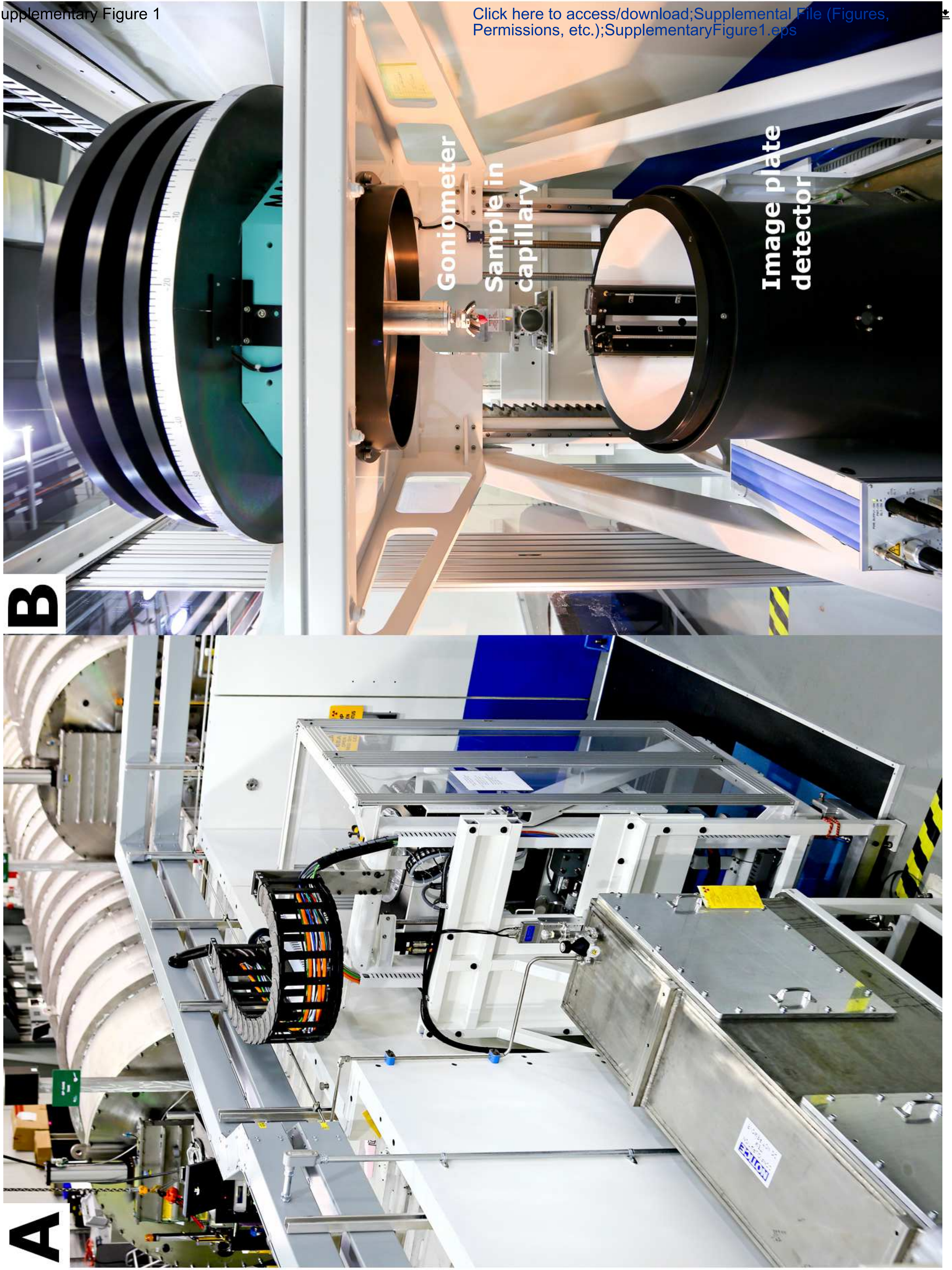
A
B
Goniometer
Sample in capillary
Image plate detector

Supplementary Figure 2

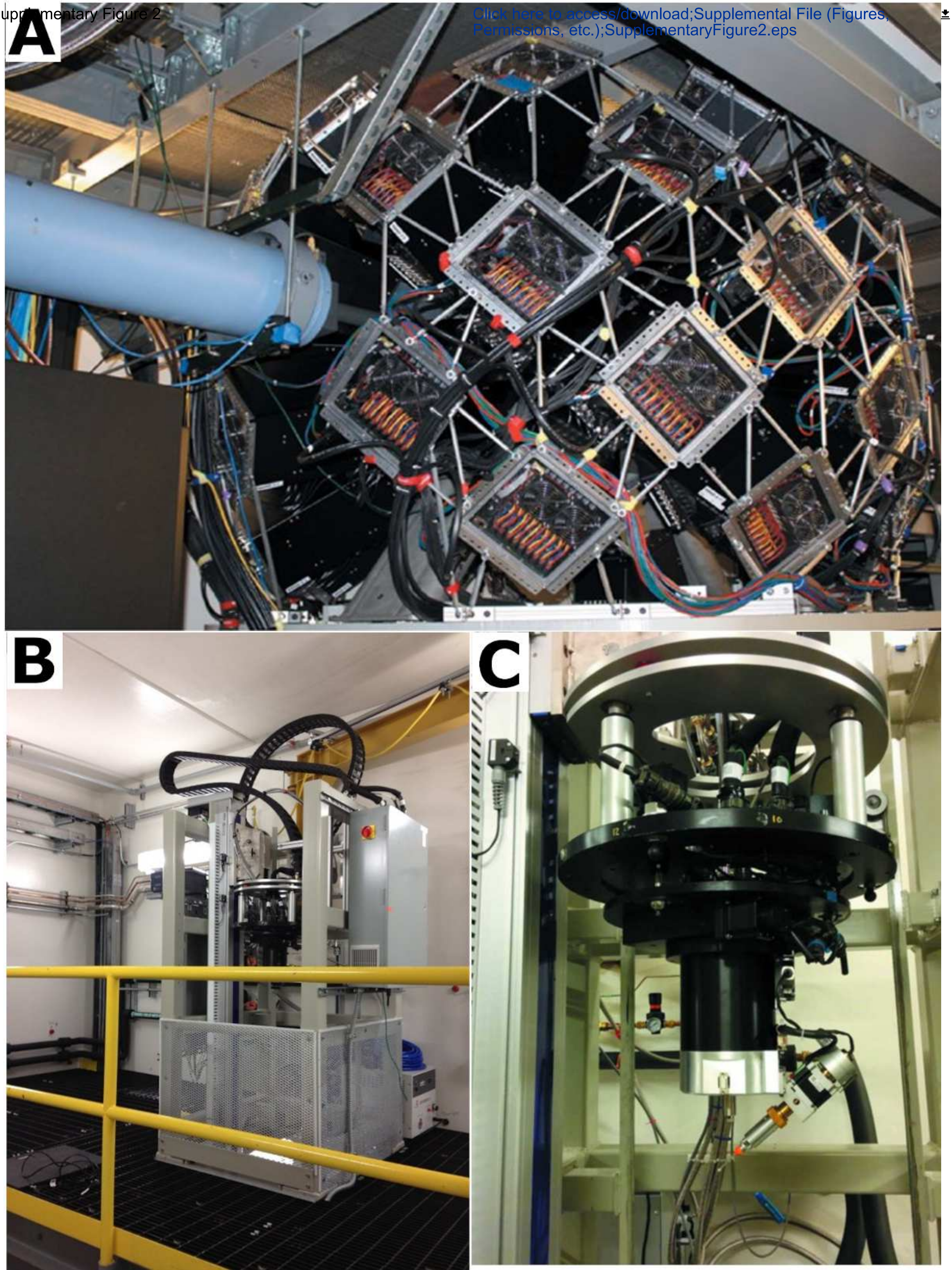

Supplementary Figure 3

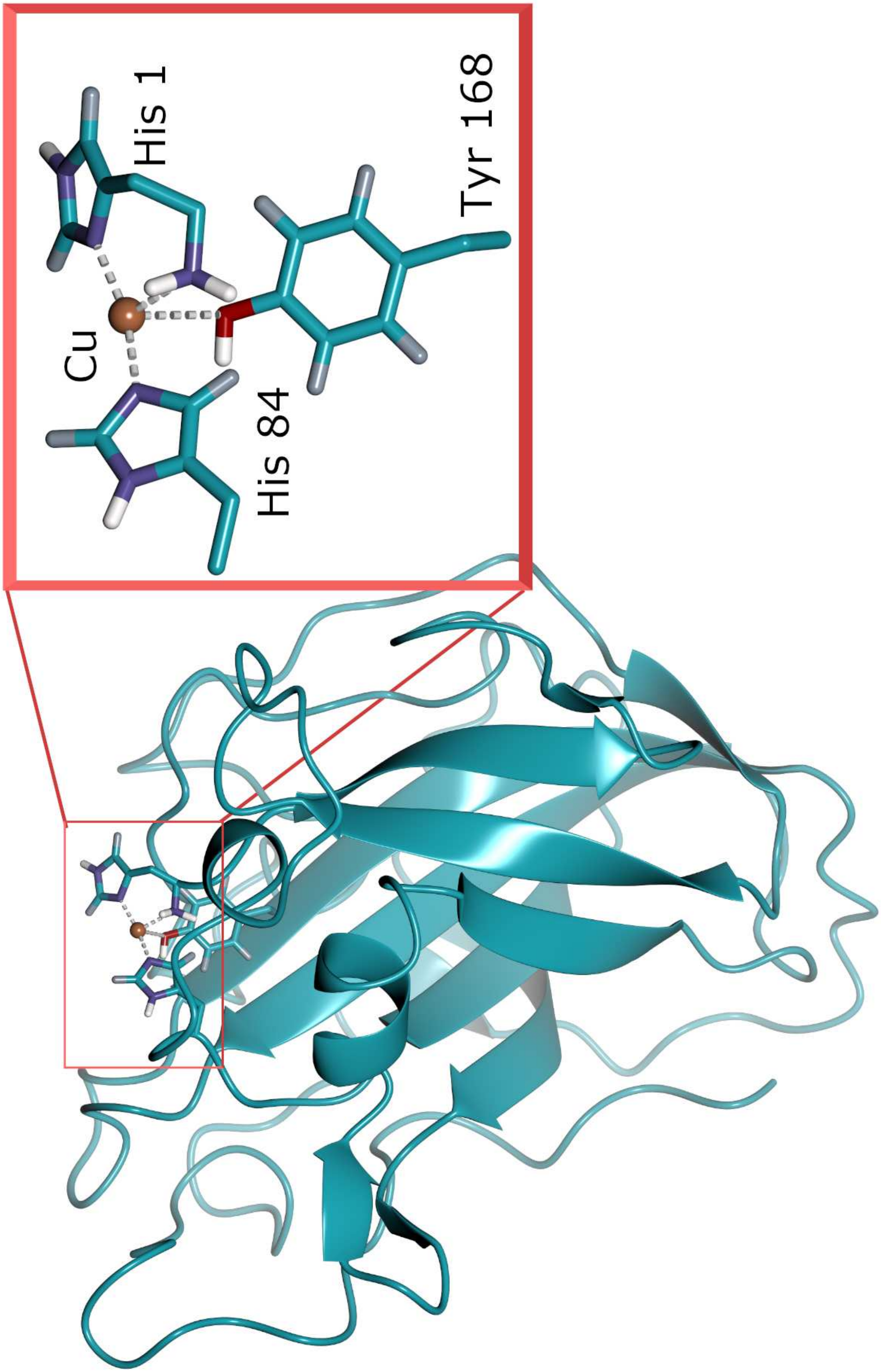
His 1
Tyr 168
Cu
His 84

Supplementary Figure 4

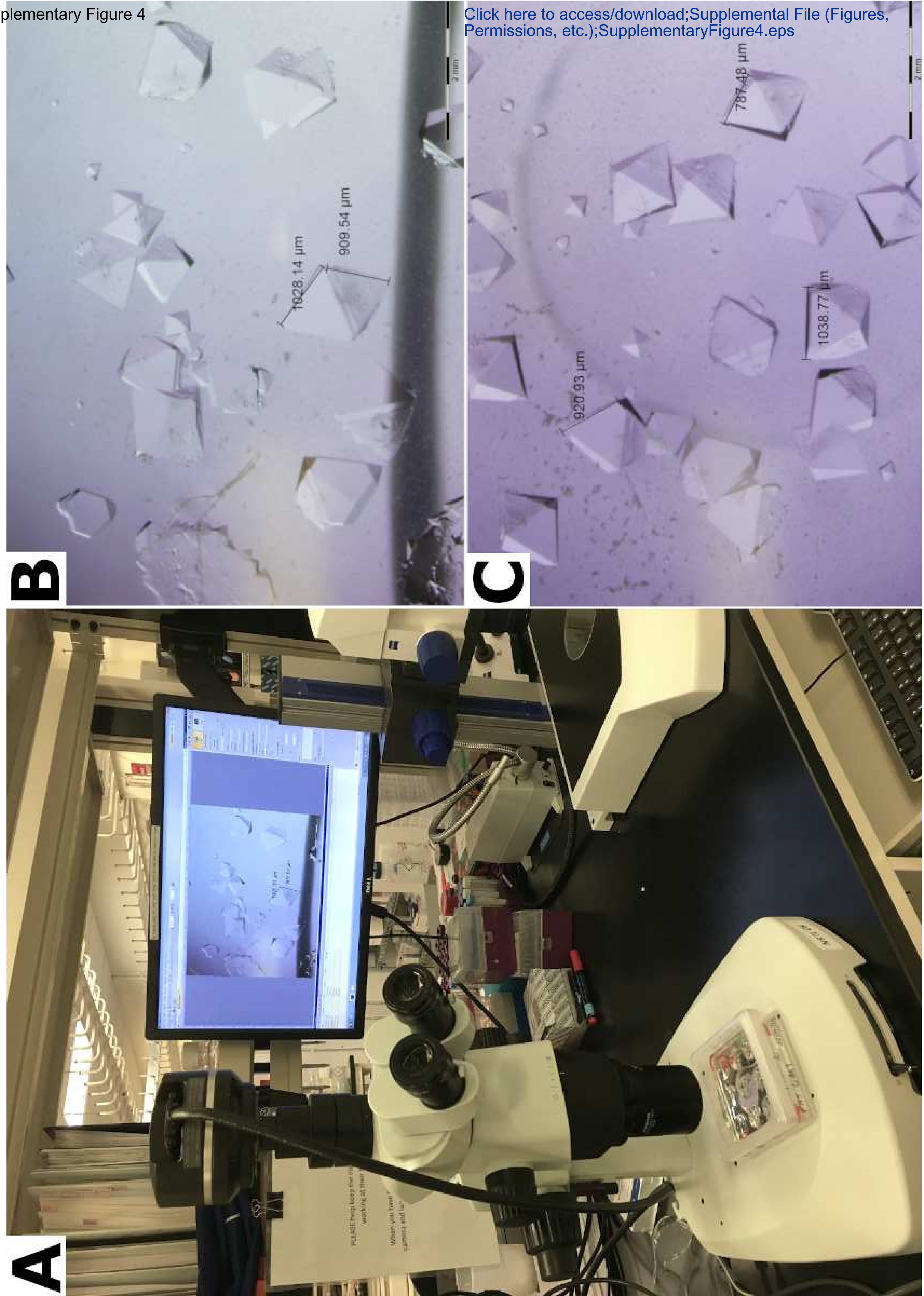
A
B
1028.14 µm
909.54 µm
2 mm
C
787.48 µm
1038.77 µm
920.93 µm
2 mm

Supplementary Figure 5

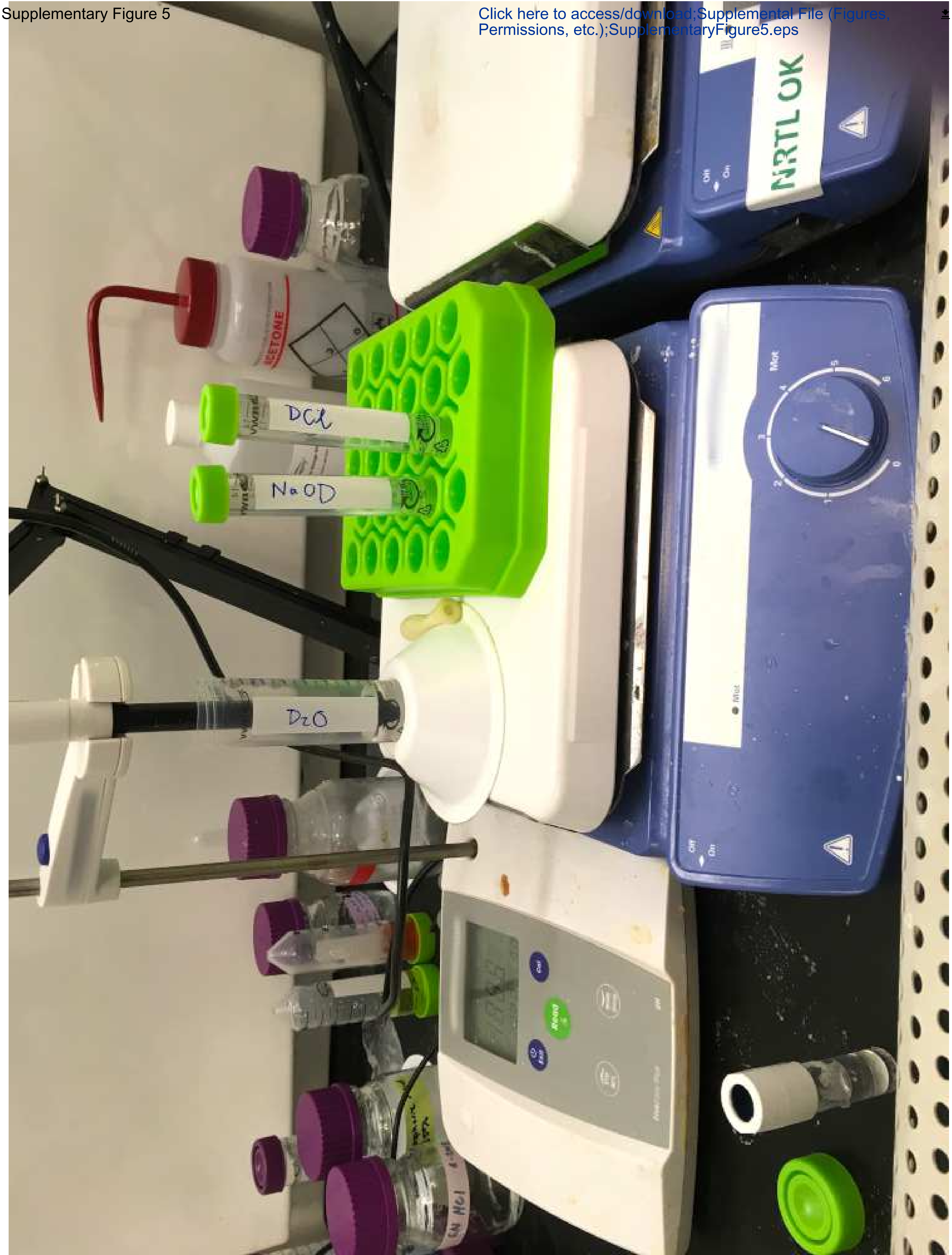
ACETONE
DCl
NaOD
D2O
NRTL OK
Mot
Read
1N HCl

Supplementary Figure 6

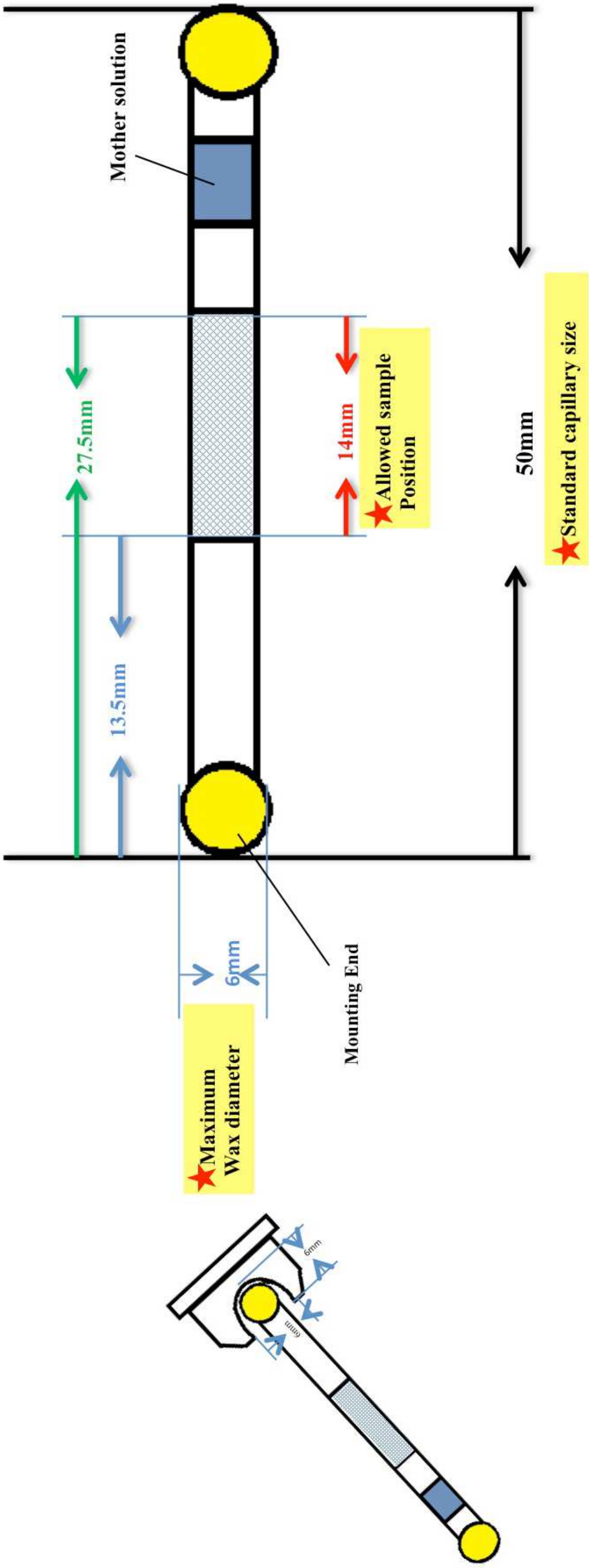
Mother solution
27.5mm
14mm
★Allowed sample Position
50mm
★Standard capillary size
13.5mm
6mm
Mounting End
★Maximum Wax diameter
6mm
6mm

Supplementary Figure 7

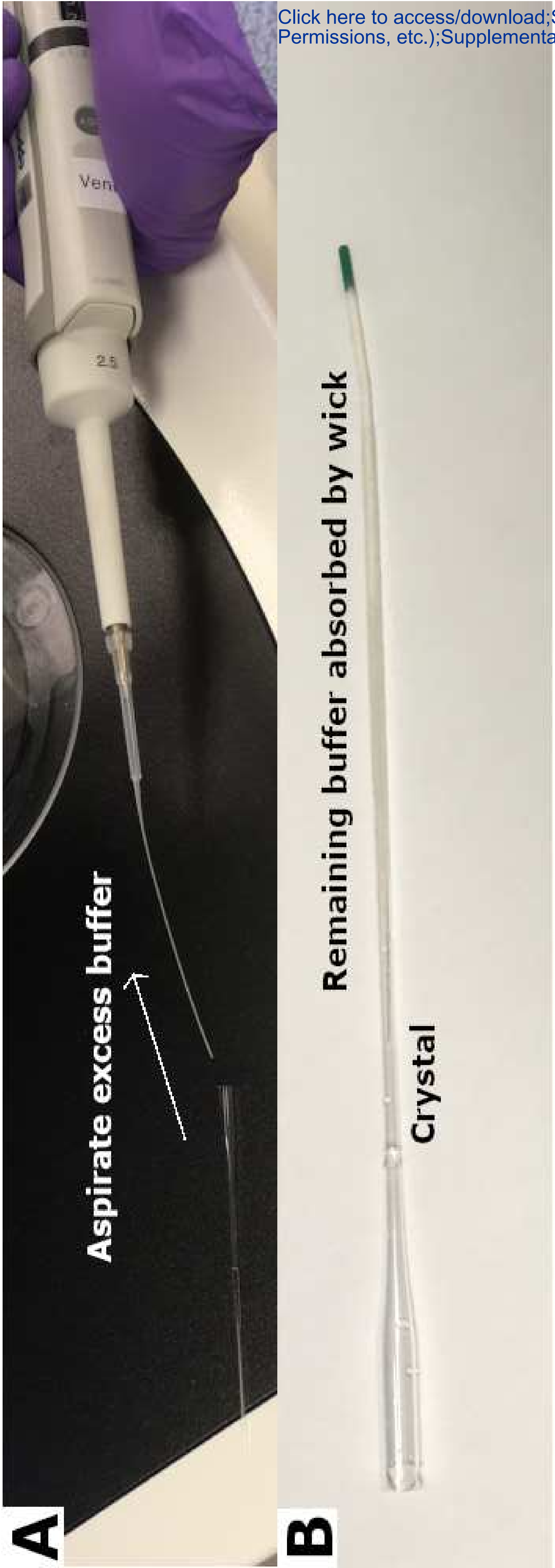
A
Aspirate excess buffer
B
Remaining buffer absorbed by wick
Crystal

Supplementary Figure 8

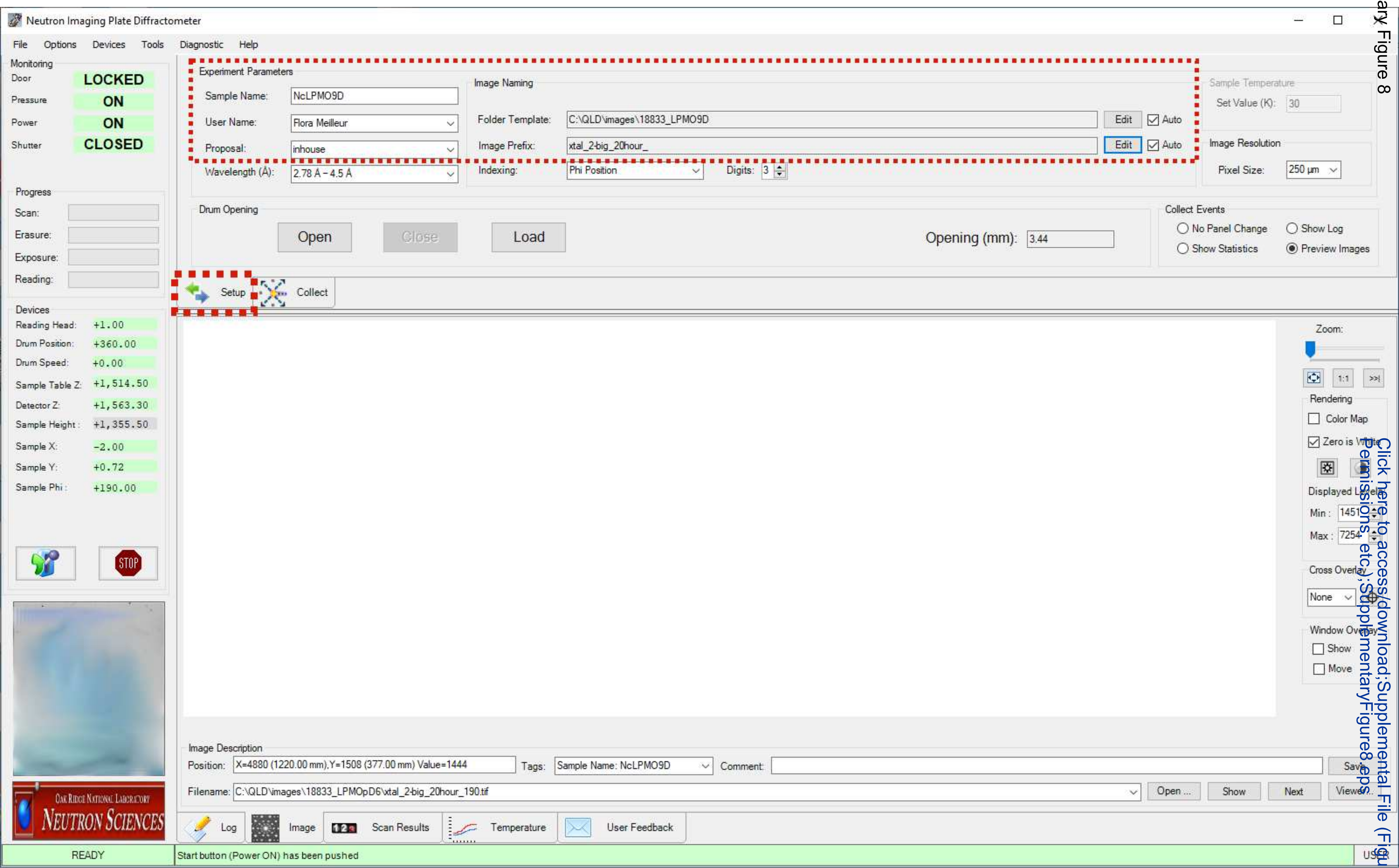

Neutron Imaging Plate Diffractometer
File
Options
Devices
Tools
Diagnostic
Help
Setup
Collect
Log
Image
Scan Results
Temperature
User Feedback
Open
Close
Load
Edit
Save
Open ...
Show
Next
Viewer...
STOP
Oak Ridge National Laboratory
Neutron Sciences

Monitoring
Door: LOCKED
Pressure: ON
Power: ON
Shutter: CLOSED

Progress
Scan:
Erasure:
Exposure:
Reading:

Devices
Reading Head: +1.00
Drum Position: +360.00
Drum Speed: +0.00
Sample Table Z: +1,514.50
Detector Z: +1,563.30
Sample Height: +1,355.50
Sample X: -2.00
Sample Y: +0.72
Sample Phi: +190.00

Experiment Parameters
Sample Name: NcLPMO9D
User Name: Flora Meilleur
Proposal: inhouse
Wavelength (Å): 2.78 Å - 4.5 Å

Image Naming
Folder Template: C:\QLD\images\18833_LPMO9D ☑ Auto
Image Prefix: xtal_2-big_20hour_ ☑ Auto
Indexing: Phi Position
Digits: 3

Sample Temperature
Set Value (K): 30

Image Resolution
Pixel Size: 250 µm

Drum Opening
Opening (mm): 3.44

Collect Events
○ No Panel Change
○ Show Log
○ Show Statistics
● Preview Images

Zoom:
1:1
Rendering
☐ Color Map
☑ Zero is White
Displayed Levels
Min: 1451
Max: 7254
Cross Overlay
None
Window Overlay
☐ Show
☐ Move

Image Description
Position: X=4880 (1220.00 mm),Y=1508 (377.00 mm) Value=1444
Tags: Sample Name: NcLPMO9D
Comment:
Filename: C:\QLD\images\18833_LPMOpD6\xtal_2-big_20hour_190.tif

READY
Start button (Power ON) has been pushed

Supplementary Figure 9

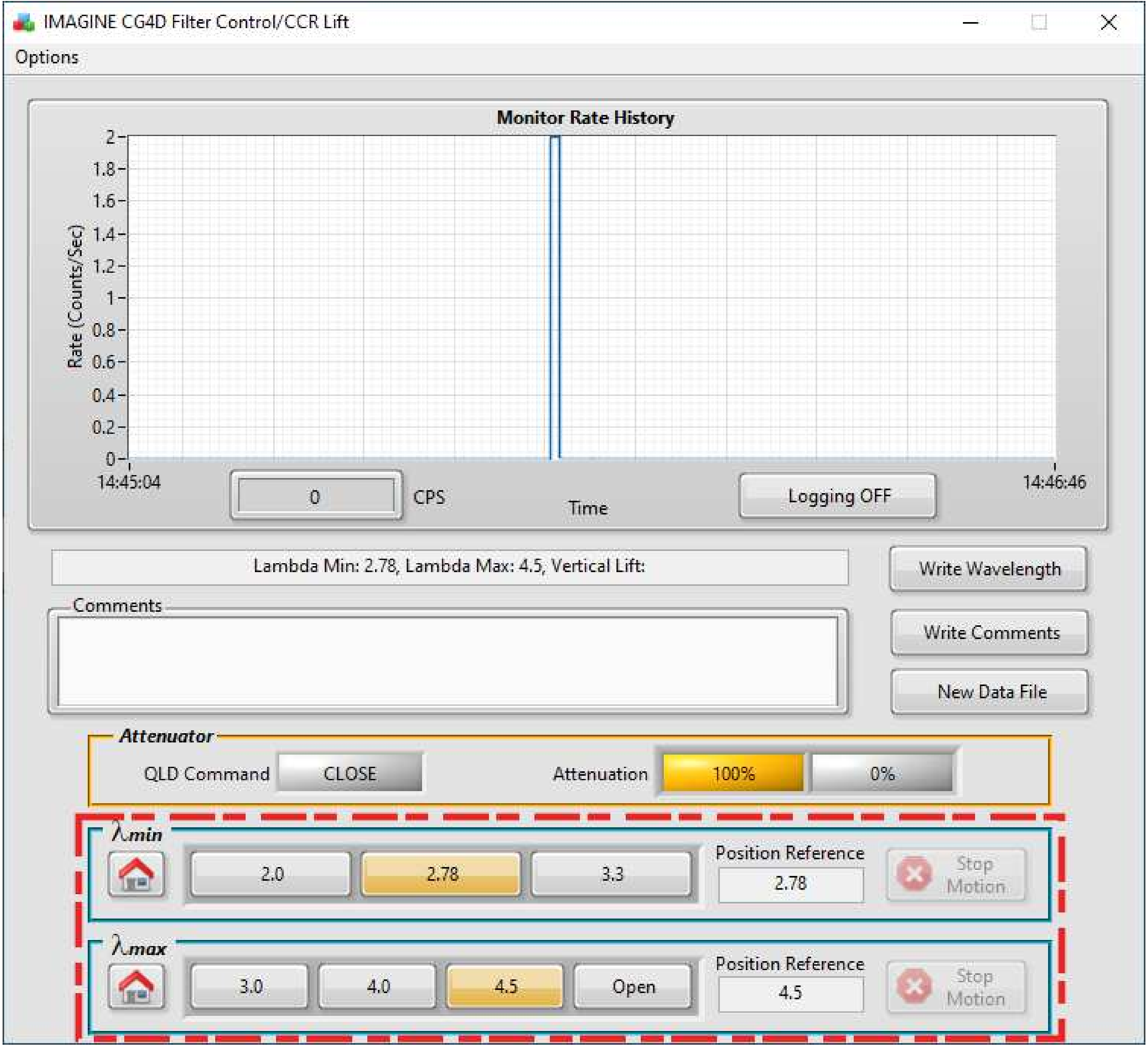

IMAGINE CG4D Filter Control/CCR Lift

CPS: 0

Lambda Min: 2.78, Lambda Max: 4.5, Vertical Lift:

Comments:

Attenuator

QLD Command: CLOSE

Attenuation: 100%

λmin Position Reference: 2.78

λmax Position Reference: 4.5

Options
Monitor Rate History
Rate (Counts/Sec)
2
1.8
1.6
1.4
1.2
1
0.8
0.6
0.4
0.2
0
14:45:04
Time
14:46:46
Logging OFF
Write Wavelength
Write Comments
New Data File
0%
2.0
2.78
3.3
Stop Motion
3.0
4.0
4.5
Open
Stop Motion

Supplementary Figure 10

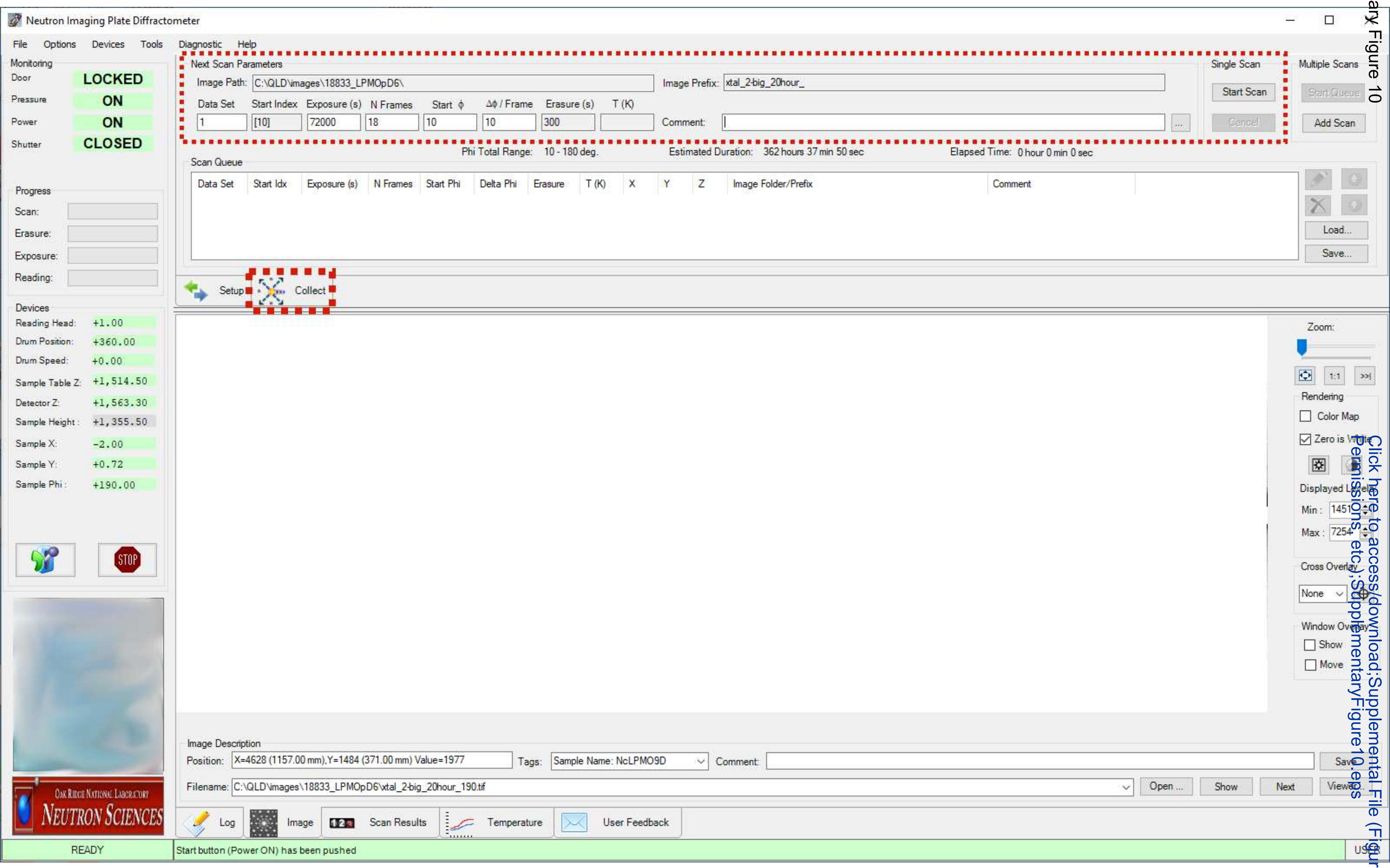
Neutron Imaging Plate Diffractometer
File
Options
Devices
Tools
Diagnostic
Help
Single Scan
Start Scan
Cancel
Multiple Scans
Start Queue
Add Scan
Load...
Save...
Setup
Collect
Zoom:
1:1
Rendering
Color Map
Zero is White
Displayed Levels
Cross Overlay
Window Overlay
Open ...
Show
Next
Viewer
Save
Log
Image
Scan Results
Temperature
User Feedback
STOP
Oak Ridge National Laboratory
Neutron Sciences

Monitoring

Door	LOCKED
Pressure	ON
Power	ON
Shutter	CLOSED

Progress

Scan:

Erasure:

Exposure:

Reading:

Devices

Reading Head:	+1.00
Drum Position:	+360.00
Drum Speed:	+0.00
Sample Table Z:	+1,514.50
Detector Z:	+1,563.30
Sample Height :	+1,355.50
Sample X:	-2.00
Sample Y:	+0.72
Sample Phi :	+190.00

Next Scan Parameters

Image Path: C:\QLD\images\18833_LPMOpD6\

Image Prefix: xtal_2-big_20hour_

Data Set	Start Index	Exposure (s)	N Frames	Start ϕ	Δϕ / Frame	Erasure (s)	T (K)
1	[10]	72000	18	10	10	300	

Comment:

Phi Total Range: 10 - 180 deg.

Estimated Duration: 362 hours 37 min 50 sec

Elapsed Time: 0 hour 0 min 0 sec

Scan Queue

Data Set	Start Idx	Exposure (s)	N Frames	Start Phi	Delta Phi	Erasure	T (K)	X	Y	Z	Image Folder/Prefix	Comment

Min : 1451

Max : 7254

Cross Overlay: None

Window Overlay: ☐ Show ☐ Move

Rendering: ☐ Color Map ☑ Zero is White

Image Description

Position: X=4628 (1157.00 mm),Y=1484 (371.00 mm) Value=1977

Tags: Sample Name: NcLPMO9D

Comment:

Filename: C:\QLD\images\18833_LPMOpD6\xtal_2-big_20hour_190.tif

READY

Start button (Power ON) has been pushed

Supplementary Figure 11

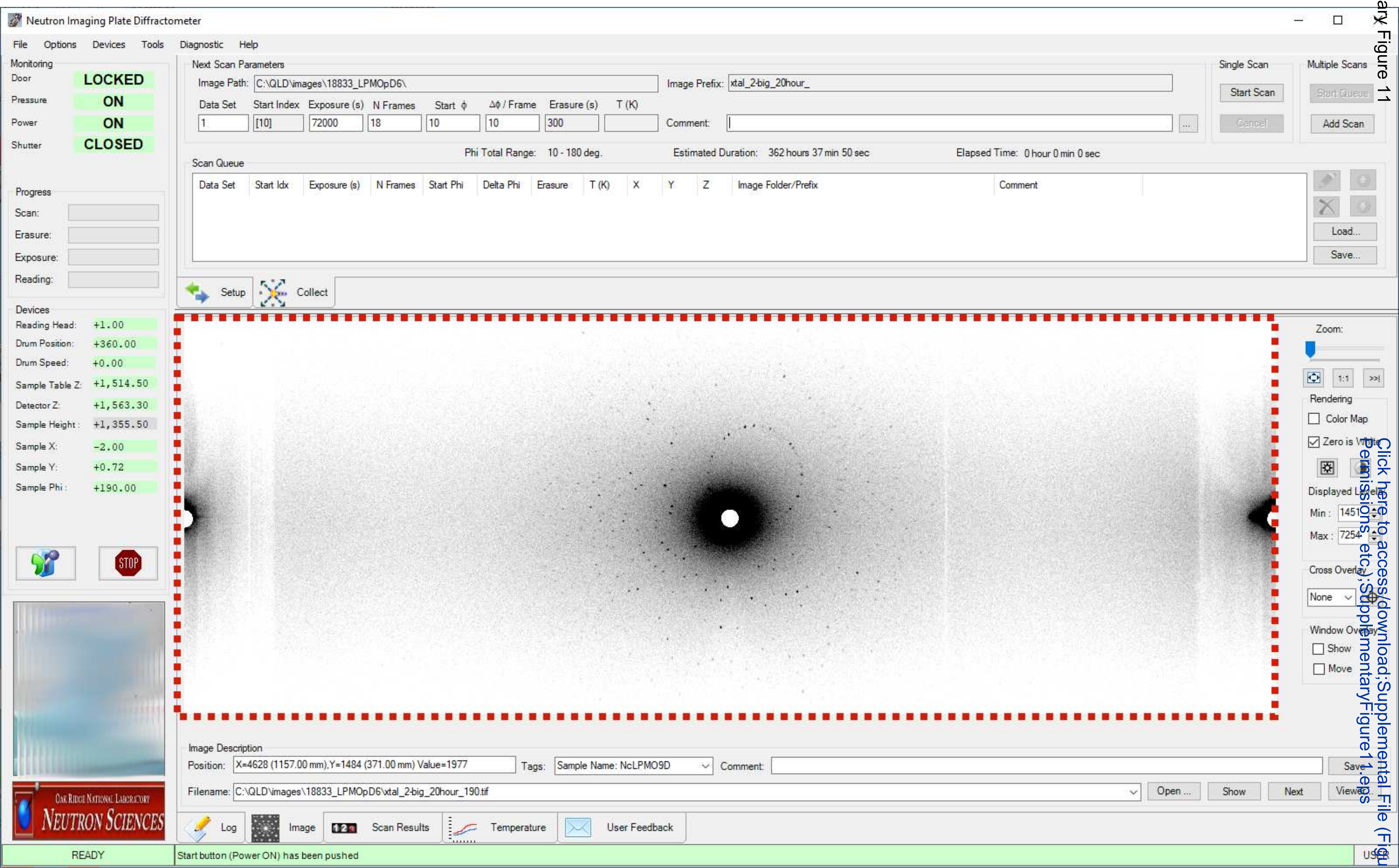
Neutron Imaging Plate Diffractometer
File
Options
Devices
Tools
Diagnostic
Help
Single Scan
Start Scan
Cancel
Multiple Scans
Start Queue
Add Scan
Load...
Save...
Setup
Collect
Zoom:
1:1
Open ...
Show
Next
Viewer
Save
Log
Image
Scan Results
Temperature
User Feedback
STOP
OAK RIDGE NATIONAL LABORATORY
NEUTRON SCIENCES

Monitoring
Door: LOCKED
Pressure: ON
Power: ON
Shutter: CLOSED

Progress
Scan:
Erasure:
Exposure:
Reading:

Devices
Reading Head: +1.00
Drum Position: +360.00
Drum Speed: +0.00
Sample Table Z: +1,514.50
Detector Z: +1,563.30
Sample Height: +1,355.50
Sample X: -2.00
Sample Y: +0.72
Sample Phi: +190.00

Next Scan Parameters
Image Path: C:\QLD\images\18833_LPMOpD6\
Image Prefix: xtal_2-big_20hour_

Data Set	Start Index	Exposure (s)	N Frames	Start ϕ	Δϕ / Frame	Erasure (s)	T (K)
1	[10]	72000	18	10	10	300	

Comment:

Phi Total Range: 10 - 180 deg.
Estimated Duration: 362 hours 37 min 50 sec
Elapsed Time: 0 hour 0 min 0 sec

Scan Queue

Data Set	Start Idx	Exposure (s)	N Frames	Start Phi	Delta Phi	Erasure	T (K)	X	Y	Z	Image Folder/Prefix	Comment

Rendering
☐ Color Map
☑ Zero is White
Displayed Levels
Min : 1451
Max : 7254
Cross Overlay: None
Window Overlay
☐ Show
☐ Move

Image Description
Position: X=4628 (1157.00 mm),Y=1484 (371.00 mm) Value=1977
Tags: Sample Name: NcLPMO9D
Comment:
Filename: C:\QLD\images\18833_LPMOpD6\xtal_2-big_20hour_190.tif

READY
Start button (Power ON) has been pushed

Supplementary Figure 12

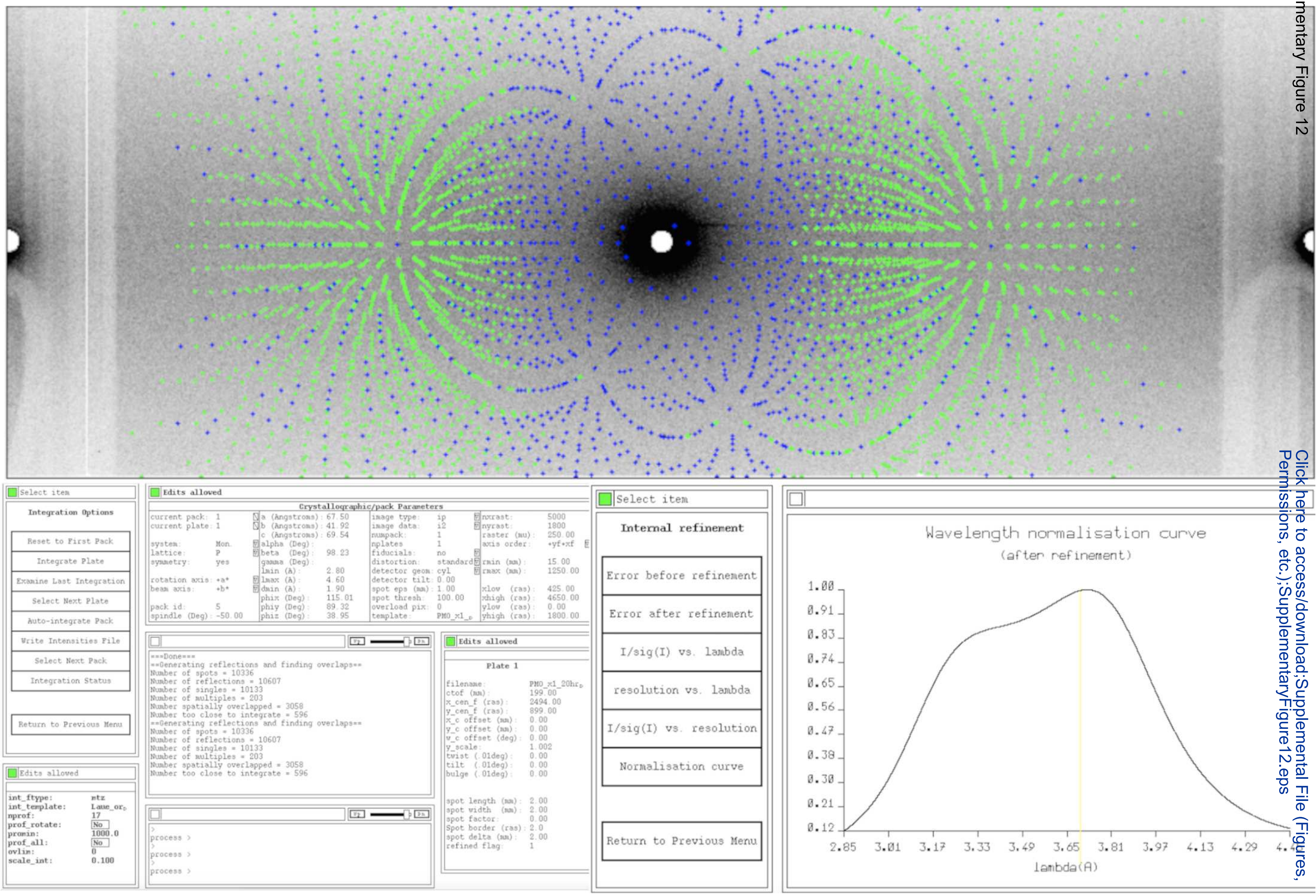
Select item
Integration Options
Reset to First Pack
Integrate Plate
Examine Last Integration
Select Next Plate
Auto-integrate Pack
Write Intensities File
Select Next Pack
Integration Status
Return to Previous Menu
Edits allowed
Crystallographic/pack Parameters
Edits allowed
Plate 1
Select item
Internal refinement
Error before refinement
Error after refinement
I/sig(I) vs. lambda
resolution vs. lambda
I/sig(I) vs. resolution
Normalisation curve
Return to Previous Menu
Wavelength normalisation curve
(after refinement)
1.00
0.91
0.83
0.74
0.65
0.56
0.47
0.38
0.30
0.21
0.12
2.85
3.01
3.17
3.33
3.49
3.65
3.81
3.97
4.13
4.29
4.4
lambda(A)

```
int_ftype:        mtz
int_template:     Laue_or
nprof:            17
prof_rotate:      No
promin:           1000.0
prof_all:         No
ovlim:            0
scale_int:        0.100
```

```
current pack:  1          a (Angstroms): 67.50    image type:      ip          nxrast:        5000
current plate: 1          b (Angstroms): 41.92    image data:      i2          nyrast:        1800
                          c (Angstroms): 69.54    numpack:         1           raster (mu):   250.00
system:        Mon.       alpha (Deg):            nplates          1           axis order:    +yf+xf
lattice:       P          beta  (Deg):   98.23    fiducials:       no
symmetry:      yes        gamma (Deg):            distortion:      standard    rmin (mm):     15.00
                          lmin (A):      2.80     detector geom:   cyl         rmax (mm):     1250.00
rotation axis: +a*        lmax (A):      4.60     detector tilt:   0.00
beam axis:     +b*        dmin (A):      1.90     spot eps (mm):   1.00        xlow  (ras):   425.00
                          phix (Deg):    115.01   spot thresh:     100.00      xhigh (ras):   4650.00
pack id:       5          phiy (Deg):    89.32    overload pix:    0           ylow  (ras):   0.00
spindle (Deg): -50.00     phiz (Deg):    38.95    template:        PMO_x1_     yhigh (ras):   1800.00
```

```
===Done===
==Generating reflections and finding overlaps==
Number of spots = 10336
Number of reflections = 10607
Number of singles = 10133
Number of multiples = 203
Number spatially overlapped = 3058
Number too close to integrate = 596
==Generating reflections and finding overlaps==
Number of spots = 10336
Number of reflections = 10607
Number of singles = 10133
Number of multiples = 203
Number spatially overlapped = 3058
Number too close to integrate = 596
```

```
>
process >
>
process >
>
process >
```

```
filename:            PMO_x1_20hr
ctof (mm):           199.00
x_cen_f (ras):       2494.00
y_cen_f (ras):       899.00
x_c offset (mm):     0.00
y_c offset (mm):     0.00
w_c offset (deg):    0.00
y_scale:             1.002
twist (.01deg):      0.00
tilt  (.01deg):      0.00
bulge (.01deg):      0.00

spot length (mm):    2.00
spot width  (mm):    2.00
spot factor:         0.00
Spot border (ras):   2.0
spot delta (mm):     2.00
refined flag:        1
```

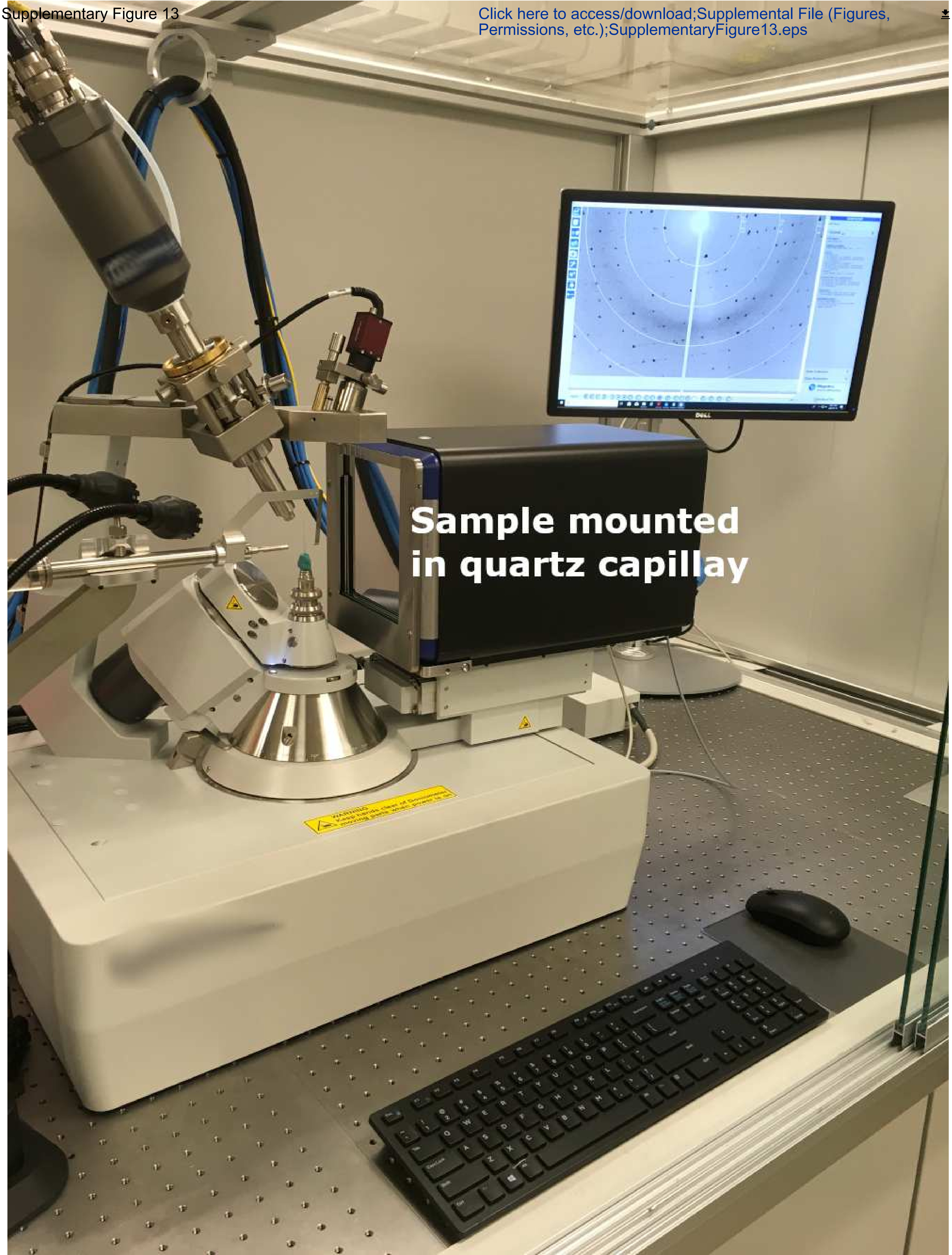

Sample mounted in quartz capillay

Supplementary Figure 14

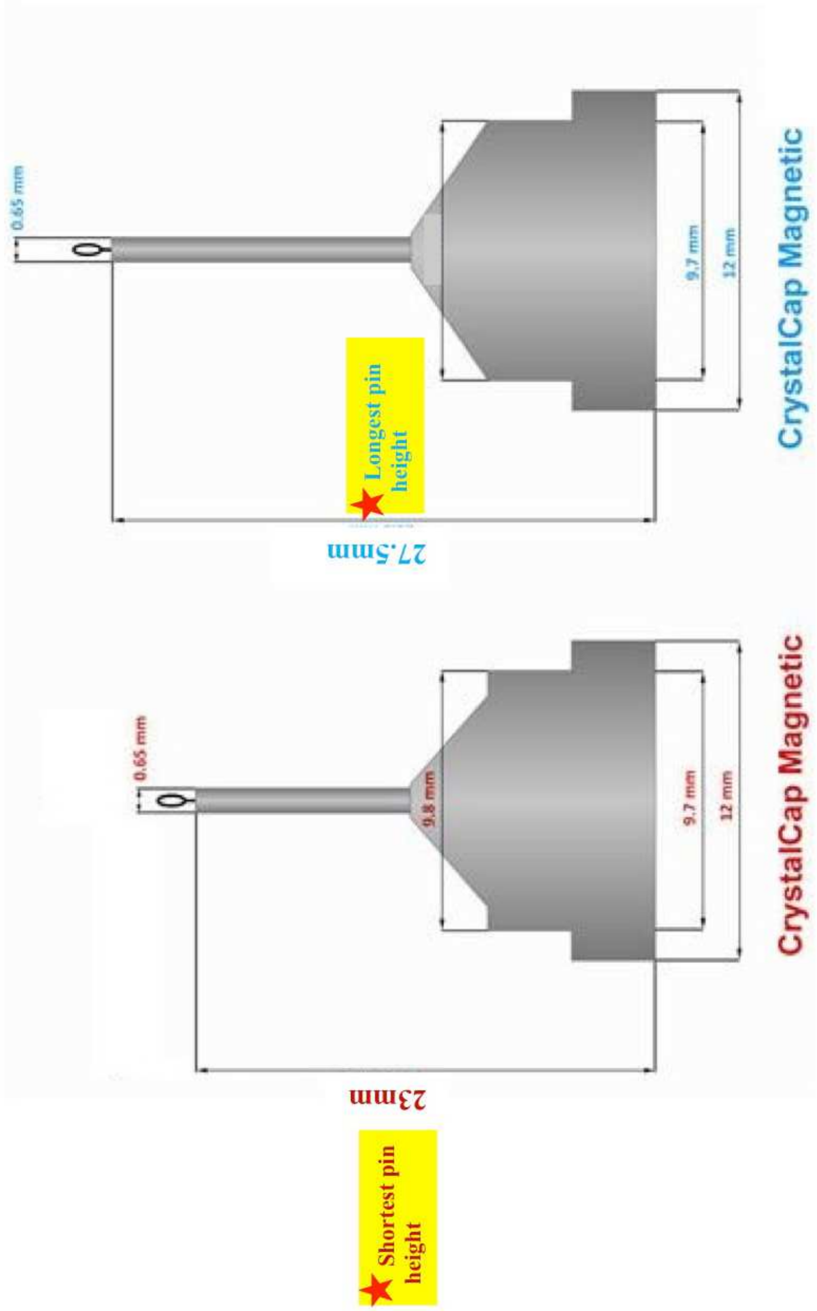
CrystalCap Magnetic
0.65 mm
9.7 mm
12 mm
Longest pin height
27.5mm
CrystalCap Magnetic
0.65 mm
9.8 mm
9.7 mm
12 mm
23mm
Shortest pin height

Supplementary Figure 15

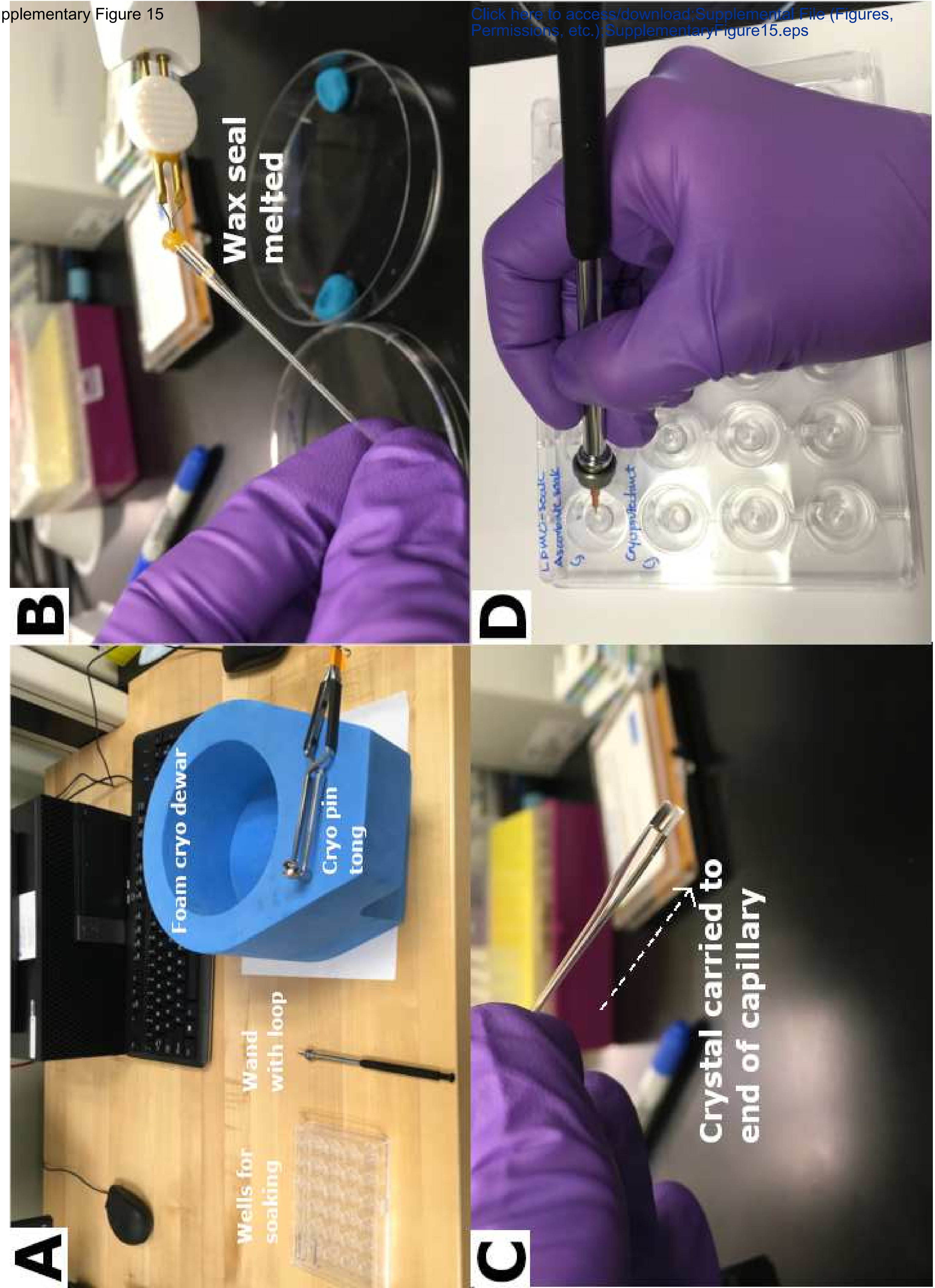
A
Foam cryo dewar
Cryo pin tong
Wand with loop
Wells for soaking
B
Wax seal melted
C
Crystal carried to end of capillary
D
LPMO-Soak
Ascorbate soak
6
Cryoprotectant
6

Supplementary Figure 16

Click here to access/download;Supplemental File (Figures, Permissions, etc.);SupplementaryFigure16.eps

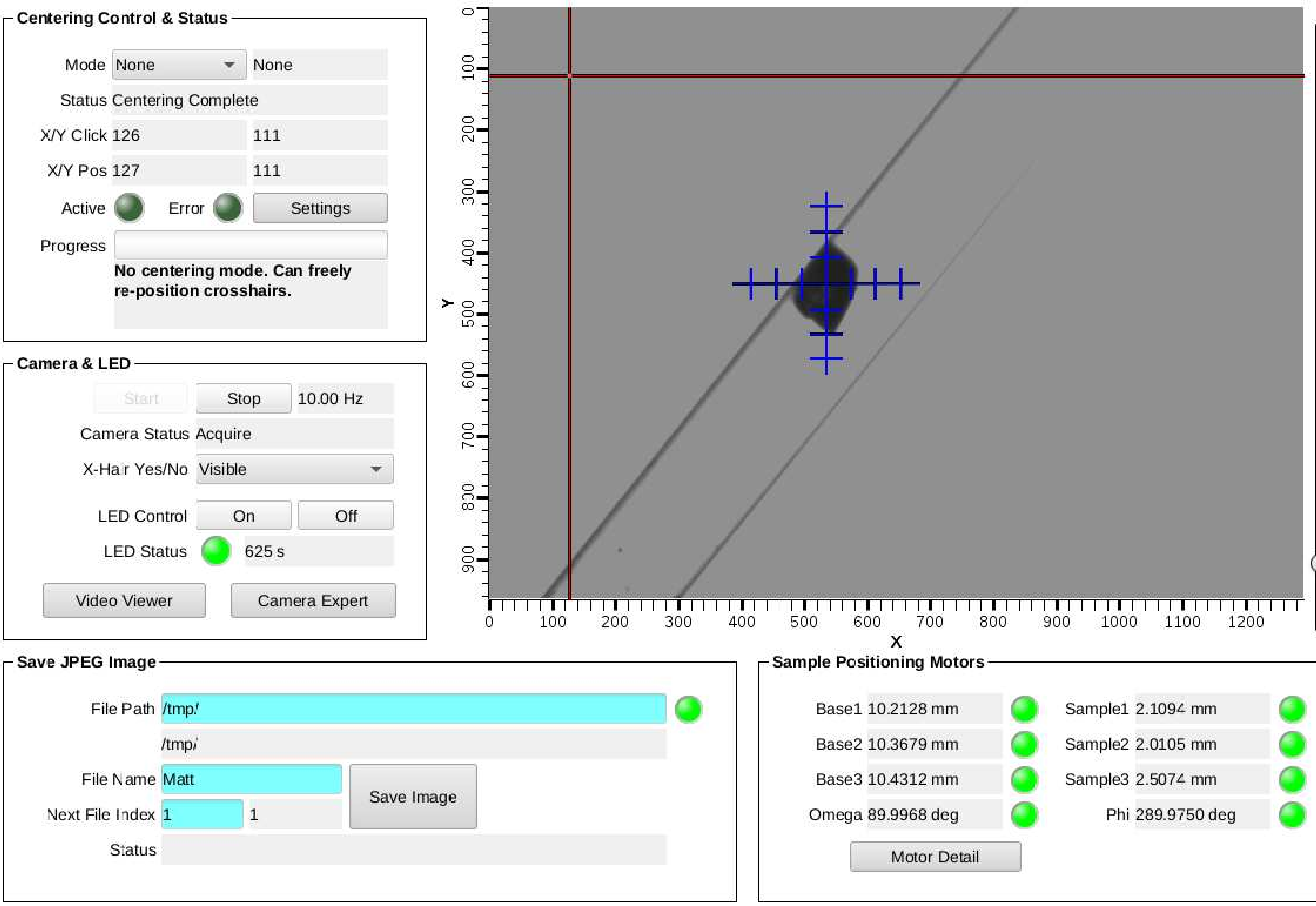
Y
0
100
200
300
400
500
600
700
800
900
X
0
100
200
300
400
500
600
700
800
900
1000
1100
1200
Start
Stop
On
Off
Settings
Video Viewer
Camera Expert
Save Image
Motor Detail

Centering Control & Status

Mode None None

Status Centering Complete

X/Y Click 126 111

X/Y Pos 127 111

Active ● Error ●

Progress

No centering mode. Can freely re-position crosshairs.

Camera & LED

10.00 Hz

Camera Status Acquire

X-Hair Yes/No Visible

LED Control

LED Status ● 625 s

Save JPEG Image

File Path /tmp/ ●

/tmp/

File Name Matt

Next File Index 1 1

Status

Sample Positioning Motors

Base1	10.2128 mm	●	Sample1	2.1094 mm	●
Base2	10.3679 mm	●	Sample2	2.0105 mm	●
Base3	10.4312 mm	●	Sample3	2.5074 mm	●
Omega	89.9968 deg	●	Phi	289.9750 deg	●

Supplementary Figure 17

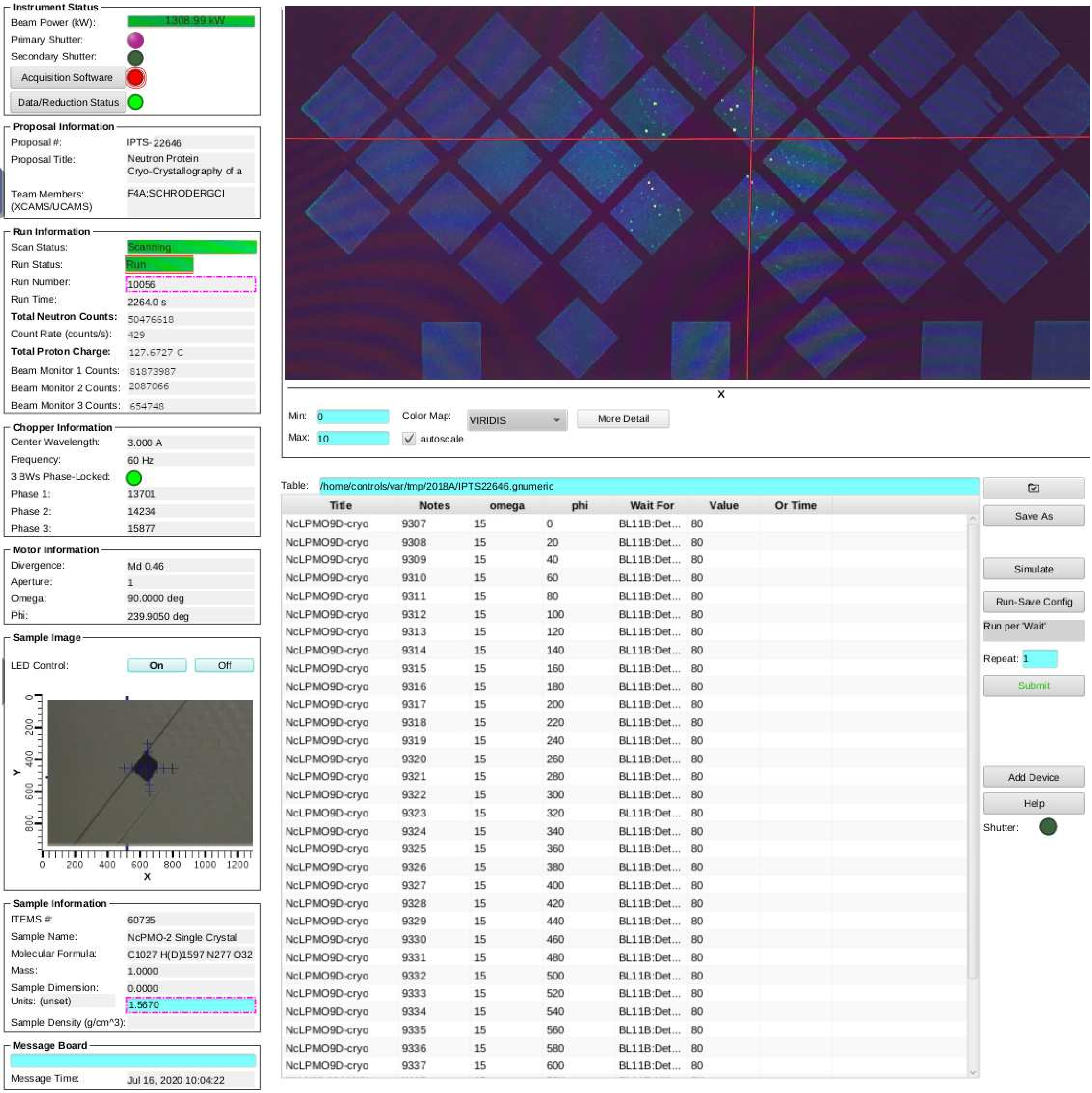

Instrument Status

Beam Power (kW): 1308.99 kW

Primary Shutter:

Secondary Shutter:

Proposal Information

Proposal #: IPTS-22646

Proposal Title: Neutron Protein Cryo-Crystallography of a

Team Members: (XCAMS/UCAMS) F4A;SCHRODERGCI

Run Information

Scan Status: Scanning

Run Status: Run

Run Number: 10056

Run Time: 2264.0 s

Total Neutron Counts: 50476618

Count Rate (counts/s): 429

Total Proton Charge: 127.6727 C

Beam Monitor 1 Counts: 81873987

Beam Monitor 2 Counts: 2087066

Beam Monitor 3 Counts: 654748

Chopper Information

Center Wavelength: 3.000 A

Frequency: 60 Hz

3 BWs Phase-Locked:

Phase 1: 13701

Phase 2: 14234

Phase 3: 15877

Motor Information

Divergence: Md 0.46

Aperture: 1

Omega: 90.0000 deg

Phi: 239.9050 deg

Sample Image

Sample Information

ITEMS #: 60735

Sample Name: NcPMO-2 Single Crystal

Molecular Formula: C1027 H(D)1597 N277 O32

Mass: 1.0000

Sample Dimension: 0.0000

Units: (unset) 1.5670

Sample Density (g/cm^3):

Message Board

Message Time: Jul 16, 2020 10:04:22

Min: 0

Max: 10

Color Map: VIRIDIS

☑ autoscale

Table: /home/controls/var/tmp/2018A/IPTS22646.gnumeric

Run per 'Wait'

Repeat: 1

Title	Notes	omega	phi	Wait For	Value	Or Time
NcLPMO9D-cryo	9307	15	0	BL11B:Det...	80	
NcLPMO9D-cryo	9308	15	20	BL11B:Det...	80	
NcLPMO9D-cryo	9309	15	40	BL11B:Det...	80	
NcLPMO9D-cryo	9310	15	60	BL11B:Det...	80	
NcLPMO9D-cryo	9311	15	80	BL11B:Det...	80	
NcLPMO9D-cryo	9312	15	100	BL11B:Det...	80	
NcLPMO9D-cryo	9313	15	120	BL11B:Det...	80	
NcLPMO9D-cryo	9314	15	140	BL11B:Det...	80	
NcLPMO9D-cryo	9315	15	160	BL11B:Det...	80	
NcLPMO9D-cryo	9316	15	180	BL11B:Det...	80	
NcLPMO9D-cryo	9317	15	200	BL11B:Det...	80	
NcLPMO9D-cryo	9318	15	220	BL11B:Det...	80	
NcLPMO9D-cryo	9319	15	240	BL11B:Det...	80	
NcLPMO9D-cryo	9320	15	260	BL11B:Det...	80	
NcLPMO9D-cryo	9321	15	280	BL11B:Det...	80	
NcLPMO9D-cryo	9322	15	300	BL11B:Det...	80	
NcLPMO9D-cryo	9323	15	320	BL11B:Det...	80	
NcLPMO9D-cryo	9324	15	340	BL11B:Det...	80	
NcLPMO9D-cryo	9325	15	360	BL11B:Det...	80	
NcLPMO9D-cryo	9326	15	380	BL11B:Det...	80	
NcLPMO9D-cryo	9327	15	400	BL11B:Det...	80	
NcLPMO9D-cryo	9328	15	420	BL11B:Det...	80	
NcLPMO9D-cryo	9329	15	440	BL11B:Det...	80	
NcLPMO9D-cryo	9330	15	460	BL11B:Det...	80	
NcLPMO9D-cryo	9331	15	480	BL11B:Det...	80	
NcLPMO9D-cryo	9332	15	500	BL11B:Det...	80	
NcLPMO9D-cryo	9333	15	520	BL11B:Det...	80	
NcLPMO9D-cryo	9334	15	540	BL11B:Det...	80	
NcLPMO9D-cryo	9335	15	560	BL11B:Det...	80	
NcLPMO9D-cryo	9336	15	580	BL11B:Det...	80	
NcLPMO9D-cryo	9337	15	600	BL11B:Det...	80	

Supplementary Figure 18

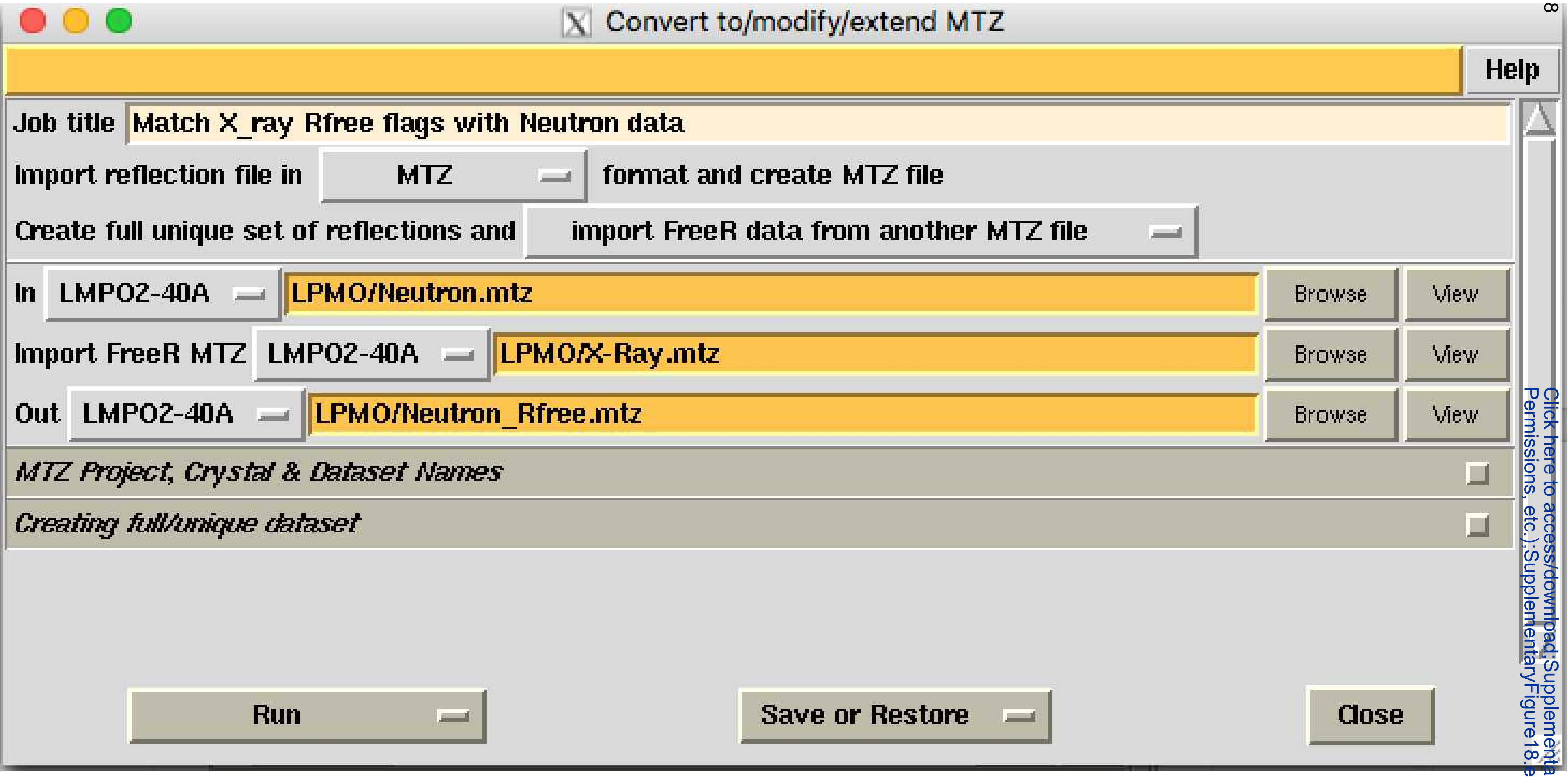

Help
MTZ Project, Crystal & Dataset Names ☐
Creating full/unique dataset ☐
Browse
View
Run
Save or Restore
Close

Convert to/modify/extend MTZ

Job title: Match X_ray Rfree flags with Neutron data

Import reflection file in MTZ format and create MTZ file

Create full unique set of reflections and import FreeR data from another MTZ file

In LMPO2-40A LPMO/Neutron.mtz

Import FreeR MTZ LMPO2-40A LPMO/X-Ray.mtz

Out LMPO2-40A LPMO/Neutron_Rfree.mtz

Supplementary Figure 19

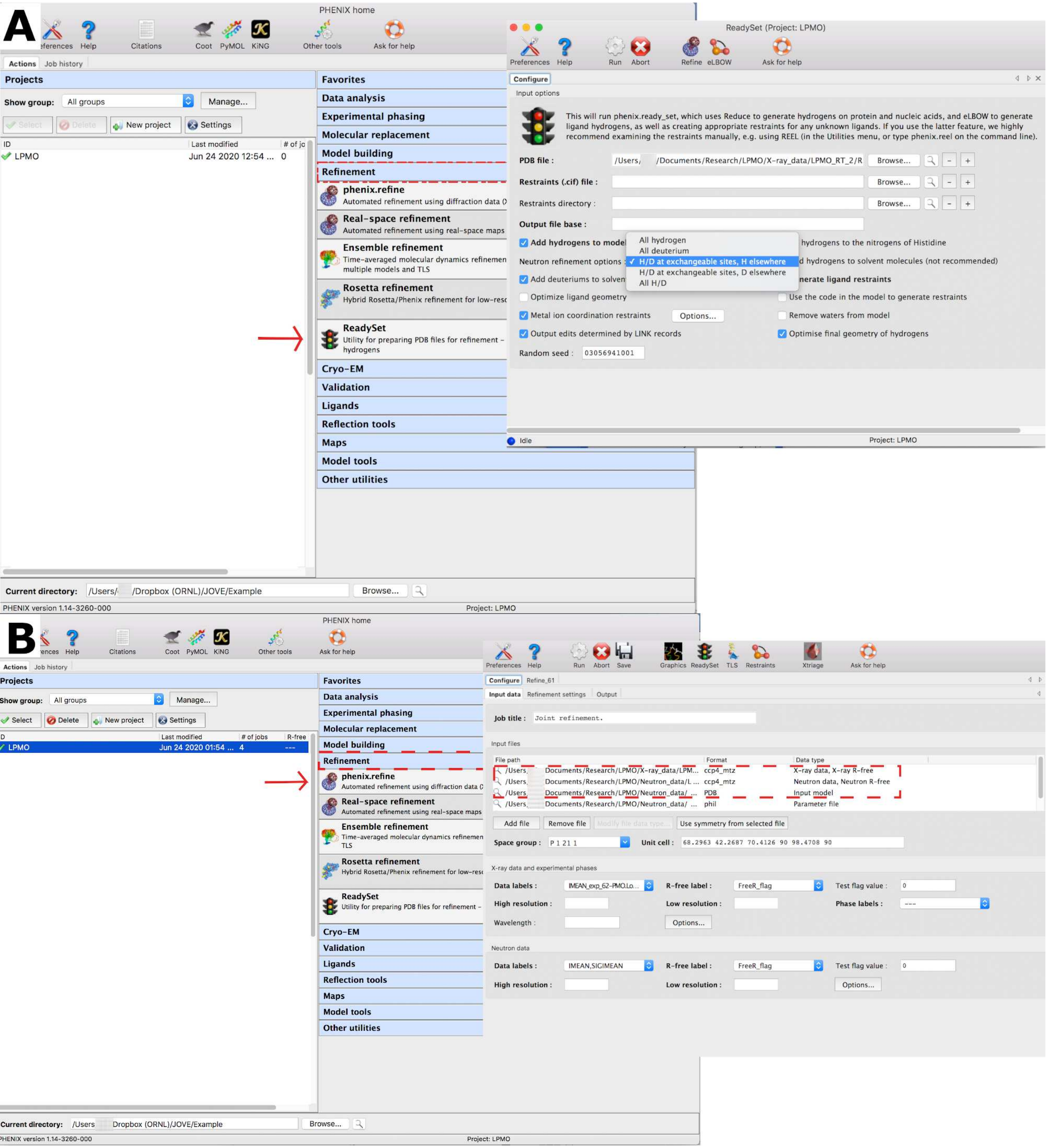
A
PHENIX home
Preferences
Help
Citations
Coot
PyMOL
KiNG
Other tools
Ask for help
Actions
Job history
Projects
Show group:
All groups
Manage...
Select
Delete
New project
Settings
Favorites
Data analysis
Experimental phasing
Molecular replacement
Model building
Refinement
phenix.refine
Automated refinement using diffraction data
Real-space refinement
Automated refinement using real-space maps
Ensemble refinement
Time-averaged molecular dynamics refinement
Rosetta refinement
Hybrid Rosetta/Phenix refinement for low-resolution
ReadySet
Utility for preparing PDB files for refinement – hydrogens
Cryo-EM
Validation
Ligands
Reflection tools
Maps
Model tools
Other utilities
Current directory:
Browse...
ReadySet (Project: LPMO)
Refine
eLBOW
Run
Abort
Configure
Input options
Browse...
Options...
Idle
B
Save
Graphics
ReadySet
TLS
Restraints
Xtriage
Refine_61
Input data
Refinement settings
Output
Add file
Remove file
Modify file data type...
Use symmetry from selected file
Options...

Panel A

ID	Last modified	# of jobs
✓ LPMO	Jun 24 2020 12:54 ...	0

Current directory: /Users/[redacted]/Dropbox (ORNL)/JOVE/Example

PHENIX version 1.14-3260-000 Project: LPMO

This will run phenix.ready_set, which uses Reduce to generate hydrogens on protein and nucleic acids, and eLBOW to generate ligand hydrogens, as well as creating appropriate restraints for any unknown ligands. If you use the latter feature, we highly recommend examining the restraints manually, e.g. using REEL (in the Utilities menu, or type phenix.reel on the command line).

PDB file : /Users/[redacted]/Documents/Research/LPMO/X-ray_data/LPMO_RT_2/R

Restraints (.cif) file :

Restraints directory :

Output file base :

☑ Add hydrogens to model … hydrogens to the nitrogens of Histidine

Neutron refinement options :
- All hydrogen
- All deuterium
- ✓ H/D at exchangeable sites, H elsewhere
- H/D at exchangeable sites, D elsewhere
- All H/D

…d hydrogens to solvent molecules (not recommended)

☑ Add deuteriums to solven… …nerate ligand restraints

☐ Optimize ligand geometry ☐ Use the code in the model to generate restraints

☑ Metal ion coordination restraints ☐ Remove waters from model

☑ Output edits determined by LINK records ☑ Optimise final geometry of hydrogens

Random seed : 03056941001

Panel B

ID	Last modified	# of jobs	R-free
✓ LPMO	Jun 24 2020 01:54 ...	4	---

Job title : Joint refinement.

Input files

File path	Format	Data type
/Users/[redacted]/Documents/Research/LPMO/X-ray_data/LPM...	ccp4_mtz	X-ray data, X-ray R-free
/Users/[redacted]/Documents/Research/LPMO/Neutron_data/L ...	ccp4_mtz	Neutron data, Neutron R-free
/Users/[redacted]/Documents/Research/LPMO/Neutron_data/ ...	PDB	Input model
/Users/[redacted]/Documents/Research/LPMO/Neutron_data/ ...	phil	Parameter file

Space group : P 1 21 1 Unit cell : 68.2963 42.2687 70.4126 90 98.4708 90

X-ray data and experimental phases

Data labels : IMEAN_exp_62-PMO.Lo... R-free label : FreeR_flag Test flag value : 0

High resolution : Low resolution : Phase labels : ---

Wavelength :

Neutron data

Data labels : IMEAN,SIGIMEAN R-free label : FreeR_flag Test flag value : 0

High resolution : Low resolution :

Current directory: /Users[redacted]Dropbox (ORNL)/JOVE/Example

PHENIX version 1.14-3260-000 Project: LPMO

Supplementary Figure 20

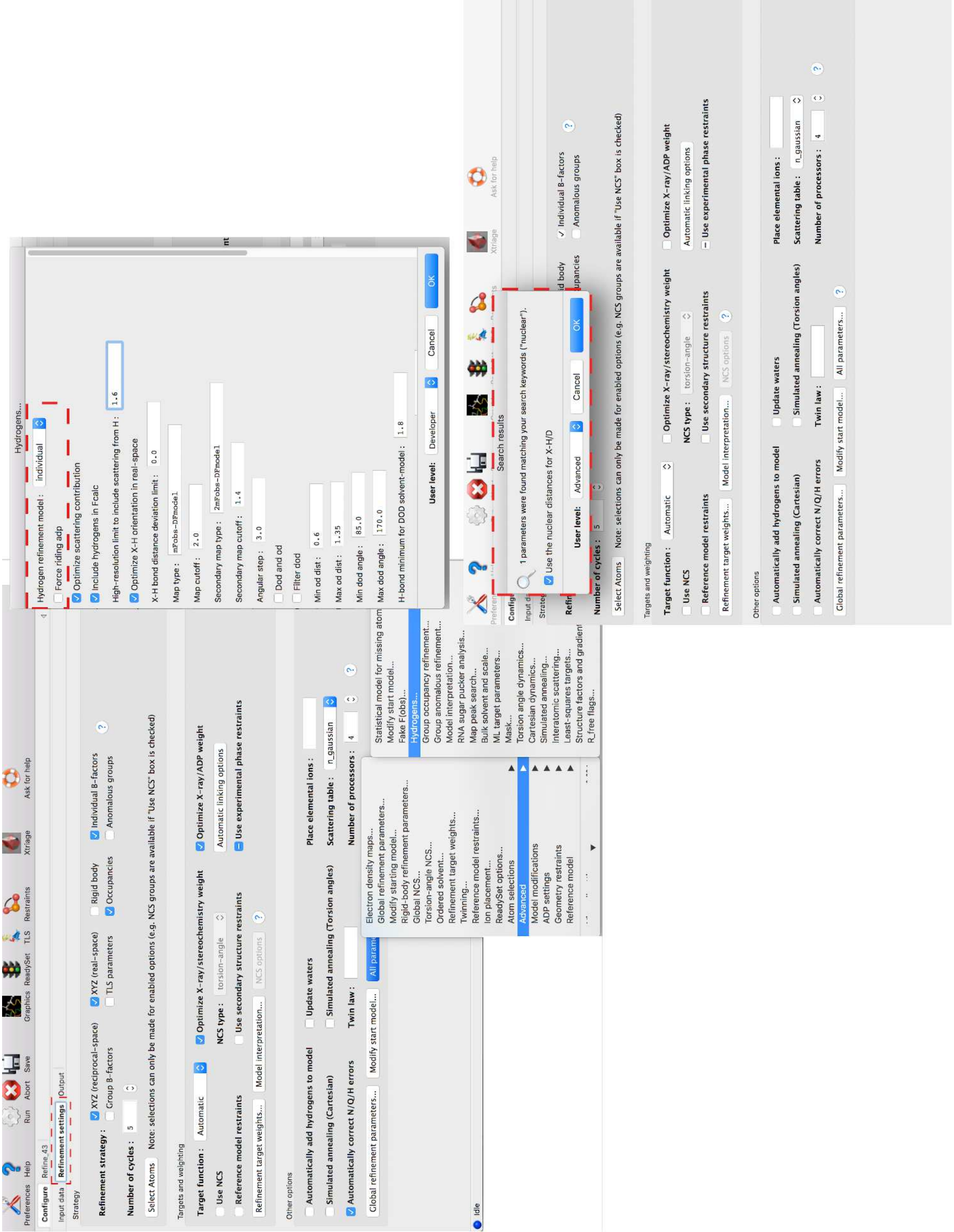
Preferences
Help
Run
Abort
Save
Graphics
ReadySet
TLS
Restraints
Xtriage
Ask for help
Configure
Refine_43
Input data
Refinement settings
Output
Strategy
Targets and weighting
Other options
Select Atoms
Model interpretation...
Refinement target weights...
NCS options
Global refinement parameters...
Modify start model...
All parameters...
Electron density maps...
Global refinement parameters...
Modify starting model...
Rigid-body refinement parameters...
Global NCS...
Torsion-angle NCS...
Ordered solvent...
Refinement target weights...
Twinning...
Reference model restraints...
Ion placement...
ReadySet options...
Atom selection
Advanced
Model modifications
ADP settings
Geometry restraints
Reference model
Statistical model for missing atoms
Modify start model...
Fake F(obs)...
Hydrogens...
Group occupancy refinement...
Group anomalous refinement...
Model interpretation...
RNA sugar pucker analysis...
Map peak search...
Bulk solvent and scale...
ML target parameters...
Mask...
Torsion angle dynamics...
Cartesian dynamics...
Simulated annealing...
Interatomic scattering...
Least-squares targets...
Structure factors and gradients...
R_free flags...
Idle
Hydrogens...
Cancel
OK
Search results
Cancel
OK

Refinement strategy : ☑ XYZ (reciprocal-space) ☑ XYZ (real-space) ☐ Rigid body ☑ Individual B-factors ☐ Group B-factors ☐ TLS parameters ☑ Occupancies ☐ Anomalous groups

Number of cycles : 5

Note: selections can only be made for enabled options (e.g. NCS groups are available if "Use NCS" box is checked)

Target function : Automatic ☑ Optimize X-ray/stereochemistry weight ☑ Optimize X-ray/ADP weight

☐ Use NCS NCS type : torsion-angle Automatic linking options

☐ Reference model restraints ☐ Use secondary structure restraints ☑ Use experimental phase restraints

☐ Automatically add hydrogens to model ☐ Update waters Place elemental ions :

☐ Simulated annealing (Cartesian) ☐ Simulated annealing (Torsion angles) Scattering table : n_gaussian

☑ Automatically correct N/Q/H errors Twin law : Number of processors : 4

Hydrogen refinement model : individual

☐ Force riding adp

☑ Optimize scattering contribution

☑ Include hydrogens in Fcalc

High-resolution limit to include scattering from H : 1.6

☑ Optimize X-H orientation in real-space

X-H bond distance deviation limit : 0.0

Map type : mFobs-DFmodel

Map cutoff : 2.0

Secondary map type : 2mFobs-DFmodel

Secondary map cutoff : 1.4

Angular step : 3.0

☐ Dod and od

☐ Filter dod

Min od dist : 0.6

Max od dist : 1.35

Min dod angle : 85.0

Max dod angle : 170.0

H-bond minimum for DOD solvent-model : 1.8

User level: Developer

1 parameters were found matching your search keywords ("nuclear").

☑ Use the nuclear distances for X-H/D

User level: Advanced

Supplementary Figure 21

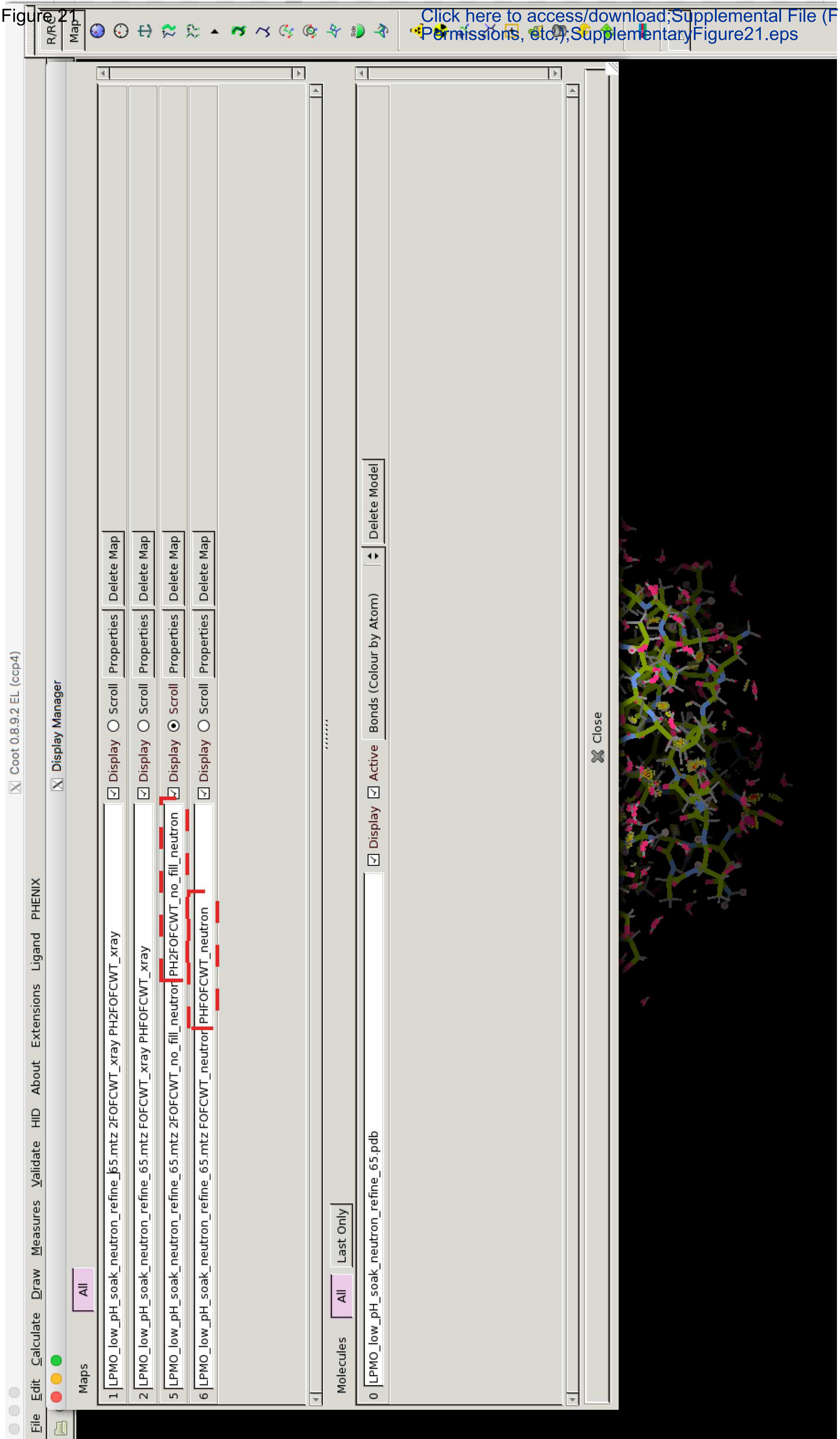
Coot 0.8.9.2 EL (ccp4)
File
Edit
Calculate
Draw
Measures
Validate
HID
About
Extensions
Ligand
PHENIX
R/RC
Map
Display Manager
Maps
All
Display
Scroll
Properties
Delete Map
Molecules
All
Last Only
Display
Active
Delete Model
Close

Maps

1 LPMO_low_pH_soak_neutron_refine_65.mtz 2FOFCWT_xray PH2FOFCWT_xray ☑ Display ○ Scroll

2 LPMO_low_pH_soak_neutron_refine_65.mtz FOFCWT_xray PHFOFCWT_xray ☑ Display ○ Scroll

5 LPMO_low_pH_soak_neutron_refine_65.mtz 2FOFCWT_no_fill_neutron PH2FOFCWT_no_fill_neutron ☑ Display ● Scroll

6 LPMO_low_pH_soak_neutron_refine_65.mtz FOFCWT_neutron PHFOFCWT_neutron ☑ Display ○ Scroll

Molecules

0 LPMO_low_pH_soak_neutron_refine_65.pdb ☑ Display ☑ Active Bonds (Colour by Atom)

Supplementary Figure 22

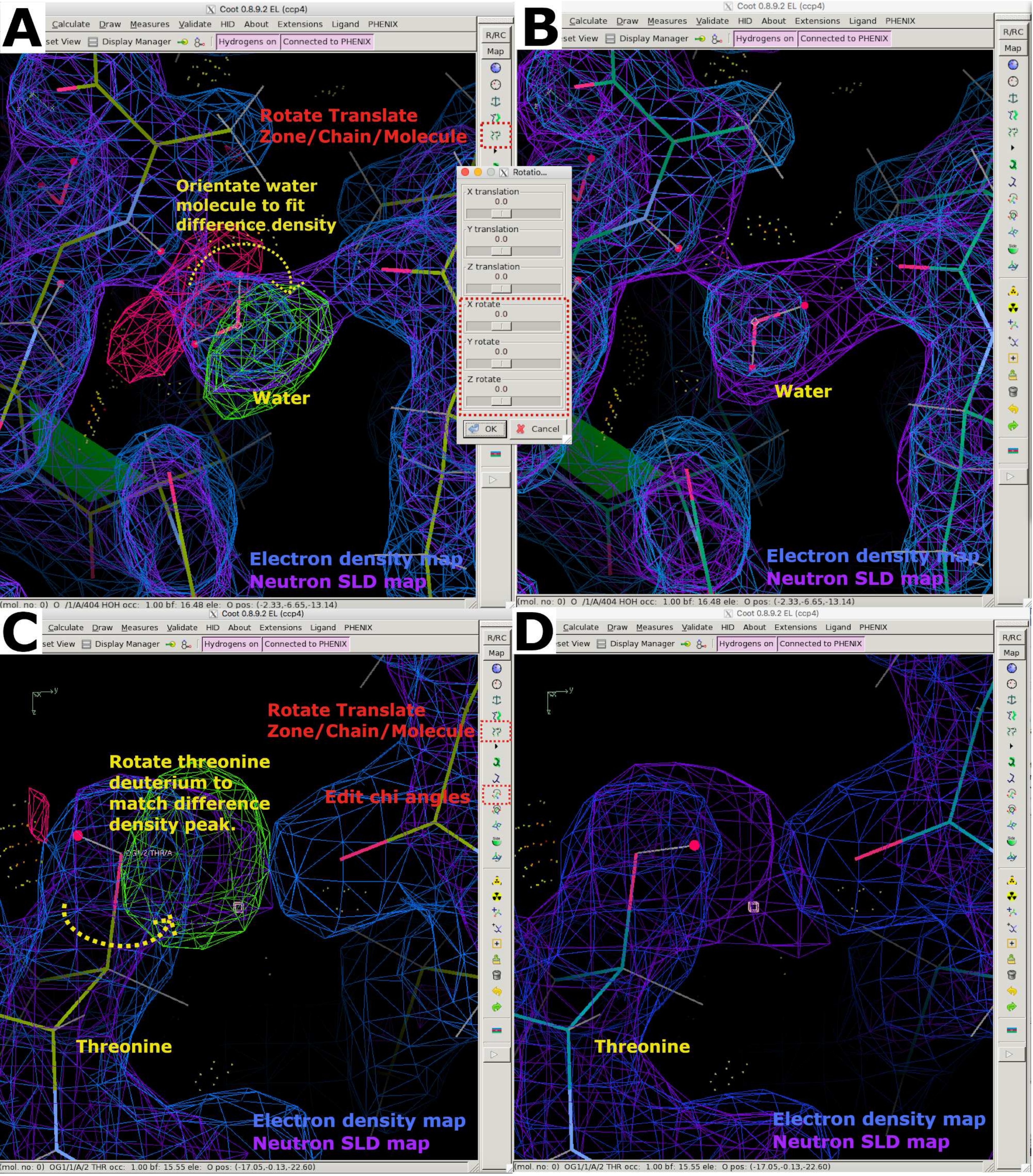
A
Coot 0.8.9.2 EL (ccp4)
Calculate Draw Measures Validate HID About Extensions Ligand PHENIX
set View Display Manager Hydrogens on Connected to PHENIX
R/RC
Map
Rotate Translate Zone/Chain/Molecule
Orientate water molecule to fit difference density
Water
Rotatio...
X translation 0.0
Y translation 0.0
Z translation 0.0
X rotate 0.0
Y rotate 0.0
Z rotate 0.0
OK
Cancel
Electron density map
Neutron SLD map
B
Coot 0.8.9.2 EL (ccp4)
Calculate Draw Measures Validate HID About Extensions Ligand PHENIX
set View Display Manager Hydrogens on Connected to PHENIX
R/RC
Map
Water
Electron density map
Neutron SLD map
C
Coot 0.8.9.2 EL (ccp4)
Calculate Draw Measures Validate HID About Extensions Ligand PHENIX
set View Display Manager Hydrogens on Connected to PHENIX
R/RC
Map
Rotate Translate Zone/Chain/Molecule
Rotate threonine deuterium to match difference density peak.
Edit chi angles
OG1/2 THR/A
Threonine
Electron density map
Neutron SLD map
D
Coot 0.8.9.2 EL (ccp4)
Calculate Draw Measures Validate HID About Extensions Ligand PHENIX
set View Display Manager Hydrogens on Connected to PHENIX
R/RC
Map
Threonine
Electron density map
Neutron SLD map

```
(mol. no: 0)  O  /1/A/404 HOH occ:  1.00 bf: 16.48 ele:  O pos: (-2.33,-6.65,-13.14)
```

```
(mol. no: 0)  O  /1/A/404 HOH occ:  1.00 bf: 16.48 ele:  O pos: (-2.33,-6.65,-13.14)
```

```
(mol. no: 0)  OG1/1/A/2 THR occ:  1.00 bf: 15.55 ele:  O pos: (-17.05,-0.13,-22.60)
```

```
(mol. no: 0)  OG1/1/A/2 THR occ:  1.00 bf: 15.55 ele:  O pos: (-17.05,-0.13,-22.60)
```

Supplementary Figure 23

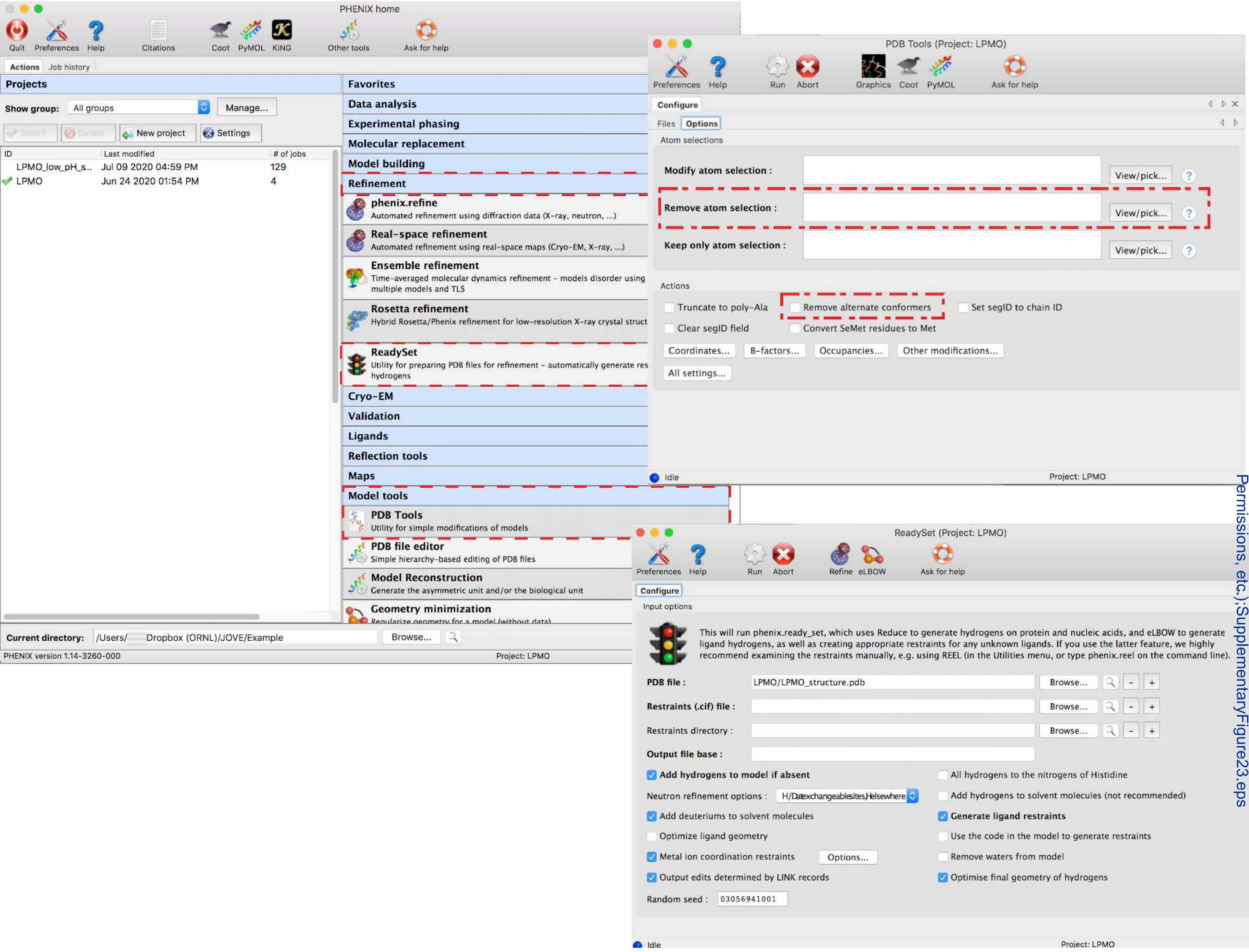
PHENIX home
Quit
Preferences
Help
Citations
Coot
PyMOL
KiNG
Other tools
Ask for help
Actions
Job history
Projects
Show group:
Manage...
Select
Delete
New project
Settings
Favorites
Data analysis
Experimental phasing
Molecular replacement
Model building
Refinement
phenix.refine
Real-space refinement
Ensemble refinement
Rosetta refinement
ReadySet
Cryo-EM
Validation
Ligands
Reflection tools
Maps
Model tools
PDB Tools
PDB file editor
Model Reconstruction
Geometry minimization
Browse...
PDB Tools (Project: LPMO)
Run
Abort
Graphics
Configure
Files
Options
Atom selections
View/pick...
Actions
Coordinates...
B-factors...
Occupancies...
Other modifications...
All settings...
ReadySet (Project: LPMO)
Refine
eLBOW
Input options
Options...

Show group: All groups

ID	Last modified	# of jobs
LPMO_low_pH_s..	Jul 09 2020 04:59 PM	129
LPMO	Jun 24 2020 01:54 PM	4

phenix.refine: Automated refinement using diffraction data (X-ray, neutron, ...)

Real-space refinement: Automated refinement using real-space maps (Cryo-EM, X-ray, ...)

Ensemble refinement: Time-averaged molecular dynamics refinement – models disorder using multiple models and TLS

Rosetta refinement: Hybrid Rosetta/Phenix refinement for low-resolution X-ray crystal struct

ReadySet: Utility for preparing PDB files for refinement – automatically generate res hydrogens

PDB Tools: Utility for simple modifications of models

PDB file editor: Simple hierarchy-based editing of PDB files

Model Reconstruction: Generate the asymmetric unit and/or the biological unit

Geometry minimization: Regularize geometry for a model (without data)

Current directory: /Users/ Dropbox (ORNL)/JOVE/Example

PHENIX version 1.14-3260-000

Project: LPMO

PDB Tools (Project: LPMO)

Modify atom selection :

Remove atom selection :

Keep only atom selection :

☐ Truncate to poly-Ala
☐ Remove alternate conformers
☐ Set segID to chain ID
☐ Clear segID field
☐ Convert SeMet residues to Met

Idle

Project: LPMO

ReadySet (Project: LPMO)

This will run phenix.ready_set, which uses Reduce to generate hydrogens on protein and nucleic acids, and eLBOW to generate ligand hydrogens, as well as creating appropriate restraints for any unknown ligands. If you use the latter feature, we highly recommend examining the restraints manually, e.g. using REEL (in the Utilities menu, or type phenix.reel on the command line).

PDB file : LPMO/LPMO_structure.pdb

Restraints (.cif) file :

Restraints directory :

Output file base :

☑ Add hydrogens to model if absent
☐ All hydrogens to the nitrogens of Histidine
Neutron refinement options : H/D at exchangeable sites, H elsewhere
☐ Add hydrogens to solvent molecules (not recommended)
☑ Add deuteriums to solvent molecules
☑ Generate ligand restraints
☐ Optimize ligand geometry
☐ Use the code in the model to generate restraints
☑ Metal ion coordination restraints
☐ Remove waters from model
☑ Output edits determined by LINK records
☑ Optimise final geometry of hydrogens

Random seed : 03056941001

Idle

Project: LPMO

Supplementary Figure 24

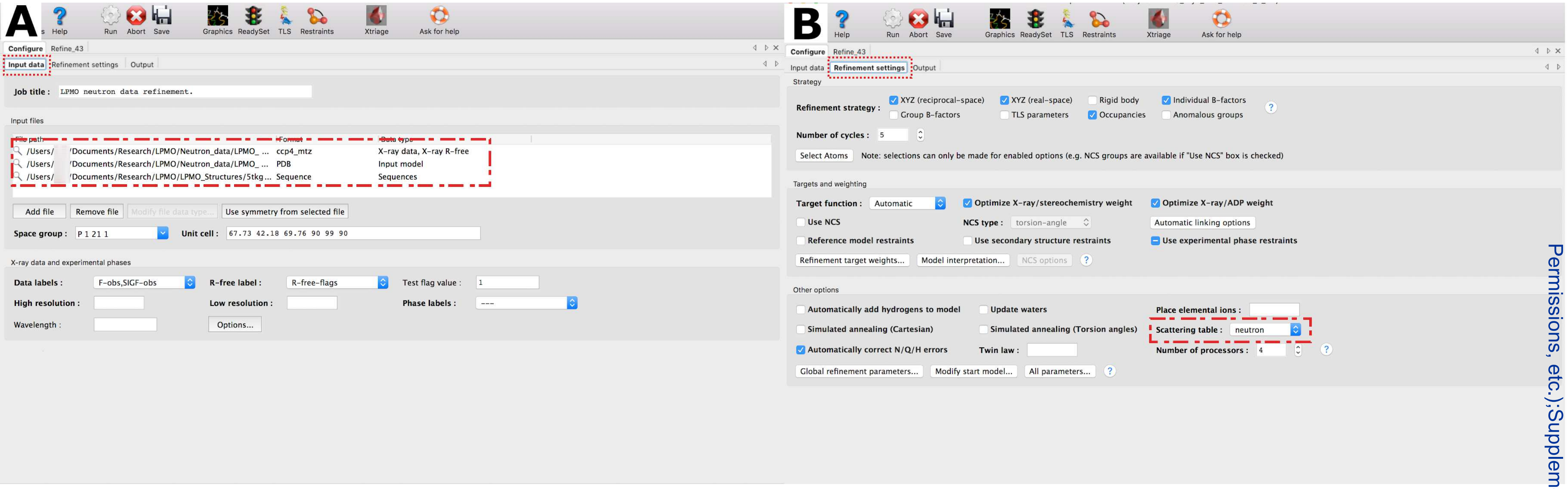

A

Job title : LPMO neutron data refinement.

Input files

File path	Format	Data type
/Users/[redacted]/Documents/Research/LPMO/Neutron_data/LPMO_ ...	ccp4_mtz	X-ray data, X-ray R-free
/Users/[redacted]/Documents/Research/LPMO/Neutron_data/LPMO_ ...	PDB	Input model
/Users/[redacted]/Documents/Research/LPMO/LPMO_Structures/5tkg...	Sequence	Sequences

Add file | Remove file | Modify file data type... | Use symmetry from selected file

Space group : P 1 21 1

Unit cell : 67.73 42.18 69.76 90 99 90

X-ray data and experimental phases

Data labels : F-obs,SIGF-obs

R-free label : R-free-flags

Test flag value : 1

High resolution :

Low resolution :

Phase labels : ---

Wavelength :

Options...

B

Strategy

Refinement strategy : ☑ XYZ (reciprocal-space) ☑ XYZ (real-space) ☐ Rigid body ☑ Individual B-factors ☐ Group B-factors ☐ TLS parameters ☑ Occupancies ☐ Anomalous groups

Number of cycles : 5

Select Atoms

Note: selections can only be made for enabled options (e.g. NCS groups are available if "Use NCS" box is checked)

Targets and weighting

Target function : Automatic

☑ Optimize X-ray/stereochemistry weight

☑ Optimize X-ray/ADP weight

☐ Use NCS

NCS type : torsion-angle

Automatic linking options

☐ Reference model restraints

☐ Use secondary structure restraints

☑ Use experimental phase restraints

Refinement target weights... | Model interpretation... | NCS options

Other options

☐ Automatically add hydrogens to model

☐ Update waters

Place elemental ions :

☐ Simulated annealing (Cartesian)

☐ Simulated annealing (Torsion angles)

Scattering table : neutron

☑ Automatically correct N/Q/H errors

Twin law :

Number of processors : 4

Global refinement parameters... | Modify start model... | All parameters...

Supplementary Figure 25

Click here to access/download;Supplemental File (Figures, Permissions, etc.);SupplementaryFigure25.eps

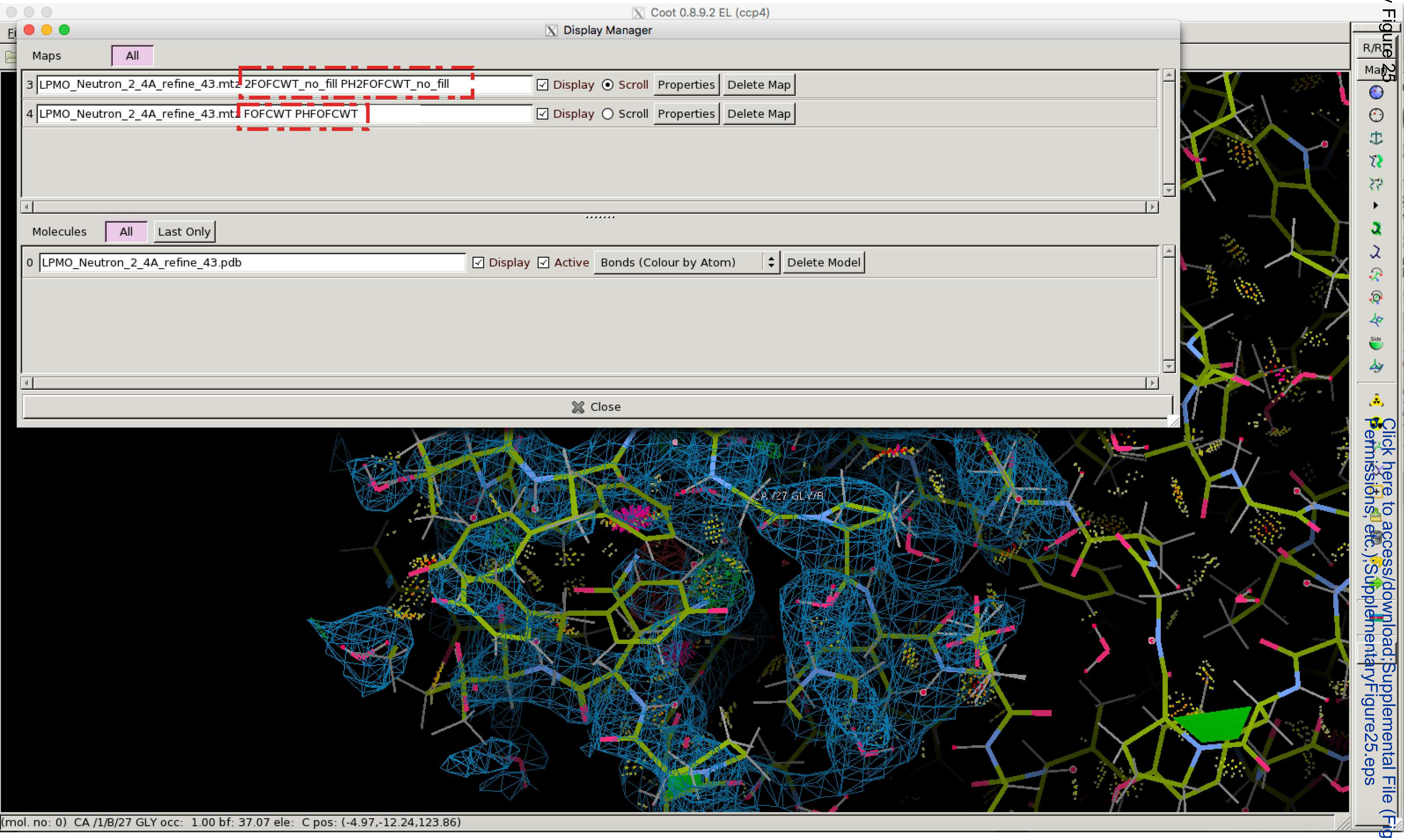

Coot 0.8.9.2 EL (ccp4)

Display Manager

Maps [All]

3 LPMO_Neutron_2_4A_refine_43.mtz 2FOFCWT_no_fill PH2FOFCWT_no_fill ☑ Display ● Scroll [Properties] [Delete Map]

4 LPMO_Neutron_2_4A_refine_43.mtz FOFCWT PHFOFCWT ☑ Display ○ Scroll [Properties] [Delete Map]

Molecules [All] [Last Only]

0 LPMO_Neutron_2_4A_refine_43.pdb ☑ Display ☑ Active Bonds (Colour by Atom) [Delete Model]

[Close]

(mol. no: 0) CA /1/B/27 GLY occ: 1.00 bf: 37.07 ele: C pos: (-4.97,-12.24,123.86)

Supplementary Figure 26

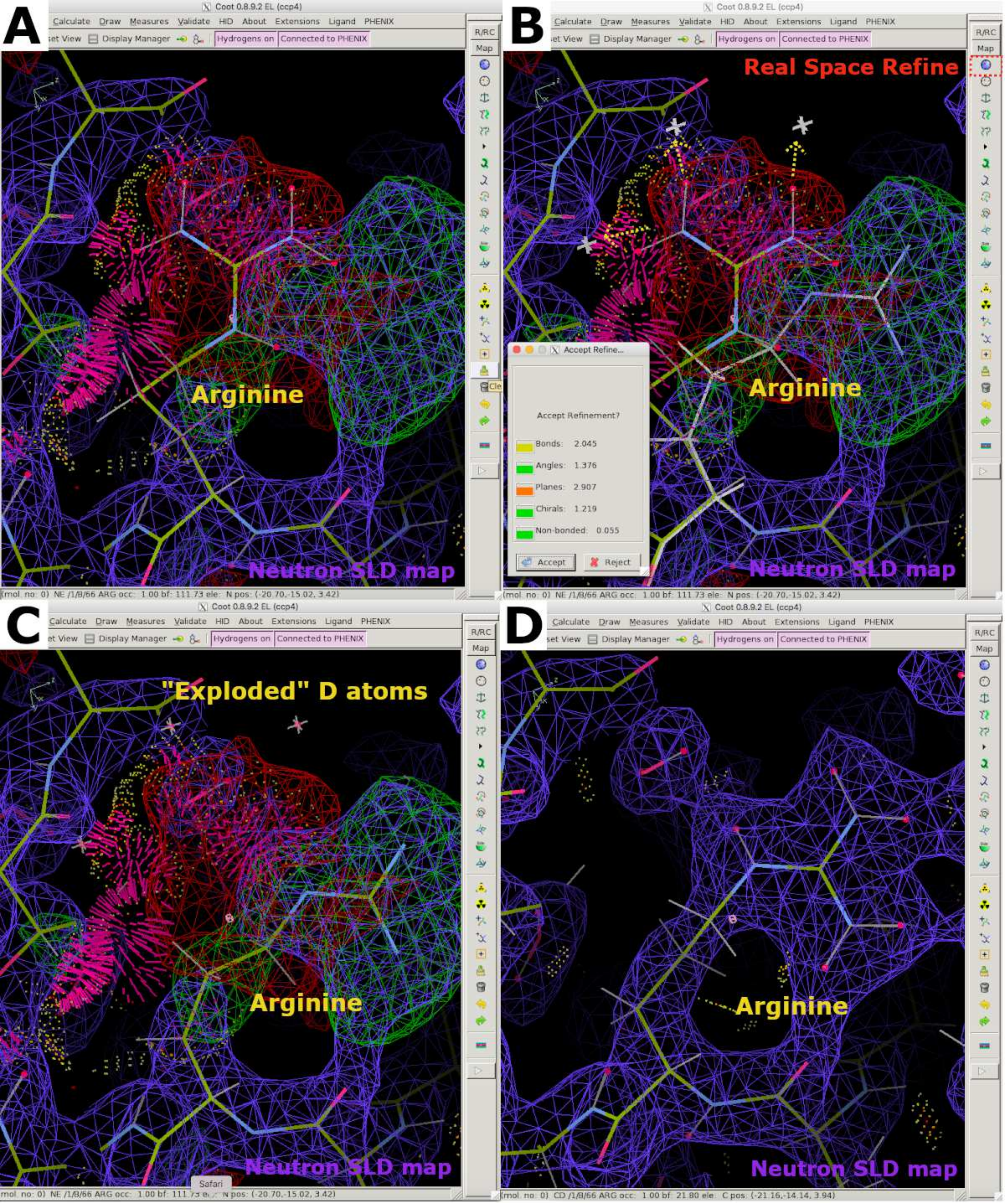
A
Coot 0.8.9.2 EL (ccp4)
Calculate Draw Measures Validate HID About Extensions Ligand PHENIX
Reset View Display Manager
Hydrogens on
Connected to PHENIX
R/RC
Map
Arginine
Neutron SLD map
B
Coot 0.8.9.2 EL (ccp4)
Calculate Draw Measures Validate HID About Extensions Ligand PHENIX
Reset View Display Manager
Hydrogens on
Connected to PHENIX
R/RC
Map
Real Space Refine
Accept Refine...
Arginine
Neutron SLD map
C
Coot 0.8.9.2 EL (ccp4)
Calculate Draw Measures Validate HID About Extensions Ligand PHENIX
Reset View Display Manager
Hydrogens on
Connected to PHENIX
R/RC
Map
"Exploded" D atoms
Arginine
Neutron SLD map
Safari
D
Coot 0.8.9.2 EL (ccp4)
Calculate Draw Measures Validate HID About Extensions Ligand PHENIX
Reset View Display Manager
Hydrogens on
Connected to PHENIX
R/RC
Map
Arginine
Neutron SLD map

A:

```
(mol. no: 0) NE /1/B/66 ARG occ: 1.00 bf: 111.73 ele: N pos: (-20.70,-15.02, 3.42)
```

B:

```
Accept Refinement?

Bonds:       2.045
Angles:      1.376
Planes:      2.907
Chirals:     1.219
Non-bonded:  0.055

Accept   Reject
```

```
(mol. no: 0) NE /1/B/66 ARG occ: 1.00 bf: 111.73 ele: N pos: (-20.70,-15.02, 3.42)
```

C:

```
(mol. no: 0) NE /1/B/66 ARG occ: 1.00 bf: 111.73 ele: N pos: (-20.70,-15.02, 3.42)
```

D:

```
(mol. no: 0) CD /1/B/66 ARG occ: 1.00 bf: 21.80 ele: C pos: (-21.16,-14.14, 3.94)
```

Supplementary Figure 27

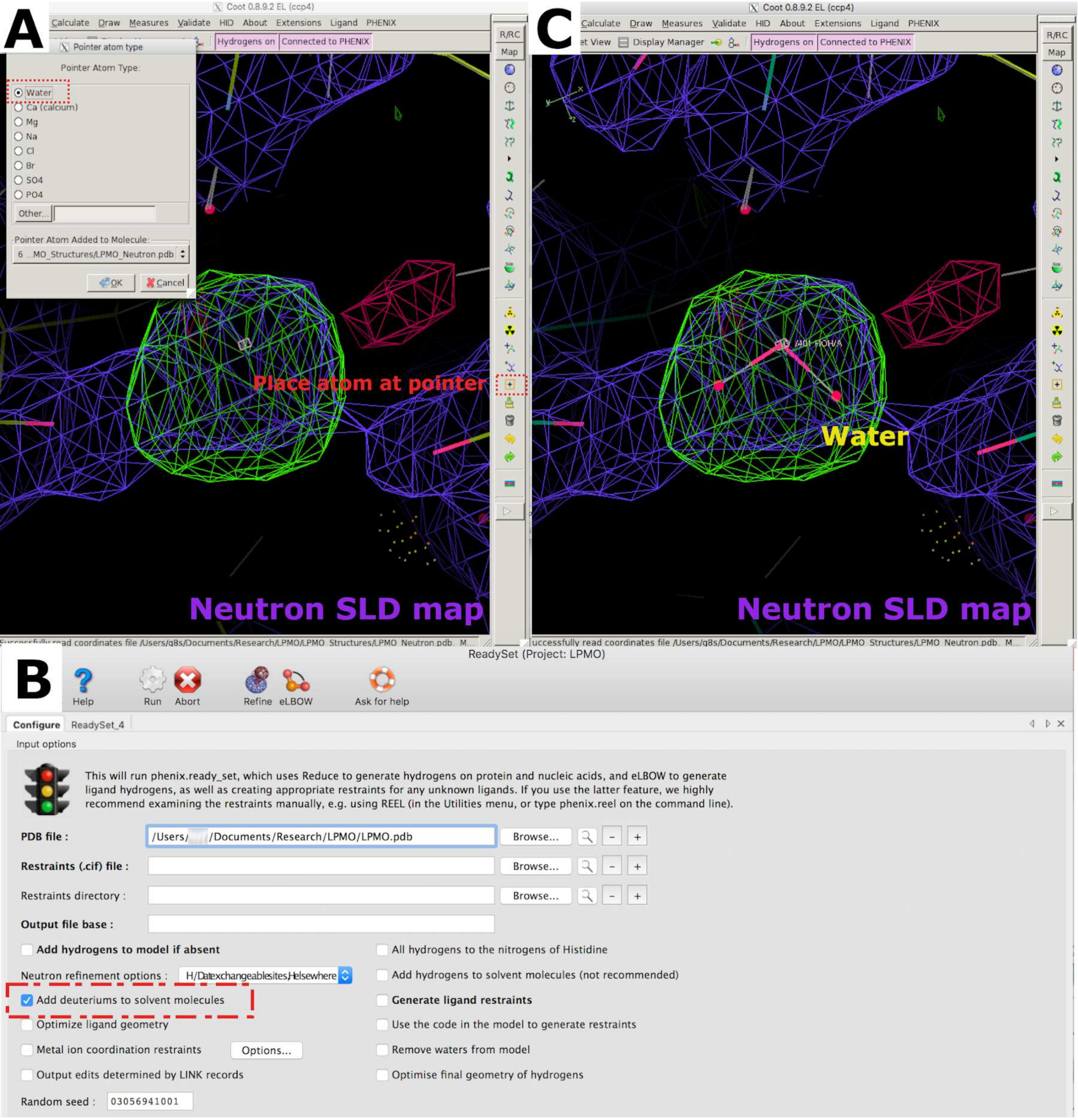
A
Coot 0.8.9.2 EL (ccp4)
Calculate Draw Measures Validate HID About Extensions Ligand PHENIX
Hydrogens on
Connected to PHENIX
Pointer atom type
Place atom at pointer
Neutron SLD map
R/RC
Map
OK
Cancel
Other...
C
Coot 0.8.9.2 EL (ccp4)
Calculate Draw Measures Validate HID About Extensions Ligand PHENIX
et View
Display Manager
Hydrogens on
Connected to PHENIX
/401 HOH/A
Water
Neutron SLD map
B
Help
Run
Abort
Refine
eLBOW
Ask for help
Configure
ReadySet_4
Browse...
Options...

Pointer Atom Type:

- ● Water
- ○ Ca (calcium)
- ○ Mg
- ○ Na
- ○ Cl
- ○ Br
- ○ SO4
- ○ PO4

Pointer Atom Added to Molecule: 6 ...MO_Structures/LPMO_Neutron.pdb

Successfully read coordinates file /Users/q8s/Documents/Research/LPMO/LPMO_Structures/LPMO_Neutron.pdb. M...

ReadySet (Project: LPMO)

Input options

This will run phenix.ready_set, which uses Reduce to generate hydrogens on protein and nucleic acids, and eLBOW to generate ligand hydrogens, as well as creating appropriate restraints for any unknown ligands. If you use the latter feature, we highly recommend examining the restraints manually, e.g. using REEL (in the Utilities menu, or type phenix.reel on the command line).

PDB file : /Users/[redacted]/Documents/Research/LPMO/LPMO.pdb

Restraints (.cif) file :

Restraints directory :

Output file base :

- ☐ **Add hydrogens to model if absent**
- ☐ All hydrogens to the nitrogens of Histidine
- Neutron refinement options : H/D at exchangeable sites, H elsewhere
- ☐ Add hydrogens to solvent molecules (not recommended)
- ☑ Add deuteriums to solvent molecules
- ☐ **Generate ligand restraints**
- ☐ Optimize ligand geometry
- ☐ Use the code in the model to generate restraints
- ☐ Metal ion coordination restraints
- ☐ Remove waters from model
- ☐ Output edits determined by LINK records
- ☐ Optimise final geometry of hydrogens

Random seed : 03056941001

Supplementary Figure 28

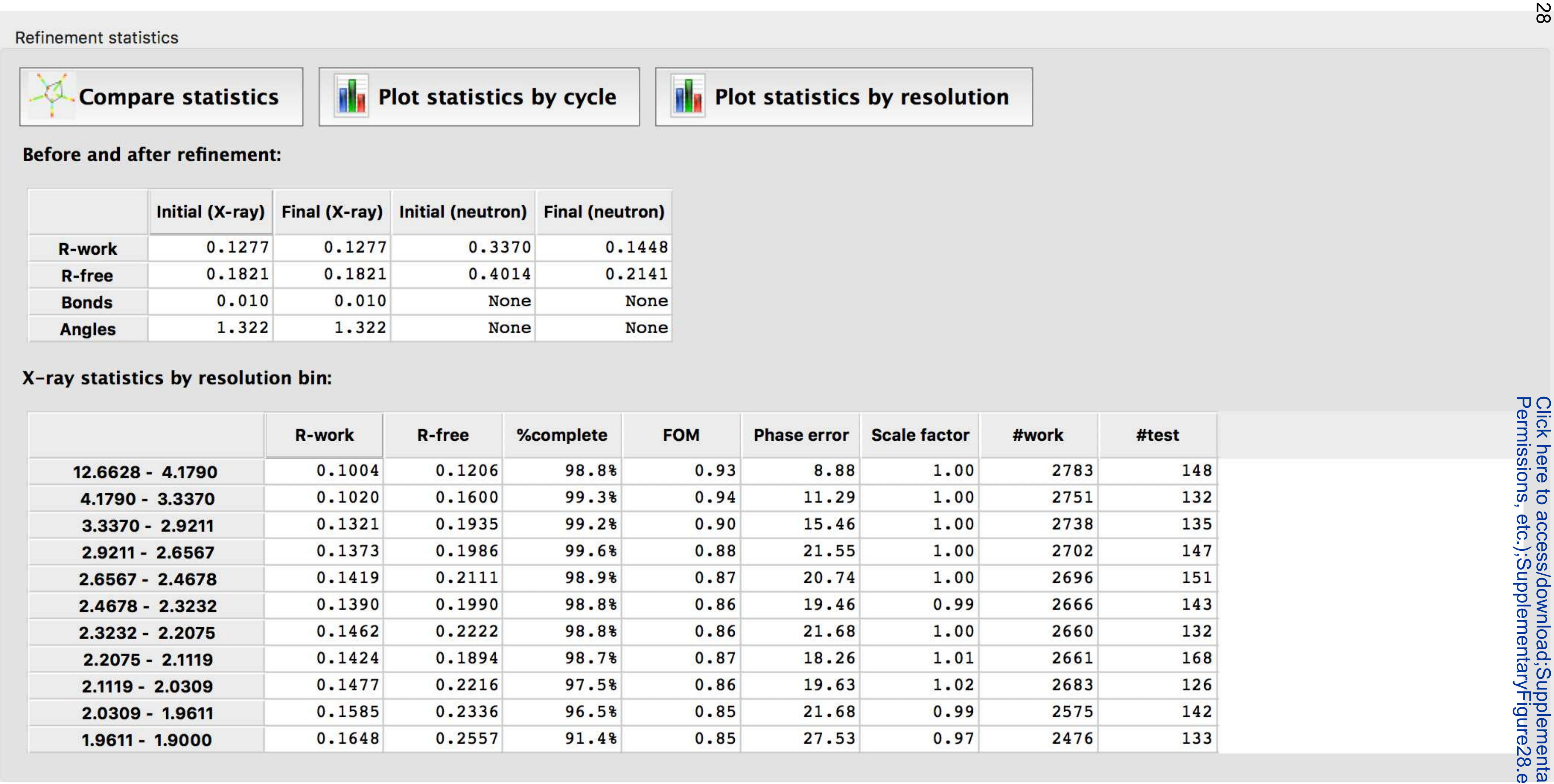
Refinement statistics
Compare statistics
Plot statistics by cycle
Plot statistics by resolution

Before and after refinement:

	Initial (X-ray)	Final (X-ray)	Initial (neutron)	Final (neutron)
R-work	0.1277	0.1277	0.3370	0.1448
R-free	0.1821	0.1821	0.4014	0.2141
Bonds	0.010	0.010	None	None
Angles	1.322	1.322	None	None

X–ray statistics by resolution bin:

	R-work	R-free	%complete	FOM	Phase error	Scale factor	#work	#test
12.6628 - 4.1790	0.1004	0.1206	98.8%	0.93	8.88	1.00	2783	148
4.1790 - 3.3370	0.1020	0.1600	99.3%	0.94	11.29	1.00	2751	132
3.3370 - 2.9211	0.1321	0.1935	99.2%	0.90	15.46	1.00	2738	135
2.9211 - 2.6567	0.1373	0.1986	99.6%	0.88	21.55	1.00	2702	147
2.6567 - 2.4678	0.1419	0.2111	98.9%	0.87	20.74	1.00	2696	151
2.4678 - 2.3232	0.1390	0.1990	98.8%	0.86	19.46	0.99	2666	143
2.3232 - 2.2075	0.1462	0.2222	98.8%	0.86	21.68	1.00	2660	132
2.2075 - 2.1119	0.1424	0.1894	98.7%	0.87	18.26	1.01	2661	168
2.1119 - 2.0309	0.1477	0.2216	97.5%	0.86	19.63	1.02	2683	126
2.0309 - 1.9611	0.1585	0.2336	96.5%	0.85	21.68	0.99	2575	142
1.9611 - 1.9000	0.1648	0.2557	91.4%	0.85	27.53	0.97	2476	133

Supplementary Figure 29

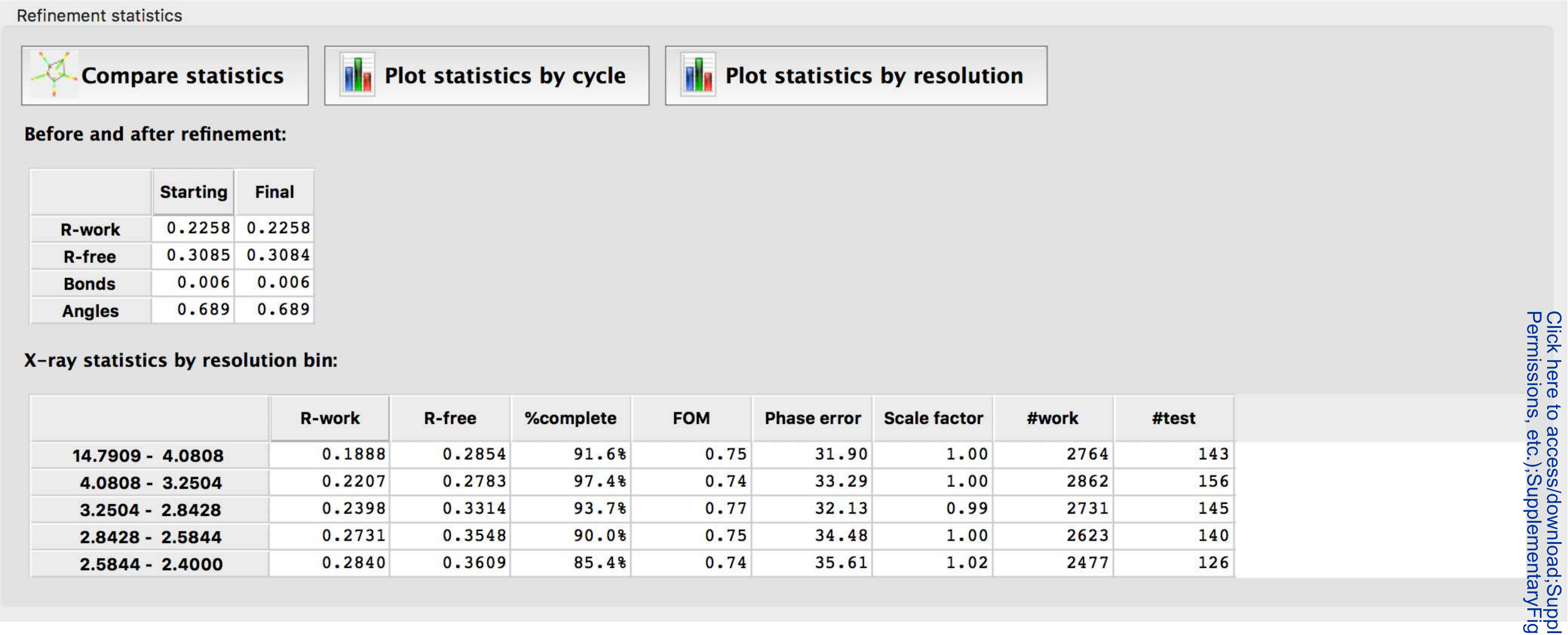
Refinement statistics
Compare statistics
Plot statistics by cycle
Plot statistics by resolution

Before and after refinement:

	Starting	Final
R-work	0.2258	0.2258
R-free	0.3085	0.3084
Bonds	0.006	0.006
Angles	0.689	0.689

X-ray statistics by resolution bin:

	R-work	R-free	%complete	FOM	Phase error	Scale factor	#work	#test
14.7909 - 4.0808	0.1888	0.2854	91.6%	0.75	31.90	1.00	2764	143
4.0808 - 3.2504	0.2207	0.2783	97.4%	0.74	33.29	1.00	2862	156
3.2504 - 2.8428	0.2398	0.3314	93.7%	0.77	32.13	0.99	2731	145
2.8428 - 2.5844	0.2731	0.3548	90.0%	0.75	34.48	1.00	2623	140
2.5844 - 2.4000	0.2840	0.3609	85.4%	0.74	35.61	1.02	2477	126